

# Activation of Hydrogen- and Halogen-Bonding Interactions in Tetrathiafulvalene-Based Crystalline Molecular Conductors

Marc Fourmigué\* and Patrick Batail\*

Laboratoire Chimie, Ingénierie Moléculaire et Matériaux (CIMMA), UMR 6200 CNRS-Université d'Angers, UFR Sciences, 2 Boulevard Lavoisier, 49045 Angers, France

Received April 15, 2004

## Contents

1. Introduction	5379
1.1. Purpose and Scope	5379
1.2. Van der Waals Interactions	5379
1.3. Overlap Interactions and Band Structure: Competing, Localized versus Delocalized Chemical Bonding Descriptions	5380
1.4. Milestones	5381
1.5. Hydrogen and Halogen Bonding	5382
2. Normal Hydrogen Bonds and Their Evolution in Radical Cation Salts	5382
2.1. Carboxylic Acids and Alcohols (OH Donors)	5383
2.1.1. Carboxylic Acids	5383
2.1.2. Neutral Hydroxylated Tetrathiafulvalenes	5385
2.1.3. Radical Cation Salts of Hydroxylated Tetrathiafulvalenes	5387
2.2. Amides and Thioamides (NH Donor)	5389
2.2.1. Neutral Amide and Thioamide Tetrathiafulvalenes	5389
2.2.2. Radical Cation Salts of Amide and Thioamide Tetrathiafulvalenes	5395
2.3. Hydrogen Bonding in the Anionic Network	5400
3. C—H···O(N, Hal) Hydrogen Bonds	5402
3.1. Hydrogen Bonding with C <sub>sp</sub> <sup>2</sup> —H Groups	5402
3.2. Hydrogen Bonding with sp <sup>3</sup> -CH <sub>2</sub> Groups	5405
3.3. C—H···O Hydrogen Bonding within the Anionic Network	5406
4. Halogen Bonding	5406
4.1. Halogen Bonding in the Solid State	5406
4.2. Neutral Halogenated Tetrathiafulvalenes	5407
4.3. Radical Cation Salts of Halogenated Tetrathiafulvalenes	5408
4.3.1. C—Hal···Hal <sub>anion</sub> Interactions	5408
4.3.2. C—Hal···O <sub>S<sub>anion</sub></sub> Interactions	5410
4.3.3. C—Hal···N Interactions	5411
4.3.4. Evolution of Halogen Bonding in TTF Salts	5413
4.4. Halogen Bonding Interactions in the Anionic Network	5414
5. Concluding Remarks	5415
6. Acknowledgments	5416
7. References	5416

## 1. Introduction

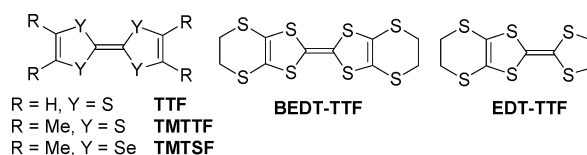
### 1.1. Purpose and Scope

The purpose of this review is to provide a perspective on the effort accomplished to direct intermolecular interactions in crystalline molecular conductors based on tetrathiafulvalene (TTF) derivatives, focusing on the use of directional, electrostatic, normal, and weak hydrogen bonds and halogen bonds. It will therefore concern tetrathiafulvalene molecules functionalized by hydrogen-bonding donor or acceptor groups such as alcohols, carboxylic acids, and amides as well as halogenated tetrathiafulvalenes and their salts, specifically concentrating on the crystal structures they adopt in the solid state. This will be conducted by proceeding to an examination throughout the entire deciphering process on how intermolecular patterns of noncovalent bonding interactions change from the parent, neutral solids to their radical cation salts.

### 1.2. Van der Waals Interactions

The solid-state structure of neutral tetrathiafulvalene-based molecules (Chart 1) is essentially con-

Chart 1



trolled by short-range, *nondirectional* van der Waals forces, which define the molecular shape, size, and close-packing properties. In addition to C···H, C···C, and H···H interactions, S···S interactions have to be taken into account in the realm of TTF solid-state chemistry.<sup>1</sup> By and large, these interactions typically govern the formation of different patterns of association of aromatics molecules, such as (i) the herringbone<sup>2</sup> structure adopted by small aromatics such as naphthalene, anthracene, or a polymorph of TTF itself,<sup>3</sup> (ii) the sandwich herringbone pattern of dimers observed with larger aromatics (pyrene, perylene) and exemplified in the structure of neutral BEDT-TTF shown in Figure 1, or (iii) the combination of stacking and herringbone geometries (so-called  $\gamma$ -packing) found with coronene and also in the

\* To whom correspondence should be addressed. E-mail addresses: marc.fourmigue@univ-angers.fr and patrick.batail@univ-angers.fr.



Marc Fourmigué received his diploma from the Ecole Supérieure de Physique et Chimie Industrielles (ESPCI, Paris) in 1986, followed by a DEA (M.S.) in Material Sciences with Pr. J. Simon at the ESPCI. After a Ph.D. under the supervision of K. Bechgaard (Copenhagen, Denmark) and P. Batail (Laboratoire de Physique des Solides, Orsay, France) in 1988, he got a CNRS position as Chargé de Recherche in 1990, spent six months in Santa Barbara, CA, in Pr. Fred Wudl's lab at University of California—Santa Barbara in 1994, and moved to the Institut Jean Rouxel (IMN) in Nantes shortly after. He is currently Directeur de Recherche at CNRS in Angers University (France). His current research interests lie in the areas of conducting and magnetic molecular solids, crystal engineering, and main-group chemistry focusing on tetrathiafulvalene derivatives and dithiolenes complexes.



Patrick Batail obtained his Doctorat d'Etat (Inorganic Chemistry) in 1976 at the University of Rennes I, where he became Assistant-Délégué (1973–1977) and then Chargé de Recherche CNRS from 1977 to 1985. He was an IBM postdoctoral fellow from 1978 to 1980 at the IBM Research Laboratory in San José, CA, where he worked with Jerry B. Torrance and Jim J. Mayerle on the neutral-to-ionic transition in TTF–chloranil. In 1985 he moved to the Laboratoire de Physique des Solides at the University of Paris-Sud at Orsay to become Directeur de Recherche CNRS. In 1990 he also became Professeur Chargé de Cours at the Ecole Polytechnique in Palaiseau. In 1995 he moved to the Institut des Matériaux de Nantes, and is currently Directeur de Recherches CNRS at the University of Angers since 2001. His research interests concern the chemistry of molecular materials, especially long range ordered hybrid solids whose low dimensional character and associated electronic instabilities are controlled by the nature of their organic–inorganic interface, and the chemistry of organic solution soluble minerals and lyotropic complex fluids with a mineral core. He held a number of visiting positions at the IBM Almaden Research Laboratory (1983), the Tokyo Institute of Technology (1989), and the Materials Research Laboratory at UCSB in 1996.

neutral TTF molecule<sup>4</sup> (Figure 2). On the basis of accurate *ab initio* calculations at the optimum geometry,<sup>5</sup> the strength of these interactions has been evaluated to be  $-0.69$ ,  $-0.45$ , and  $-0.35$  kcal mol<sup>-1</sup>

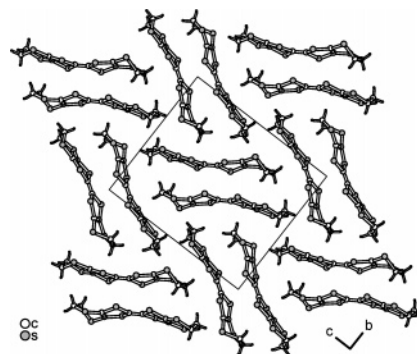


**Figure 1.** Herringbone pattern of dimers in crystals of neutral BEDT-TTF.

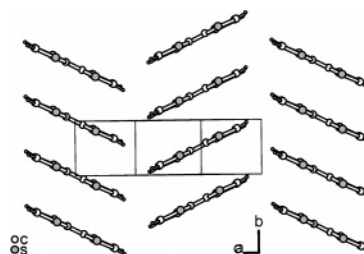


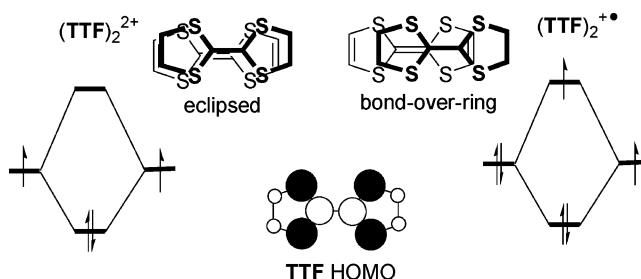
**Figure 2.** Combination of stacking and herringbone patterns in the  $\gamma$ -packing motif of neutral TTF.

for the C–H $\cdots$ C<sub>sp<sup>2</sup></sub>, C–H $\cdots$ S, and S $\cdots$ S interactions, respectively, providing a clear confirmation of their attractive nature.<sup>6</sup>

### 1.3. Overlap Interactions and Band Structure: Competing, Localized versus Delocalized Chemical Bonding Descriptions

Because we are faced in the radical cation salts or charged transfer salts with planar, *radical* molecules, another intermolecular interaction takes place in the solid state, that is their strong tendency to form a two-electron bond through direct overlap of their single occupied molecular orbitals (SOMOs). An essential characteristic of the tetrathiafulvalene molecule is the shape of its SOMO (Scheme 1), an orbital

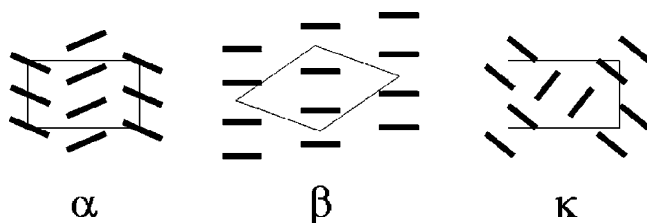
**Scheme 1**



whose  $\pi$  character essentially extends on the central C<sub>2</sub>S<sub>4</sub> motif. The gradual coming together of two such TTF<sup>•+</sup> species into a face-to-face arrangement thus corresponds to the formation of  $\sigma$  bonding and  $\sigma^*$  antibonding combinations of the two SOMOs. With a two-electron occupancy (Scheme 1, left), a strong  $\sigma$  bond between the two radicals is formed and the dyadic, dicationic (TTF)<sub>2</sub><sup>2+</sup> entity becomes fully diamagnetic. This dyadic entity can be considered as the

elementary building unit for the construction of extended one- or two-dimensional structures found in conducting systems, because it also captures the essence of the mixed valence dyadic system  $[\text{TTF}]_2^{+\cdot}$ , where the antibonding combination  $\sigma^*$  accommodates the supplementary electron (Scheme 1, right). In this configuration, the net bond strength is weaker but the attractive interaction is still present. As a consequence, the plane-to-plane distance increases and the molecules shift from the eclipsed conformation in the dicationic dyad—where the overlap interaction energy reaches its maximum—to a so-called bond-over-ring conformation—with less overlap but better mutual interpenetration. A very similar scheme prevails in extended structures where an infinity of partially occupied SOMOs interact to form energy bands, some of them filled and some partially filled and at the origin of a possible metallic behavior, provided their dispersion is larger than on-site Coulomb repulsions. However, the details of band dispersion and dimensionality are exceedingly sensitive to minute modifications of the relative orientations of each independent radical molecule in the solid state, and weak intermolecular interactions such as hydrogen or halogen bonding are thus expected to strongly modify the band structures and associated electronic behavior, by comparison with salts of nonfunctionalized tetrathiafulvalene derivatives. In that respect, in the numerous salts of “classical” TTF, TMTTF, TMTSF, BEDT-TTF, or EDT-TTF donor molecules described so far (Chart 1), essentially three intermolecular interactions are expected to play a prominent role: (i) long-range Coulombic interactions between charged species, be they a radical cation or the counterion, (ii) medium range overlap interactions of the open-shell radical cations, and (iii) short-range van der Waals interactions already present in the neutral component. The delicate balance between those interactions determines the final crystal structure and affects its properties. Besides the well-known one-dimensional stacks observed in the TTF, TMTTF, or TMTSF salts, BEDT-TTF or EDT-TTF salts are also found to organize into recurrent layered, two-dimensional structures, characterized with all molecules lying with their long axes parallel to each other. Many such arrangements have been reported and have been classified as  $\alpha$ -,  $\beta$ -,  $\beta'$ -,  $\delta$ -, or  $\kappa$ -phases (Scheme 2),<sup>7</sup> each of them allowing for different and specific overlap interaction networks and associated band structures and Fermi surfaces.

**Scheme 2. Different Two-Dimensional Structural Organizations Observed in the Layered BEDT-TTF Salts<sup>a</sup>**



<sup>a</sup> The BEDT-TTF molecules represented with the black lines are viewed along the molecular long axis.

## 1.4. Milestones

Looking back with a crystal engineering eye on several decades of increasingly intense research on structural chemistry issues in crystalline molecular conductors, a set of three seminal, important milestones are singled out at the onset of this review, based on the early recognition that weak  $\text{C}-\text{H}\cdots\text{X}$  interactions, particularly between the  $\text{C}_{\text{sp}^2}-\text{H}$  or  $\text{C}_{\text{sp}^3}-\text{H}$  groups of the donor molecule and the anionic counterpart, play an important role in determining the precise electronic properties of a given salt, as discussed below.

The earliest one is perhaps the discovery<sup>8,9</sup> in 1980 that the neutral-to-ionic phase transition in TTF-chloranil occurs in synchronicity with activation, accompanying a structural transition, of a two-dimensional network of weak  $\text{C}_{\text{sp}^2}-\text{H}\cdots\text{O}$  hydrogen bonds shown in Figure 3.

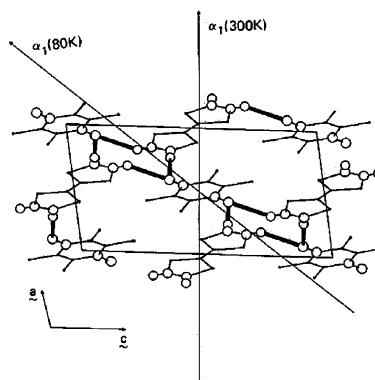


**Figure 3.** Projection of the structure of TTF-chloranil onto the  $ac$  plane, showing the network of  $\text{C}-\text{H}\cdots\text{O}$  contacts (thick lines). The orientations of the largest principal axis of the thermal contraction tensor above and below the neutral-to-ionic phase transition are also depicted. (Reproduced from ref 8. Copyright 1981 American Chemical Society.)

Then, there was the landmark 1987 paper by Whangbo et al.<sup>10</sup> which demonstrated that a set of weak  $\text{C}_{\text{sp}^3}-\text{H}\cdots\text{X}$  hydrogen bonds, shown in Figure 4, was responsible for the occurrence of a modulation

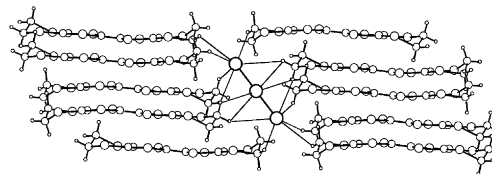


**Figure 4.** Structure of  $\beta$ -(BEDT-TTF)<sub>2</sub>AuI<sub>2</sub> with the 12 BEDT-TTF molecules that surround one AuI<sub>2</sub><sup>-</sup> anion with  $\text{H}\cdots\text{I}$  and  $\text{H}\cdots\text{Au}$  contacts less than 3.5 Å.<sup>10</sup>

of the structure of  $\beta$ -(BEDT-TTF)<sub>2</sub>I<sub>3</sub> which vanishes under hydrostatic pressures as low as 0.5 kbar, and for affecting the superconducting transition temperature  $T_C$  and the dependence of  $T_C$  on the nature of  $\text{X}^-$  in  $\beta$ -(BEDT-TTF)<sub>2</sub>X. The softness of the BEDT-TTF molecules with respect to translational and/or librational modes of vibration could be correlated with the strength of the shortest  $\text{C}-\text{H}\cdots\text{X}^-$  contacts, which means “that ET molecules are anchored around anions  $\text{X}^-$  as if effectively weak hydrogen bonding

exists in the C–H···X<sup>−</sup> contacts”. Such contacts also govern whether the two ethylene groups of BEDT-TTF adopt a staggered or eclipsed conformation.  $T_c$  increases from 1.4 K in  $\beta$ -(BEDT-TTF)<sub>2</sub>I<sub>3</sub> up to 8 K in  $\beta^*$ -(BEDT-TTF)<sub>2</sub>I<sub>3</sub> upon application of only 0.5 kbar, which stabilizes the staggered conformation of the outer ethylene fragments and makes for a softer lattice than that of  $\beta$ -(BEDT-TTF)AuI<sub>2</sub> or  $\beta$ -(BEDT-TTF)I<sub>3</sub>. Comparable C–H···anion interactions present in Bechgaard salts with ClO<sub>4</sub><sup>−</sup>, ReO<sub>4</sub><sup>−</sup>, PF<sub>6</sub><sup>−</sup>, and AsF<sub>6</sub><sup>−</sup> counterions involve less polarizable atoms such as oxygen or fluorine in C–H···O or C–H···F contacts. As a consequence, the lattice is expected to be stiffer than that observed with the more polarizable iodine or bromine atoms in C–H···I or C–H···Br interactions, hence the lower  $T_c$  in these salts when compared with BEDT-TTF salts.

Finally, at a moment when the organic–inorganic hybrid ideas in materials chemistry were taking shape,<sup>11</sup> the layered structure of  $\beta$ -(BEDT-TTF)<sub>8</sub>[SiW<sub>12</sub>O<sub>40</sub>] was reported,<sup>12,13</sup> in 1989, to exhibit a singular, non-centrosymmetric character which originates in a set of “interfacial” C–H···O hydrogen bonds with the top and bottom closed-packed oxygen atom surface layers of the polyoxometalate anions, thanks to the orthogonal topology inherent to their tetrahedral symmetry (see Figure 5).

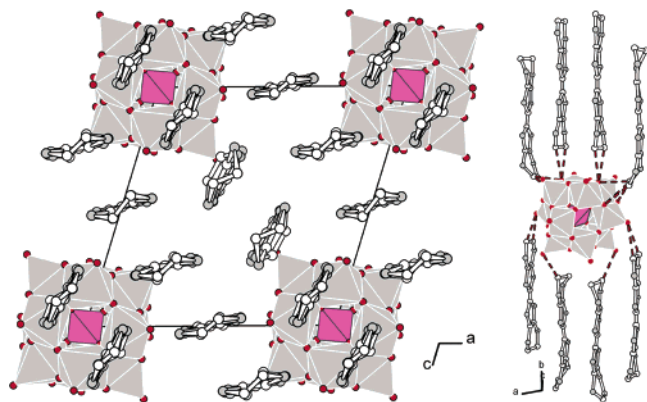


**Figure 5.** Set of two illustrations exemplifying how the upper and lower faces of a single [SiW<sub>12</sub>O<sub>40</sub><sup>4−</sup>] anion are capped by BEDT-TTF molecules in monoclinic, space group  $I2$ ,  $\alpha$ -(BEDT-TTF)<sub>4</sub>(SiW<sub>12</sub>O<sub>40</sub>).<sup>12</sup>

These three milestones have served as an incentive to develop the synthesis and solid-state chemistry of tetrathiafulvalene cores functionalized by hydrogen bond donor/acceptor groups whose early developments have been reviewed by M. Bryce in 1995.<sup>14</sup> Also the possibility that hydrogen bonding might influence electronic properties through direct electron–proton coupling phenomena provides an added impetus for these studies.<sup>15</sup> Although the scope of this review is not restricted to the use of hydrogen-bonding interactions, today the singular electrostatic, directional, and strongest intermolecular interaction is one crystal engineers work with confidence and is the most readily deciphered one, as discussed in the following sections.

### 1.5. Hydrogen and Halogen Bonding

In the past several years, there have been a number of excellent reviews<sup>16–19</sup> on the broad topic

of crystal engineering, defined by Desiraju as “the understanding of intermolecular interactions in the context of crystal packing and in the utilization of such understanding in the design of new solids with desired physical and chemical properties”. Directional intermolecular interactions of diverse strengths are the favorite tools of crystals engineers, since the orientation of molecules in the solid state can be predicted with a reasonable degree of accuracy. Three such interactions stand out: (i) hydrogen bonding, (ii) weaker C–H···X hydrogen bonding, and (iii) halogen bonding. Hydrogen bonds of the type O–H···O or N–H···O are described as normal with bond energies<sup>20</sup> ranking from 19 kcal mol<sup>−1</sup> in NH<sub>4</sub><sup>+</sup>···OH<sub>2</sub> and 13.5 kcal mol<sup>−1</sup> in HO–H···Cl<sup>−</sup> to 5 kcal mol<sup>−1</sup> in HO–H···OH<sub>2</sub> model systems. The weaker C–H···X interaction energies involving activated C–H groups amount to 2.2 kcal mol<sup>−1</sup> in HC≡C–H···OH<sub>2</sub> or 1 kcal mol<sup>−1</sup> in H<sub>2</sub>C=CH–H···OH<sub>2</sub> systems. Notice that halogen bonds can be compared to normal hydrogen bonds. For example, the C–Cl···N≡C bond energy has been calculated to amount to 2.4 kcal mol<sup>−1</sup> (10 kJ) in the chlorocynoacetylene dimer,<sup>21</sup> while it was estimated to amount to 6 kcal mol<sup>−1</sup> in the F<sub>3</sub>C–I···NH<sub>3</sub> system.<sup>22</sup> These three interaction categories have been investigated in the field of molecular conductors in the last 20 years as an efficient tool to rationalize, orient, and control their solid-state structures and hence influence their electronic properties. One essential, preliminary step lies thus in the conception, preparation, and characterization of tetrathiafulvalene donor molecules functionalized with hydrogen bond donor or acceptor substituents such as –OH, –CO<sub>2</sub>H, or –CONHR moieties or with halides (–Cl, –Br, –I). This article does not intend to review the synthetic effort accomplished to prepare TTF molecules appended with the former substituents but focuses on the analysis of their crystal structures, when available, in their neutral form as well as in their radical cation salts, concentrating first on hydrogen bonding in section 2, weaker C–H···X hydrogen bonds in section 3, and halogen bonding in section 4.

### 2. Normal Hydrogen Bonds and Their Evolution in Radical Cation Salts

The distinctive geometrical characteristics of a hydrogen bond have been discussed extensively in books or review articles<sup>20,23</sup> and will not be detailed further. Typical values to be remembered for the H···A distance are 1.60–1.80 Å for O–H···O bonds and 1.80–2.00 Å for N–H···O bonds. Note that, in the discussion of the structural characteristics of hydrogen bonds described in this review, we will systematically use the hydrogen atom positions reported by different authors in their original papers without any modification, such as, for example, distance normalization based on neutron derived distances of the X–H distance.<sup>24</sup> As seen in Table 1, where standard X–H neutron distances are compared with those distances used, for example, in SHELXL for calculated hydrogen atom positions (HFIX),<sup>25</sup> the maximum differences do not exceed

**Table 1. Comparison of Standard Neutron X–H Distances<sup>24</sup> with SHELXL<sup>25</sup> Calculated X–H Distances and Maximum Differences**

X–H group	standard value	SHELXL value	max diff
C–H	1.083	0.93–0.98	0.153
N–H	1.009	0.86–0.89	0.149
O–H	0.983	0.82	0.163

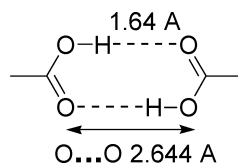
+0.15 Å, implying that the distance criteria defined with normalized values can be slightly increased when using SHELXL values while the directionality requirements should be strengthened. The D–H···A hydrogen bond angle ranges between 150 and 180°. This marked directionality of the hydrogen bond is well established and is the basis for efficient and reliable topologies<sup>16</sup> of intermolecular motifs that contain groups such as –OH, –CO<sub>2</sub>H, –CONH<sub>2</sub>, and –CONHR.

Tetrathiafulvalenes bearing a –OH function as hydrogen bond donor (carboxylic acids, alcohols) will be described first in section 2.1, followed by those bearing a –NH function as hydrogen bond donor, essentially primary and secondary amides, in section 2.2. In each case, the X-ray crystal structures of neutral donor molecules will be examined before their radical cation salts. Finally, a selection of salts where hydrogen bonding is observed exclusively within the anionic layer will be described.

## 2.1. Carboxylic Acids and Alcohols (OH Donors)

### 2.1.1. Carboxylic Acids

Carboxylic acids self-assemble to form a robust symmetrical eight-membered cyclic dimer motif shown in Scheme 3. It should be stressed, however, that the

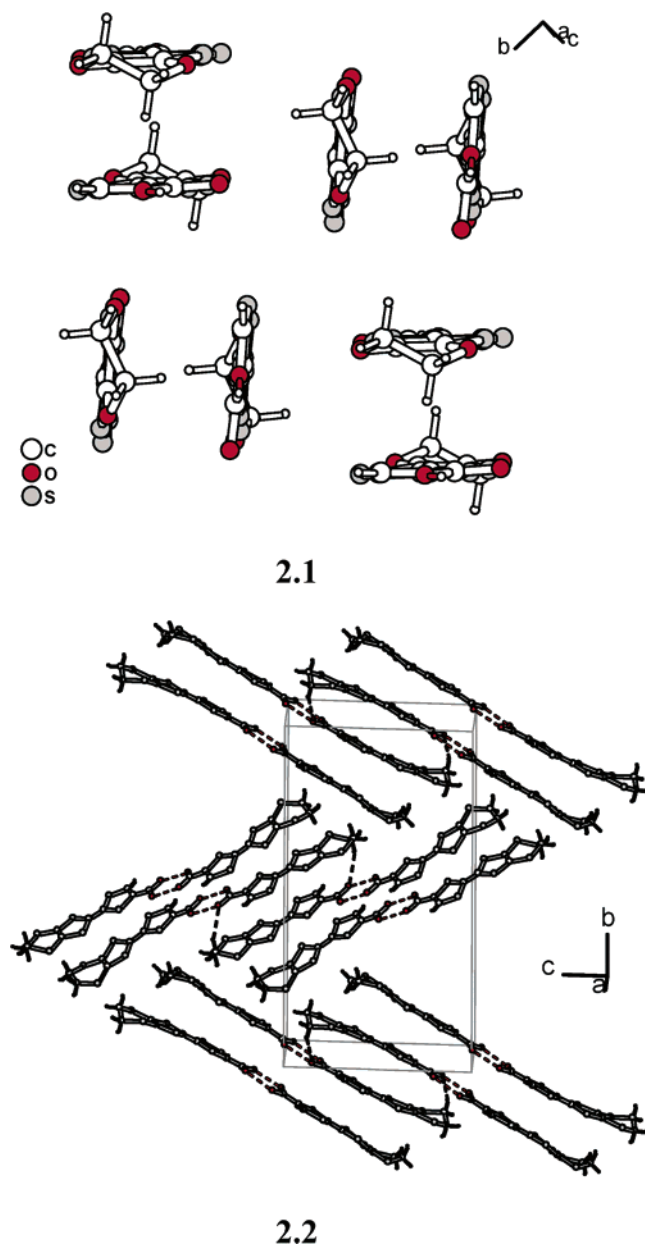
**Scheme 3. Mean Geometry of the Carboxylic Acid Dimer in Crystals<sup>23</sup>**

probability of formation of this dimeric motif is of the order of 33%, thus the preference of CO<sub>2</sub>H groups for a wide variety of other hydrogen bond acceptor competitors (CO<sub>2</sub><sup>−</sup>, P=O, pyridine, F<sup>−</sup>, Cl<sup>−</sup>). As stated by Steiner, “engineering the carboxylic acid dimer clearly requires the absence of successful competitors”.<sup>23</sup> We will see in the following that the few crystallographically characterized tetrathiafulvalene carboxylic acids adopt this dimer motif, giving rise to bimolecular units without further possibilities for hydrogen bond interactions.

Besides the presence of the carboxylic acid dimer motif, the structure of EDO-TTF–COOH is singular, as two-dimensional  $\kappa$ -type slabs (**2.1**) along *b* in a (*a* + *c*, *b*) plane develop out of dimers of the former dimers<sup>26</sup> while a herringbone arrangement of similar dimers of hydrogen-bonded dimers is observed in the structure of the EDT-TTF–CO<sub>2</sub>H analogue (**2.2**) (see Table 2).<sup>27</sup>

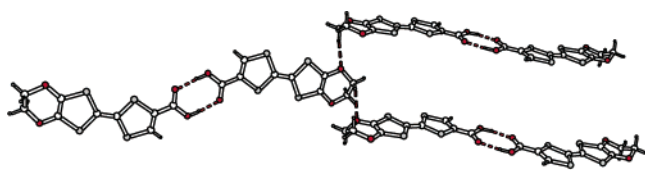
**Table 2. Structural Characteristics of the Tetrathiafulvalene Carboxylic Acid Dimers**

compound	O···H (Å)	O···O (Å)	ref
EDO-TTF–CO <sub>2</sub> H	1.71	2.64	26
EDT-TTF–CO <sub>2</sub> H		2.58	27
Me <sub>3</sub> TTF–CO <sub>2</sub> H	1.62	2.63	28
[Me <sub>3</sub> TTFPO <sub>3</sub> H] <sup>+</sup>		2.41	29
		2.49	
( <i>n</i> -C <sub>5</sub> H <sub>11</sub> ) <sub>2</sub> TTF(Me)CO <sub>2</sub> H		2.61	30
TTF(CH <sub>2</sub> ) <sub>11</sub> CO <sub>2</sub> H		2.63	31



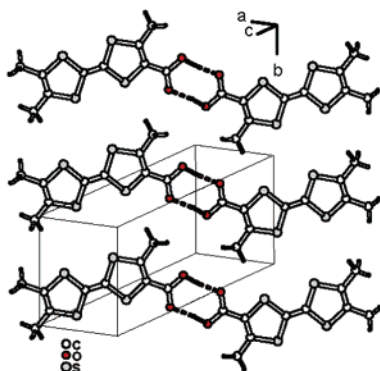
The difference between the two organizations reflects the difference in net van der Waals interaction stabilization energies between EDO-TTF–CO<sub>2</sub>H and EDT-TTF–CO<sub>2</sub>H upon substitution of two sulfur atoms by oxygen atoms as well as the effect of C<sub>sp3</sub>–H···O hydrogen bonding between the ethylenic bridges and different oxygen atom acceptors. Indeed, in EDT-TTF–CO<sub>2</sub>H (**2.2**), one C<sub>sp3</sub>–H···O interaction with the carboxylic group is identified (H···O = 2.63 Å, C<sub>sp3</sub>(–H)···O = 3.50 Å, C–H···O = 149°) while, in EDO-TTF–CO<sub>2</sub>H (**2.3**), a C<sub>sp3</sub>–H···O

interaction ( $H\cdots O = 2.54 \text{ \AA}$ ,  $C_{sp^3}(-H)\cdots O = 3.33$ ,  $C-H\cdots O = 138^\circ$ ) also prevails, this time with the oxygen atom of the ethylene dioxo substituent which directs the molecular planes of  $O-H\cdots O$  hydrogen-bonded dimers  $[EDO-TTF-COOH]_2$  to be orthogonal to each other, as shown in **2.3**.

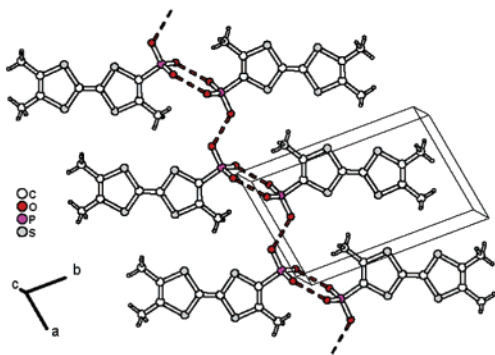


2.3

In  $Me_3TTF-CO_2H$ , carboxylic dimers arrange parallel to each other into a flat ribbon extending along  $b$ , as shown in **2.4a**.<sup>28</sup> Likewise, a similar dimer motif, also connected into a flat ribbon, here extending along  $a$  and via additional  $O-H\cdots O$  hydrogen bonds, is identified in **2.4b** for the zwitterionic radical derived



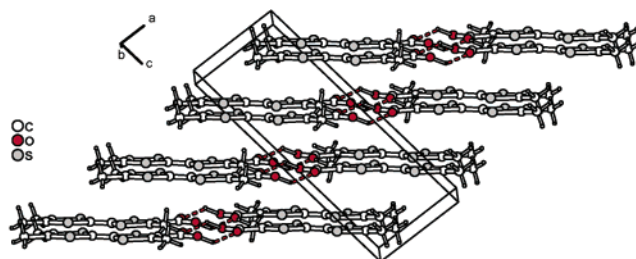
2.4a



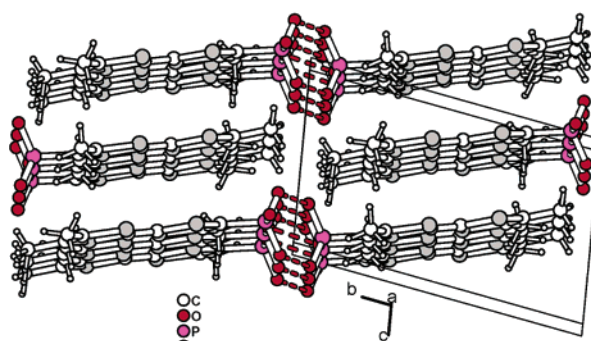
2.4b

from the trimethyltetrathiafulvalene phosphonic acid,  $[Me_3TTF-PO_3H^-]^+$ .<sup>29</sup> Notice the  $(a,b)$  and  $(a,c)$  slabs developing out of the van der Waals' self-association of ribbons in  $Me_3TTF-CO_2H$ , **2.5a**, and in  $[Me_3TTF-PO_3H^-]^+$ , **2.5b**, respectively, a similar set of two remarkable two-dimensional architectures rarely obtained for neutral, monomolecular solids. Interestingly, a clear-cut two-dimensional hydrophilic-hydrophobic partition occurs in **2.5a**, which contrasts with the three-dimensional repartition of hydrophilic and hydrophobic regions in **2.5b**. Notice also that, in  $[Me_3TTF-PO_3H^-]^+$  (**2.5b**), the slabs of radical molecules adopt a  $\beta$ -type topology with HOMO $\cdots$ HOMO interaction energies and a two-dimensional dispersion comparable to those found in  $\beta$ -(BEDT-TTF)<sub>2</sub>I<sub>3</sub>,

despite a rather different mode of overlap, with an unprecedented, strong  $\sigma$ -type  $(p_\pi)_C-(p_\pi)_S$  overlap along  $c$ .

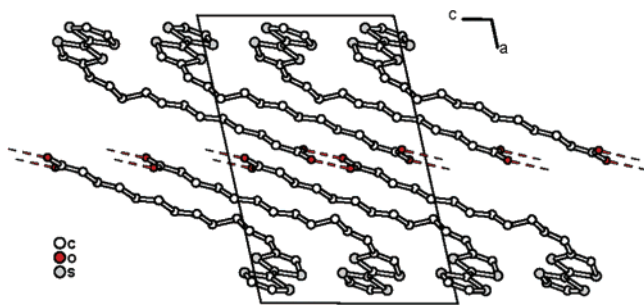


2.5a



2.5b

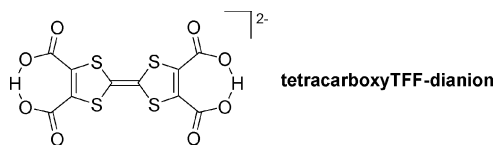
In addition to the rigid acid derivatives described above, two other TTF acids have been reported with long alkyl chains attached either on the TTF core in  $(n-C_5H_{11})_2TTF(Me)CO_2H$ <sup>30</sup> or between the TTF and  $CO_2H$  moieties in 12-(tetrathiafulvalenyl)-11-dodecenoic acid.<sup>31</sup> In both cases, the strong carboxylic acid hydrogen-bonded dimers combine with a van der Waals segregation of the long alkyl chains on the one hand and the TTF core on the other hand to generate the layered architecture of 12-(tetrathiafulvalenyl)-11-dodecenoic shown in **2.6**, which features a hydrophilic-hydrophobic partition and thin slices of overlapping TTF cores extended side-by-side along  $c$ .



2.6

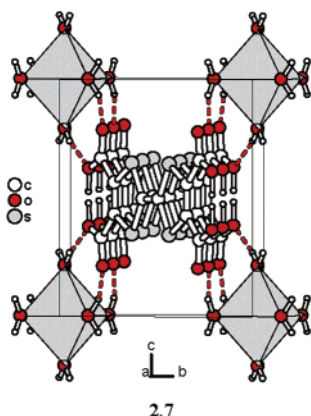
Developing an efficient, general methodology for the preparation of the bis(deprotonated) TTF tetraacid  $TTF(CO_2H)_4$ , Mercier et al. isolated  $[TTF-(CO_2H)_2(CO_2)_2]^{2-}$  (Chart 2) as its  $n-Bu_4N^+$  salt.<sup>32</sup> The dianionic TTF moieties were found fully embedded in a sea of  $N$ -alkyl chains, with two intramolecular, symmetrical  $O-H\cdots O=C$  hydrogen bonds, which leave the dianion a potential hydrogen bond acceptor

Chart 2



only, as observed in the TTF-based composite salt,  $(\text{TTF}^+)_2[\text{TTF}(\text{COOH})_2(\text{COO}^-)_2]$  described below in section 3.1. Note that the hydrogen atom could not be located between the two oxygen atoms while the  $\text{O}\cdots\text{O}$  distance amounts to 2.387 Å, comparable to that observed in the hydrogenomaleate anion (2.41–2.43 Å), for example.<sup>33</sup>

Starting from the same tetracarboxylic acid, Beer et al. reported that slow diffusion in aqueous silica gel of  $\text{TTF}(\text{CO}_2\text{H})_4$  in the presence of  $[\text{Co}^{\text{II}}(\text{NO}_3)_2]\cdot 6\text{H}_2\text{O}$  affords,  $[\text{Co}^{\text{II}}(\text{H}_2\text{O})_6][\text{TTF}(\text{CO}_2\text{H})_2(\text{CO}_2)_2]\cdot 2\text{H}_2\text{O}$ , a microporous water solvate whose framework robustness is based on short hydrogen bonds between 8 of the 12 protons in the hexaaquometal cation and 6 of the 8 carboxyl oxygen atoms (**2.7**). The two



protons of the doubly deprotonated acid form short, intramolecular hydrogen bonds to the neighboring carboxyl groups with  $\text{O}\cdots\text{O}$  distances of 2.44 Å, slightly longer than those in the *n*-Bu<sub>4</sub>N<sup>+</sup> salt described above. Interestingly, the disordered water molecules interspersed within one-dimensional channels running along *a* may be liberated at 50 °C while monocrystallinity is retained across the desolvation, which causes a triclinic to monoclinic transformation to  $[\text{Co}(\text{H}_2\text{O})_6][\text{TTF}(\text{CO}_2\text{H})_2(\text{CO}_2)_2]$ . The remarkable flexibility and durability of this microporous framework are seen as the result of a synergy between the large collection of independent hydrogen-bonding and nonbonding intermolecular interactions present in the salt.

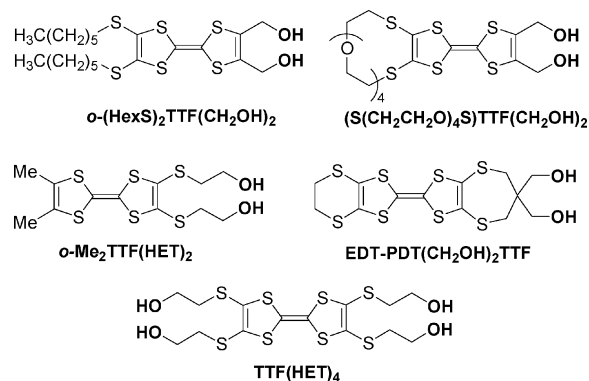
Despite the remarkable efficiency of the carboxylic acid function to crystallize in a robust dimer, there is neither a TTF carboxylic acid which has been successfully oxidized to the corresponding radical cation nor a carboxylate which has been successfully oxidized to the corresponding crystalline zwitterionic  $[\text{TTF}-\text{CO}_2^-]^+$ .<sup>35</sup> Our own experience in the electrocrystallization of TTF carboxylic acids such as  $\text{Me}_3\text{TTF}-\text{CO}_2\text{H}$  indicates indeed their propensity to decompose upon oxidation through a Kolbe electro-decarboxylation mechanism to generate radical cation salts of the unsubstituted TTF core.<sup>28</sup>

### 2.1.2. Neutral Hydroxylated Tetrathiafulvalenes

The crystal structures of only a few hydroxylated neutral tetrathiafulvalenes are available, and the simplest elements of the series such as  $\text{TTF}-\text{CH}_2\text{OH}$ ,  $E\text{-TTF}(\text{CH}_2\text{OH})_2$ , or  $\text{TTF}(\text{CH}_2\text{OH})_4$  have not been investigated in the solid state. Since C–OH motifs may act simultaneously as hydrogen bond donors and acceptors, they are often found to be engaged in cyclic or extended motifs stabilized by  $\sigma$ -bond cooperativity,<sup>36</sup> as discussed below. Carbohydrate X-ray and neutron diffraction data indicate that mean  $\text{H}\cdots\text{O}$  distances range from 1.82 Å in infinite chains where  $\sigma$ -bond cooperativity is significant to 1.91 Å in finite motifs. Similar values are reported for alcohols (C–OH) hydrogen bonded to water molecules with mean  $\text{H}\cdots\text{O}$  and  $\text{O}\cdots\text{O}$  distances of 1.80 and 2.75 Å, respectively. Those values will serve as reference values in the following discussion of the geometrical characteristics of the observed hydrogen bond interactions in the series of neutral hydroxylated tetrathiafulvalenes collected in Table 3 and described below.

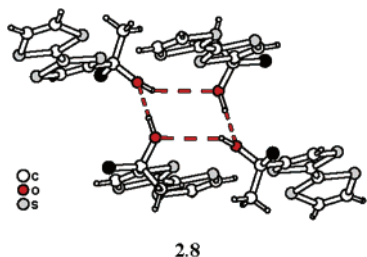
Molecules with only one hydroxyl group are found as secondary or tertiary alcohols such as  $(\text{Me}_3\text{TTF})_2\text{-CH}(\text{OH})$  and  $(\text{Fc})(\text{TTF})\text{CMe}(\text{OH})$ . In the former,<sup>37</sup> the OH group engages in a weak hydrogen bond with the oxygen atom of an EtOH solvate molecule while, when no solvent (alcohol) molecule is available, the pattern of intermolecular association of the similar

**Table 3. Structural Characteristics of the Hydrogen Bonds Identified in Neutral Hydroxylated Tetrathiafulvalenes**



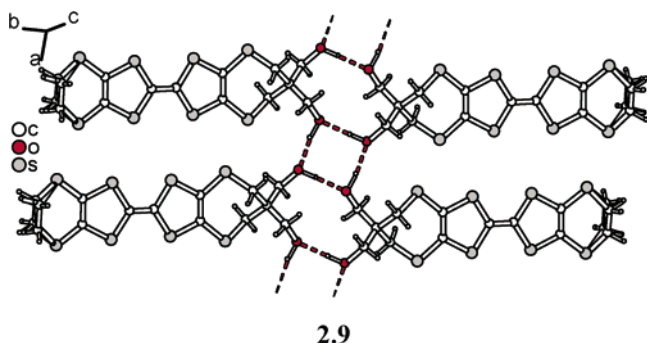
compound	H $\cdots$ O (Å)	O $\cdots$ O (Å)	O–H $\cdots$ O (deg)	ref
$(\text{Me}_3\text{TTF})_2\text{CHOH}$ , EtOH	2.44	3.47	175	37
$(\text{Fc})(\text{TTF})(\text{Me})\text{C}-\text{OH}$	2.96	3.63	134	38
	1.98	3.07	178	
<i>o</i> -(HexS) <sub>2</sub> TTF(CH <sub>2</sub> OH) <sub>2</sub>	1.85	2.70	165	40
	1.99	2.71	133	
$(\text{S}(\text{CH}_2\text{CH}_2\text{O})_4\text{S})\text{TTF}(\text{CH}_2\text{OH})_2$	2.00	2.82	172	41
	2.29	3.04	153	
	2.02	2.80	156	
<i>o</i> -Me <sub>2</sub> TTF(HET) <sub>2</sub>		2.77		42
		2.74		
		2.67		
		2.71		
EDT-PDT(CH <sub>2</sub> OH) <sub>2</sub> TTF	1.85	2.88	170	39
	1.76	2.72	159	
TTF(HET) <sub>4</sub> (MeOH) <sub>2</sub>	1.92	2.65	152	43
	2.05	2.75	165	
	1.70	2.70	161	
TTF(SCH <sub>2</sub> CH <sub>2</sub> OCH <sub>2</sub> CH <sub>2</sub> OH) <sub>4</sub>	1.88	2.65	165	43
	1.95	2.67	174	

molecule TTF-CMe(OH)Fc (Fc = ferrocenyl)<sup>38</sup> shown in **2.8** (the ferrocenyl moieties attached to the darkened carbon atoms have been omitted) is dominated by a four-point intermolecular weak hydrogen-bonded tetramer where the four hydroxyl groups are simultaneously hydrogen bond donors and acceptors.



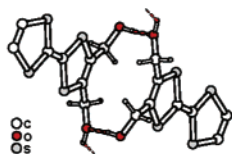
2.8

A similar tetrameric arrangement shown in **2.9** is observed in the ethylenedithio[2,2-bis(hydroxymethyl)propylenedithio]tetrathiafulvalene, EDT-PDT-(CH<sub>2</sub>OH)<sub>2</sub>TTF, where it develops along the *a* direction, stabilizing infinite ribbons of donor molecules and a clear segregation of hydrophobic and hydrophilic moieties.<sup>39</sup>

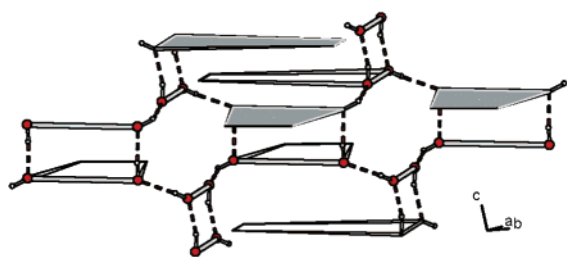


2.9

Among primary alcohol derivatives, a *tour de force* by Bryce et al., who were able to obtain and solve the disordered 150 K single-crystal structure of the *o*-bis(hydroxymethyl)-TTF also bearing two *ortho-n*-hexylthio groups, [HexS]<sub>2</sub>TTF(CH<sub>2</sub>OH)<sub>2</sub>,<sup>40</sup> provides an interesting and seemingly complex architecture, based on the elementary bimolecular building block shown in **2.10**. This precise hydrogen bond motif directs the planar [···(S)(S)-TTF-(O)(O)···] units (symbolized by distorted rectangles in **2.11**, three of which are darkened) to be orthogonal to each other.

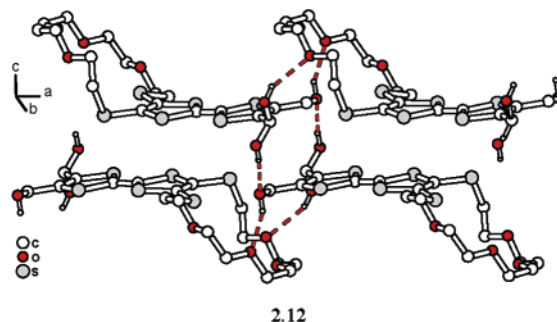


2.10



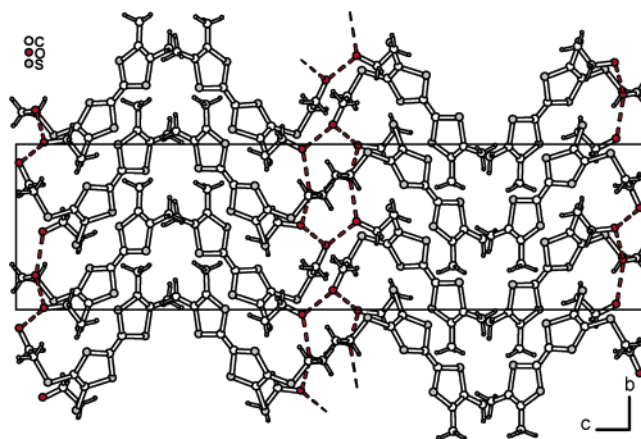
2.11

A similar motif was not encountered in the analogous crown-ether annelated, bis(hydroxymethyl)-TTF,<sup>41</sup> [-S(CH<sub>2</sub>CH<sub>2</sub>O)<sub>4</sub>CH<sub>2</sub>CH<sub>2</sub>S-]TTF(CH<sub>2</sub>OH)<sub>2</sub>, where one of the hydroxyl group is disordered and two of the three are engaged in O-H···O hydrogen bonds with the oxygen atoms of the crown-ether moiety, as shown in **2.12**.



2.12

With longer, flexible arms such as in *o*-Me<sub>2</sub>TTF-(HET)<sub>2</sub> (HET = (2-hydroxyethyl)thio), two crystallographically independent molecules bring four OH groups as hydrogen bond donors and acceptors.<sup>42</sup> Despite the fact that hydrogen atoms could not be identified, the short O···O distances unambiguously qualify the infinite chains of O-H···O hydrogen bonds shown in **2.13**, stabilizing a segregation of the rigid [*o*-Me<sub>2</sub>TTF] fragments from the alkyl chain layers.



2.13

In the methanol solvate TTF(HET)<sub>4</sub>·MeOH,<sup>43</sup> the molecule acts as a tetrafold hydrogen bond donor, toward the oxygen atoms of two neighboring molecules and of two MeOH solvent molecules, and as a tetrafold hydrogen bond acceptor, giving rise to the formation of ribbons running along the *c*-axis, connected to each other along *b* via the MeOH molecules (**2.14**). Combined with the outer thioalkyl chains' van der Waals affinity, this makes for a two-dimensional hydrophilic-hydrophobic partition and the formation of TTF stacks, with a short interplanar distance (3.36 Å) and strong S···S van der Waals interactions. The same principle of construction holds with longer arms<sup>45</sup> as in TTF[S(CH<sub>2</sub>)<sub>2</sub>O(CH<sub>2</sub>)<sub>2</sub>OH]<sub>4</sub>, where both intramolecular and intermolecular hydrogen bonds are identified between the outer hydroxyl proton

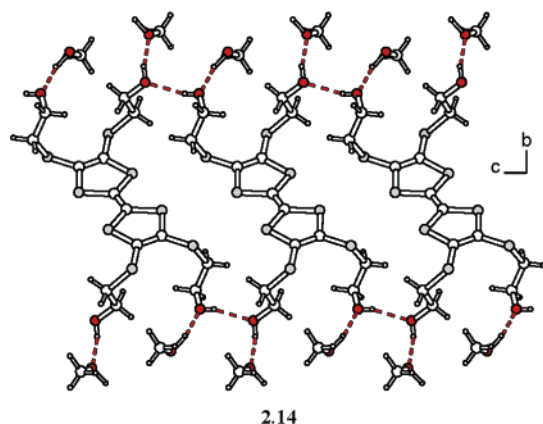


**Table 4. Structural Characteristics of Hydrogen Bonds in Radical Cation Salts of Hydroxylated Tetrathiafulvalenes Together with the Degree of Charge Transfer ( $\rho$ ) and the Room Temperature Conductivity ( $\sigma_{RT}$ ) and Its Temperature Behavior**

compound	H $\cdots$ X (Å)	O $\cdots$ X (Å)	O–H $\cdots$ X (deg)	$\rho$	$\sigma_{RT}^a$ (S cm $^{-1}$ )	ref
(EDT-TTF–CH $_2$ OH) $_2$ ClO $_4$		3.33		0.5	3	44
(EDT-TTF–CH $_2$ OH) $_2$ ReO $_4$		3.33		0.5	0.3	44
[Me $_3$ TTF–CHMe(OH)][TCNQ]	2.12 (N)	3.24	154	1	(insul)	45
(Me $_3$ TTF–CH $_2$ OH) $_2$ (Mo $_6$ O $_{19}$ )		2.78–3.05		1	(insul)	46
[EDT-TTF(CH $_2$ OH) $_2$ ] $_2$ (Mo $_6$ O $_{19}$ )		2.60–2.96		1	(insul)	46
[TTF(CH $_2$ OH) $_4$ ] $_2$ (Mo $_6$ O $_{19}$ )	1.93 (O)	2.74	166	1	(insul)	46
	1.98 (O)	2.78	165			
	2.06 (O)	2.87	173			
	2.14 (O)	2.89	154			
[BEDT-TTF(CH $_2$ OH) $_2$ ] $_2$ Cl	2.31 (Cl)	3.12	169	0.5	0.1	47
	2.34 (Cl)	3.16	173		(semicond)	
	2.31 (Cl)	3.10	160			
[EDT-PDT(CH $_2$ OH) $_2$ TTF] $_2$ I $_3$	1.85 (O)	2.66	163	0.5	3	39
	1.88(O)	2.71	167		(metal,	
	1.87 (O)	2.73	179		$T_{MI} = 235$ K)	
	1.90 (O)	2.74	179			
[ <i>o</i> -Me $_2$ TTF(SCH $_2$ CH $_2$ OH) $_2$ ] $_2$ Br	2.18 (Br)	3.21	171	1	$5 \times 10^{-4}$	42,49
	2.50 (Br)	3.24	162			
[TTF(SCH $_2$ CH $_2$ OH) $_4$ ] $_2$ BF $_4$	2.14 (F)	2.93	160	1		50
	2.09 (O)	2.89	166			
	1.93 (O)	2.75	174			
	2.10 (F)	2.87	157			

<sup>a</sup>  $T_{MI}$  = metal–insulator transition temperature.

donors and the outer oxygen atom acceptors. Thus, the hydrophilic–hydrophobic partition forces the TTF cores to stack deep within the hydrophobic region of the two-dimensional structure with again a short plane-to-plane distance (3.40 Å).

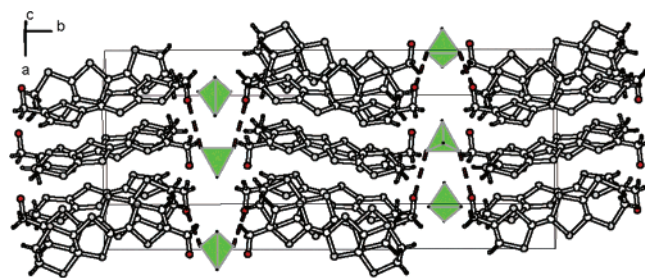


### 2.1.3. Radical Cation Salts of Hydroxylated Tetrathiafulvalenes

Only a few radical cation salts of hydroxylated TTF have been described so far, either with hydroxymethyl groups directly linked to the TTF core or with longer, flexible (2-hydroxyethyl)thio substituents (HET

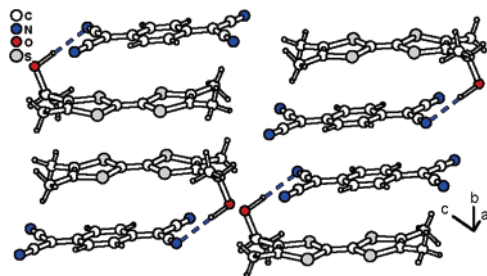
= –S–CH $_2$ CH $_2$ –OH). These salts are collected in Table 4 together with the hydrogen bonds' geometrical characteristics. Here, the counterions are expected to act as hydrogen bond acceptors to form OH $\cdots$ X $_{anion}$  interactions, in competition with the oxygen atom of the OH group(s), as indeed identified in every structure available.

[EDT-TTF(CH $_2$ OH) $_2$ ] $_2$ ClO $_4$  and [EDT-TTF(CH $_2$ OH) $_2$ ] $_2$ ReO $_4$  are early, seminal examples of structure-directing, “interfacial” cation–anion hydrogen-bonded association deliberately engaging functionalized TTFs.<sup>44</sup> The structure is dominated by the formation of orthogonal mixed-valence dimers and the  $\kappa$ -topology (see Scheme 2) of the radical cation layers illustrated in **2.15**, which also displays the single O–H $\cdots$ O–ClO $_3$  hydrogen bond identified. However, the fact that the hydroxyl hydrogen atom could not be located and the long O $\cdots$ O distance (3.33 Å) preclude any further meaningful interpretation of the strength of this interaction. While the band structure and topology of the Fermi surface are those of a metal, the conductivity of both salts is activated and amounts to 3.0 and 0.3 S cm $^{-1}$ , respectively. Application of hydrostatic pressure does not restore a metallic character, suggesting that these  $\kappa$ -phases lie at the borderline of the localized and delocalized descriptions of their electronic structures.



2.15

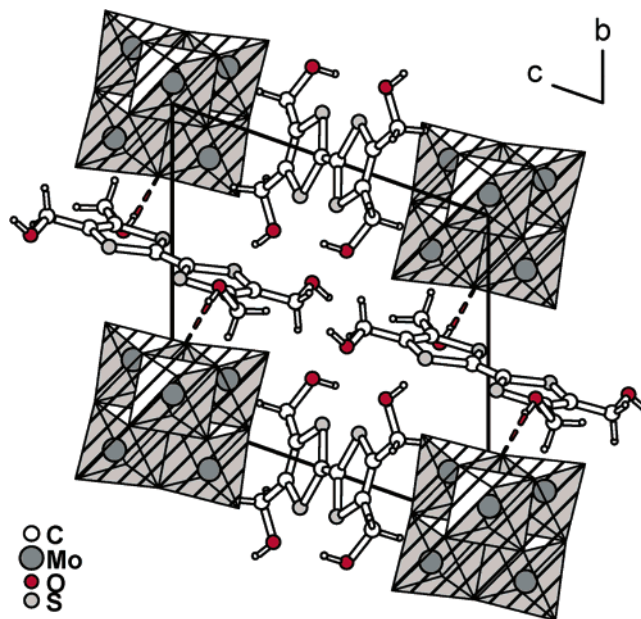
The 1:1 TCNQ salt of the racemic, tertiary alcohol,  $(\pm)\text{Me}_3\text{TTF}-\text{C}^*\text{H}(\text{Me})\text{OH}$ , crystallizes into one-dimensional chains of successive pairs of electron-donating and electron-accepting molecules extending along [110], as shown in **2.16**.<sup>45</sup> Note that the hydroxyl group is engaged in a weak, intrastack,  $\text{O}-\text{H}\cdots\text{N}\equiv\text{C}$  hydrogen bond ( $\text{H}\cdots\text{N} = 2.12 \text{ \AA}$ ,  $\text{O}(-\text{H})\cdots\text{N} = 3.24 \text{ \AA}$ ,  $\text{O}-\text{H}\cdots\text{N} = 154^\circ$ ) with a cyano group of TCNQ rather than with the hydroxyl oxygen atom.



2.16

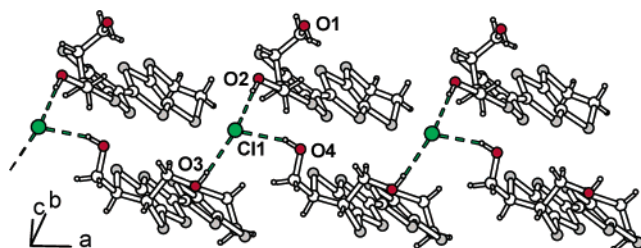
A set of three fully oxidized, radical cation salts with the Linquist anion  $\text{Mo}_6\text{O}_{19}^{2-}$ , namely,  $[\text{Me}_3\text{TTF}(\text{CH}_2\text{OH})_2\text{Mo}_6\text{O}_{19}]$ ,  $[\text{EDT-TTF}(\text{CH}_2\text{OH})_2\text{Mo}_6\text{O}_{19}]$ , and  $[\text{TTF}(\text{CH}_2\text{OH})_4\text{Mo}_6\text{O}_{19}]$ , were prepared by electrocrystallization of the corresponding hydroxymethyl TTF derivatives and analyzed with an eye on how the hydroxyl groups of the functionalized  $\pi$ -radicals interact with oxygen atoms paving the surface of such polyoxometalate anions.<sup>46</sup> For  $[\text{Me}_3\text{TTF}(\text{CH}_2\text{OH})_2\text{Mo}_6\text{O}_{19}]$  and  $[\text{EDT-TTF}(\text{CH}_2\text{OH})_2\text{Mo}_6\text{O}_{19}]$ , the  $\text{CH}_2\text{OH}$  groups are disordered over several positions in the lattice and no clear hydrogen bond pattern is identified. In  $[\text{TTF}(\text{CH}_2\text{OH})_4\text{Mo}_6\text{O}_{19}]$ , however, two discrete, independent radical cations, each located on an inversion center, are fully ordered and establish a network of  $\text{O}-\text{H}\cdots\text{O}$  hydrogen bonds where three OH groups act as hydrogen acceptors and one OH group acts as a hydrogen bond donor selectively directed toward a bridging rather than a terminal oxygen atom at the polyoxometalate anion surface, as shown in **2.17**. It is remarkable that up to four  $\text{O}-\text{H}$  hydrogen bond donors have to be engaged per electron-donating molecule in order to provide sufficient net intermolecular interaction energy to prevent the formation of the strongly coupled, diamagnetic radical cation dimers observed in  $[\text{Me}_3\text{TTF}(\text{CH}_2\text{OH})_2\text{Mo}_6\text{O}_{19}]$  and  $[\text{EDT-TTF}(\text{CH}_2\text{OH})_2\text{Mo}_6\text{O}_{19}]$ . Note in addition that, in  $[\text{TTF}(\text{CH}_2\text{OH})_4\text{Mo}_6\text{O}_{19}]$ , the strongest hydrogen bond is formed with the oxygen atom common to two

$\text{MoO}_6$  octahedra, that is, the most electronegative oxygen atom and strongest hydrogen bond acceptor, as demonstrated by ab initio calculations of the distribution of electrostatic potentials in the vicinity of the Linquist anion.



2.17

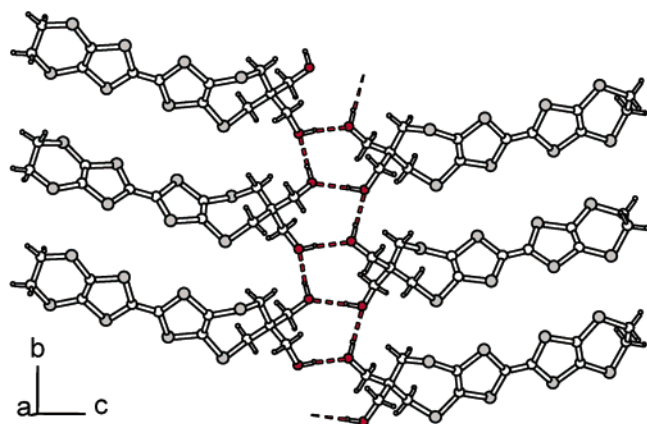
In  $[\text{BEDT-TTF}(\text{CH}_2\text{OH})_2\text{Cl}]$ ,<sup>47</sup> only three (O2–O4) out of the four crystallographically independent hydroxyl groups are hydrogen bonded to the chloride anion (**2.18**). The geometrical characteristics (Table 4) compare very well with the  $\text{O}-\text{H}\cdots\text{Cl}$  statistical values established with water molecules for the  $\text{HO}-\text{H}\cdots\text{Cl}^-$  interaction ( $2.10 < 95\%$  of  $\text{H}\cdots\text{Cl}$  distances  $< 2.46 \text{ \AA}$ ,  $3.06 < 95\%$  of  $\text{H}\cdots\text{Cl}$  distances  $< 3.38 \text{ \AA}$ )<sup>23,48</sup> which makes for a strong organic-inorganic interface. Despite its 2:1 stoichiometry and mixed valence character, the salt is a semiconductor, with  $\sigma_{\text{RT}} = 0.1 \text{ S cm}^{-1}$  and an activation energy of  $0.25 \text{ eV}$ .



2.18

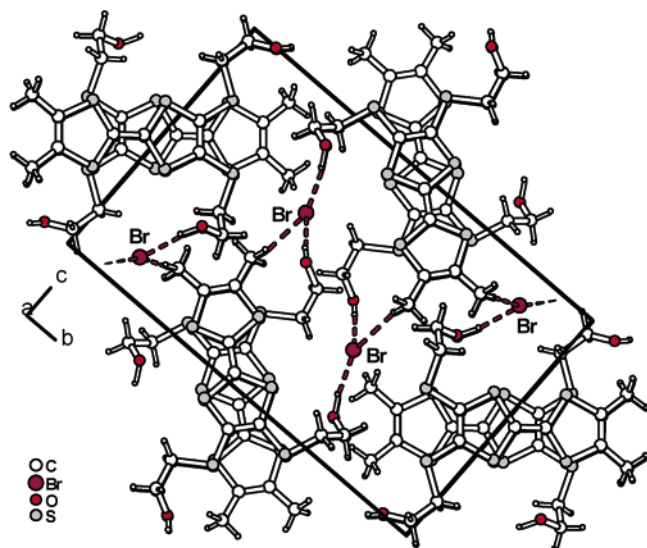
In the metallic 2:1  $\text{I}_3^-$  salt of another bis-hydroxylated donor molecule, ethylenedithio(2,2-bis(hydroxymethyl)propylenedithio)tetrathiafulvalene, the partially oxidized EDT-PDT( $\text{CH}_2\text{OH}$ )<sub>2</sub>TTF donor molecules are hydrogen bonded to each other (**2.19**) to form infinite chains running along  $b$  while no hydrogen bonds to the  $\text{I}_3^-$  anion can be identified.

On the other hand, the single bromine atom in the 1:1  $[\text{o-Me}_2\text{TTF}(\text{HET})_2]\text{Br}$  salt<sup>49</sup> accepts two strong hydrogen bonds from the  $\text{O}-\text{H}$  donors of two radical



2.19

cations and a weaker one from a methyl  $C_{sp^3}$ -H donor of a third molecule, as illustrated in **2.20**. Notice that the long molecular axes of the three molecules associated with this set of three-point hydrogen bonds are all parallel. This leaves another equivalent set of two O-H donors and one C-H donor per cluster of three molecules which forms the very same three-point hydrogen bond motif around another bromine atom, as shown in **2.20**. Note that the common direction of the long molecular axes is now orthogonal to that of the former cluster, a consequence of the glide plane along *c*.



2.20

Finally, in the 1:1  $BF_4^-$  salt of the tetrakis-(hydroxyethylthio)-TTF,<sup>50</sup>  $[TTF(HET)_4]BF_4$ , each of the four OH groups is hydrogen bonded, two with oxygen atoms of neighboring molecules and two with fluorine atoms of the  $BF_4^-$  counterion with O-H...F geometrical characteristics in the range of the statistical mean values reported for HO-H...F- $BF_3^-$  ( $H\cdots F = 2.1 \text{ \AA}$ ,  $O\cdots F = 2.94 \text{ \AA}$ ).<sup>23</sup>

In sum, hydroxylated TTFs are engaged in only weak interactions with hydrogen bond acceptors such as  $ClO_4^-$ ,  $ReO_4^-$ ,  $TCNQ^-$ , or  $Mo_6O_{19}^{2-}$  and in stronger interactions with the  $BF_4^-$ ,  $Cl^-$ , or  $Br^-$  anions. This calls for further investigations, particularly

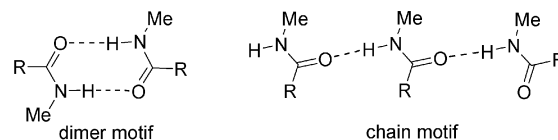
engaging comparatively rigid molecules such as EDT-TTF- $CH_2OH$ , for example. Of particular note are  $(EDT-TTF-CH_2OH)_2ClO_4$  and  $(EDT-TTF-CH_2OH)_2ReO_4$ , which were purposely prepared to form a directional, hydrogen-bonded interface between the organic and inorganic fragments compatible with the formation of an organic slab with adequate band structure and Fermi surface topology, albeit its predictability is hampered by the many possible orientations and subsequent disorder of the  $CH_2OH$  moiety relative to the redox core. A stronger control of the organic-inorganic interface is expected when TTF amides and thioamides are engaged, as described below in section 2.2.

## 2.2. Amides and Thioamides (NH Donor)

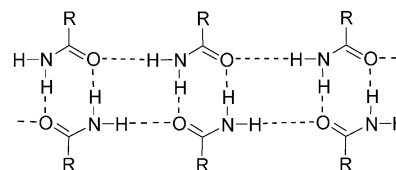
The rigidity and dual character of primary and secondary amides are known to direct the formation of self-complementary, extended N-H...O=C hydrogen bond motifs (Chart 3).<sup>51,52,53</sup> Elaborating upon

### Chart 3

Secondary amides



Primary amides: combining dimer and chain motifs



those elements of predictability, the amide linkage<sup>54</sup> has been actively used in molecular crystal chemistry and qualified as an efficient tool for the generation of extended hydrogen-bonded networks<sup>55,56</sup> as well as supramolecular complexes.<sup>57</sup> Therefore, amide functionalization of the TTF core is expected to yield a rich crystal chemistry for both neutral and oxidized forms alike, by balancing competing requirements such as hydrogen-bonding, van der Waals, and SOMO...SOMO overlap interactions. The structures and hydrogen-bonding patterns of neutral TTF amides, together with several thioamides, will be described first in section 2.2.1, and their geometrical characteristics are collected in Table 5. The different salts derived from those amide-functionalized TTFs, essentially obtained by electrocrystallization, are described and analyzed in section 2.2.2.

### 2.2.1. Neutral Amide and Thioamide Tetrathiafulvalenes

In EDT-TTF(SMe)(SCH<sub>2</sub>CONH<sub>2</sub>), the amidic function is linked to the TTF core by a flexible SCH<sub>2</sub> spacer.<sup>58</sup> The amidic group forms a strong, one-dimensional, self-complementary hydrogen-bonded chain motif running along *b* which leaves one NH function uncoordinated (**2.21**). On the other hand, one of the hydrogen atoms of the methylenic group,

**Table 5. Structural Characteristics of Hydrogen Bonds in Neutral Tetrathiafulvalene Amides<sup>a</sup>**

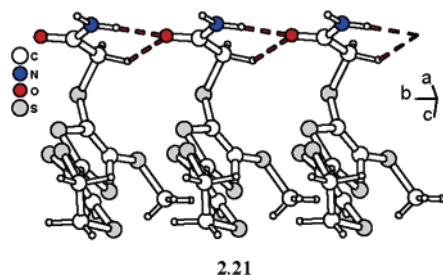
compound	H...O (Å)	N...O (Å)	N-H...O (deg)	ref
<b>Primary amides</b>				
EDT-TTF(SMe)(SCH <sub>2</sub> CONH <sub>2</sub> )	1.88	2.81	175	58
	<i>2.34</i>	<i>3.32</i>	<i>138</i>	
EDT-TTF-CONH <sub>2</sub>	2.13	2.98	172	59
	<i>2.32</i>	<i>3.06</i>	<i>144</i>	
	<i>2.03</i>	<i>2.87</i>	<i>166</i>	
	<i>2.14</i>	<i>2.88</i>	<i>145</i>	
	<i>2.73</i>	<i>3.44</i>	<i>134</i>	
	<i>2.77</i>	<i>3.32</i>	<i>118</i>	
EDT-TTF(CONH <sub>2</sub> ) <sub>2</sub>	1.93 (intra)	2.74 (intra)	157	61
	2.06	2.91	169	
	2.06	2.90	166	
	2.28	3.06	151	
<b>Secondary amides</b>				
TTF-CONH-Ph•Tol	2.68	3.44	144	63
	<i>2.56</i>	<i>3.38</i>	<i>142</i>	
EDT-TTF-CONH-Me	2.10	2.95	168	59
	<i>2.12</i>	<i>2.95</i>	<i>163</i>	
	<i>2.42</i>	<i>3.32</i>	<i>164</i>	
	<i>2.22</i>	<i>3.13</i>	<i>165</i>	
EDT-TTF-CONH-( <i>p</i> -py)	<i>2.67</i> ( <i>N<sub>Py</sub></i> )	<i>3.54</i> ( <i>N<sub>Py</sub></i> )	<i>157</i>	65
	<i>2.59</i> ( <i>N<sub>Py</sub></i> )	<i>3.48</i> ( <i>N<sub>Py</sub></i> )	<i>153</i>	
	<i>2.29</i> ( <i>O<sub>intra</sub></i> )	<i>2.88</i> ( <i>O<sub>intra</sub></i> )	<i>121</i>	
EDT-TTF-CONH-( <i>m</i> -py)	2.28 ( <i>N<sub>Py</sub></i> )	3.08 ( <i>N<sub>Py</sub></i> )	154	65
	<i>2.46</i> ( <i>N<sub>Py</sub></i> )	<i>3.33</i> ( <i>N<sub>Py</sub></i> )	<i>156</i>	
	<i>2.17</i> ( <i>O<sub>intra</sub></i> )	<i>2.79</i> ( <i>O<sub>intra</sub></i> )	<i>123</i>	
(MeS) <sub>2</sub> TTF-CONH-( <i>m</i> -py)•CH <sub>2</sub> Cl <sub>2</sub>	2.21 ( <i>N<sub>Py</sub></i> )	3.05 ( <i>N<sub>Py</sub></i> )	165	65
	<i>2.46</i> ( <i>N<sub>Py</sub></i> )	<i>3.28</i> ( <i>N<sub>Py</sub></i> )	<i>147</i>	
	<i>2.24</i> ( <i>O<sub>intra</sub></i> )	<i>2.85</i> ( <i>O<sub>intra</sub></i> )	<i>123</i>	
EDT-TTF-CONH-( <i>m</i> -bipy)	2.12 ( <i>N<sub>bipy</sub></i> )	2.90 ( <i>N<sub>bipy</sub></i> )	151	65
	2.81 ( <i>N<sub>bipy</sub></i> )	3.52 ( <i>N<sub>bipy</sub></i> )	142	
	<i>2.31</i> ( <i>O<sub>intra</sub></i> )	<i>2.88</i> ( <i>O<sub>intra</sub></i> )	<i>120</i>	
(MeS) <sub>2</sub> TTF-CONH-( <i>m</i> -bipy)•MeOH	2.02 (Os)	2.96 (Os)	167	65
	2.24 (Os)	3.16 (Os)	167	
	<i>2.39</i> ( <i>O<sub>intra</sub></i> )	<i>2.93</i> ( <i>O<sub>intra</sub></i> )	<i>117</i>	
[(MeS) <sub>2</sub> TTF-CONH] <sub>2</sub> -( <i>m</i> -bipy)•Py <sub>2</sub>	2.21 ( <i>N<sub>Py</sub></i> )	3.05 ( <i>N<sub>Py</sub></i> )	166	65
	<i>2.46</i> ( <i>N<sub>Py</sub></i> )	<i>3.36</i> ( <i>N<sub>Py</sub></i> )	<i>165</i>	
	<i>2.60</i> ( <i>N<sub>Py</sub></i> )	<i>3.89</i> ( <i>N<sub>Py</sub></i> )	<i>142</i>	
	<i>2.29</i> ( <i>O<sub>intra</sub></i> )	<i>3.87</i> ( <i>O<sub>intra</sub></i> )	<i>119</i>	
EDT-TTF(CONH-Me) <sub>2</sub>	1.84 (intra)	2.67 (intra)	160	67
	2.84	3.36	120	
EDT-TTF(CONH-Et) <sub>2</sub>	1.91 (intra)	2.71 (intra)	157	67
	2.10	2.86	147	
EDT-TTF(CONH-Pr) <sub>2</sub>	2.09 (intra)	2.91 (intra)	158	67
	2.22	2.94	142	
EDT-TTF(CONH-Bu) <sub>2</sub>	1.95 (intra)	2.78 (intra)	164	67
	2.00	2.81	157	
EDT-TTF(CONH-Pent) <sub>2</sub>	2.01	2.85	164	67
	1.99	2.84	168	
EDT-TTF(CONH-Bz) <sub>2</sub>	1.94 (intra)	2.74 (intra)	154	67
	2.26	2.87	127	
(1- <i>n</i> -butyluracil-5-yl)-TTF	2.06	2.85	174	70
	<i>2.49</i>	<i>3.35</i>	<i>155</i>	
[(1- <i>n</i> -butyluracil-5-yl)-TTF <sup>•+</sup> ] [cyananilate <sup>-</sup> ]	2.02	2.84	162	70
	1.79 (OH)	2.58 (OH)	146	
<i>o</i> -Me <sub>2</sub> TTF[C(=O)NHC(=O)NH]	1.93	2.85	171	69
	1.76 (DMF)	2.67 (DMF)	173	
<b>Secondary thioamides</b>				
TTF-C(=S)NH-Me	2.91	3.51	138	74
<i>o</i> -Me <sub>2</sub> TTF-C(=S)NH-Me	2.68	3.42	150	72
Me <sub>3</sub> TTF-C(=S)NH-Me	3.18	3.70	123	72
TTF-C(=S)NH-Ph	2.86	3.59	139	77

<sup>a</sup> Values in italics refer to C-H...X interactions.

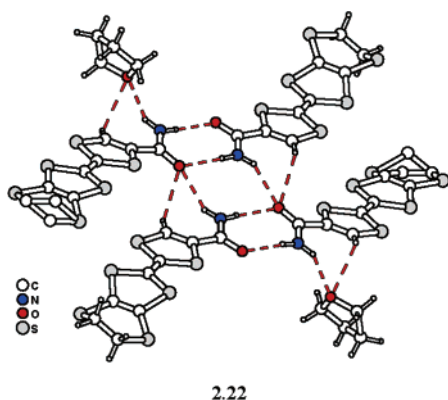
located between the TTF-S and the amidic moiety, also points toward the carbonyl oxygen atom, thus establishing a weak C-H...O hydrogen bond (Table

5). As a consequence, the EDT-TTF moieties also stack along *b*, in sharp contrast with the structures of neutral, nonfunctionalized BEDT-TTF or EDT-

TTF molecules which crystallize into a herringbone pattern of dimers.

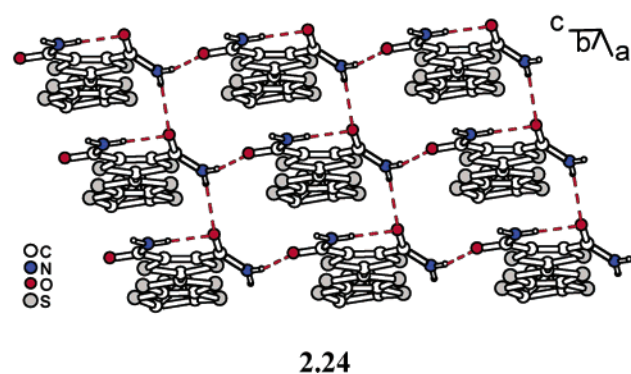
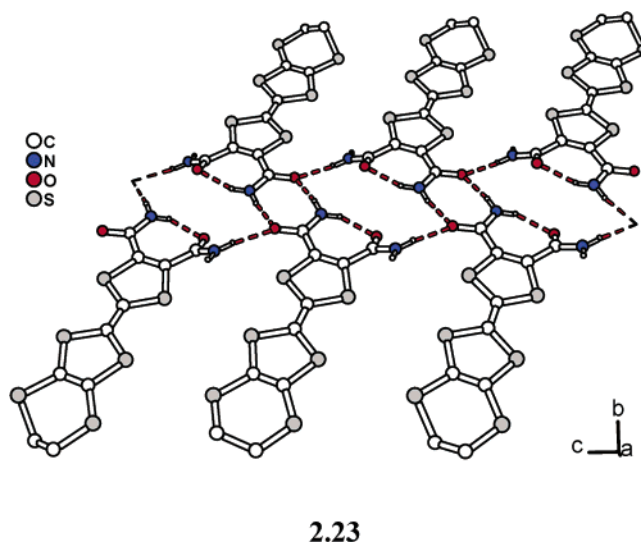


In the solvate EDT-TTF-CONH<sub>2</sub>·THF,<sup>59</sup> there are two crystallographically independent molecules associated by the combination of a eight-membered cyclic motif, further linked two by two, as shown in **2.22**. The two remaining N-H hydrogen atoms are then hydrogen bonded to the THF solvent molecule included in the structure. Notice also the C<sub>ortho</sub>-H group, located *ortho* to the electron-withdrawing amidic function, which is engaged in activated weak C-H···O interactions with both the carbonyl and the THF oxygen atoms. Such activation of the hydrogen bond character of the CH group *ortho* to the conjugated amidic function will emerge as a recurrent, distinctive feature of these EDT-TTF-amides.

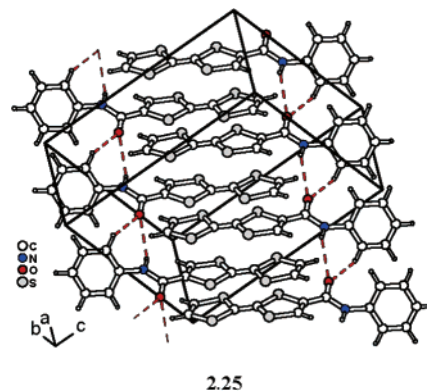


A recent thorough analysis by Allen et al. has revealed that the probability of formation of the cyclic intermolecular eight-membered motif is 80% for monoamide and reaches 95% for diamides.<sup>60</sup> This is indeed verified in EDT-TTF(CONH<sub>2</sub>)<sub>2</sub>, with the only structure reported so far of a tetrathiafulvalene derivative bearing two primary diamides,<sup>61</sup> EDT-TTF(CONH<sub>2</sub>)<sub>2</sub>, where molecules are locked in a closed conformation through an intramolecular N-H···O hydrogen bond and arrange pairwise through the eight-membered cyclic motif. Infinite ribbons running along *c* are constructed out of the dyadic motifs (**2.23**) and further connected along *a* by the fourth N-H group. This neat, topologically precise hydrogen bond network directs the formation of slabs of the β'-type (**2.24**),<sup>62</sup> a rare motif in neutral crystalline TTFs, potentially transposable in the structure of their radical cation slabs, as discussed below.

The very first TTF amide whose structure is available is the secondary amide, TTF-CONHPh, which crystallizes as a toluene solvate (**2.25**).<sup>63</sup> Inversion-related molecules form dimers with ring-over-

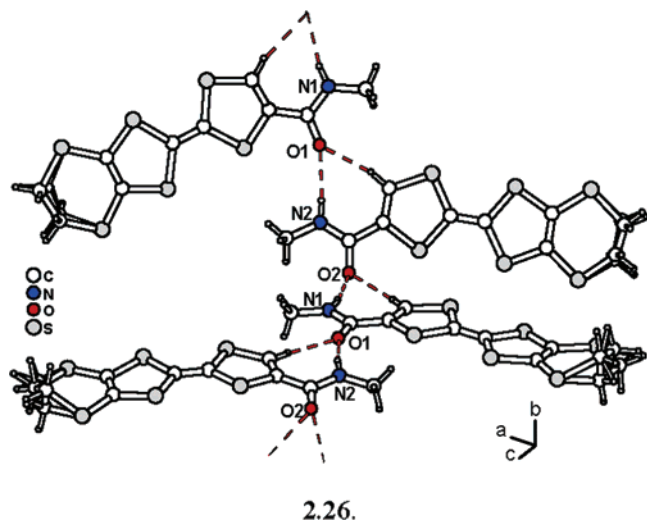


ring overlap (together with a lateral shift of 1.7 Å) and an interplanar distance of 3.75 Å. The N-H···O hydrogen bond is weak and complemented with an even shorter C<sub>phenyl</sub>-H···O interaction. Both contribute to the formation of chains running along *a*.



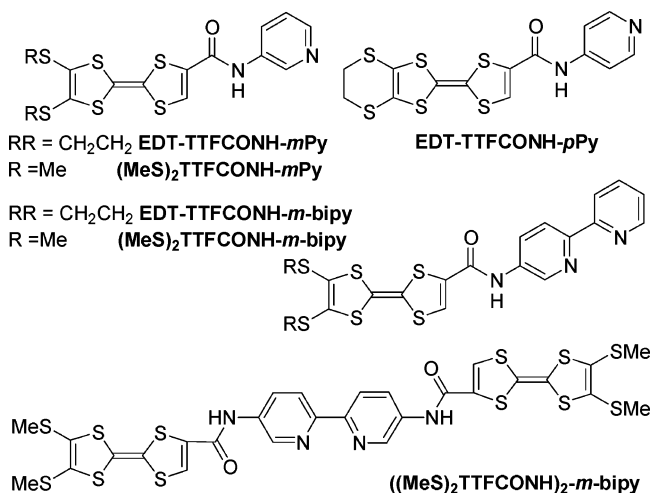
In the other neutral secondary amide described so far, EDT-TTF-CONHMe,<sup>59</sup> a stronger chain motif occurs which involves the participation of the C<sub>sp<sup>2</sup></sub>-H donor located on the TTF core, *ortho* to the electron-withdrawing amidic group (**2.26**). Both N-H···O and C-H···O hydrogen bonds lead to the formation of a cyclic seven-membered motif. A similar motif is found in the X-ray crystal structures of *N*-methylbenzamide<sup>63</sup> or *N*-methylnicotinamide.<sup>64</sup> The latter was also identified earlier in the crystal structure of the primary amide EDT-TTF-CONH<sub>2</sub> and appears as a recurrent motif among aromatic amides. On the other

hand, this strong hydrogen-bonded motif hinders the formation of dimeric TTF moieties, and besides one single short S...S contact at 3.41 Å, all other intermolecular S...S distances exceed 3.70 Å.

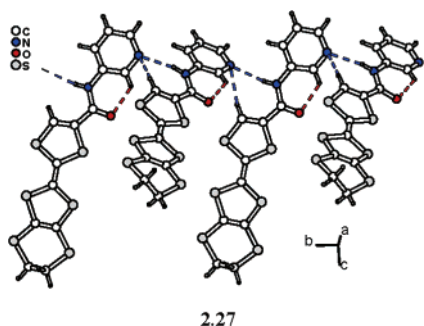


An additional element of complexity was introduced with secondary amides bearing pyridine or 2,2'-bipyridine substituents (Chart 4), as exemplified

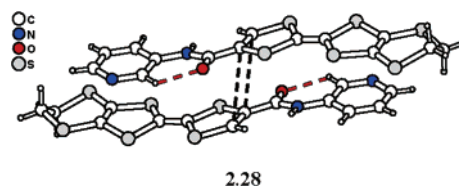
#### Chart 4



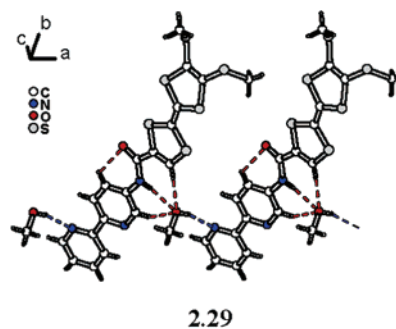
in EDT-TTF-CONH-(*m*-pyridine), where both the amidic N-H and the (TTF)<sub>C<sub>ortho</sub></sub>-H moieties are hydrogen bonded to the nitrogen atom of the pyridine, hence the relative orthogonal orientation of two neighboring molecules in the hydrogen-bonded chain along *b* shown in 2.27.<sup>65</sup>



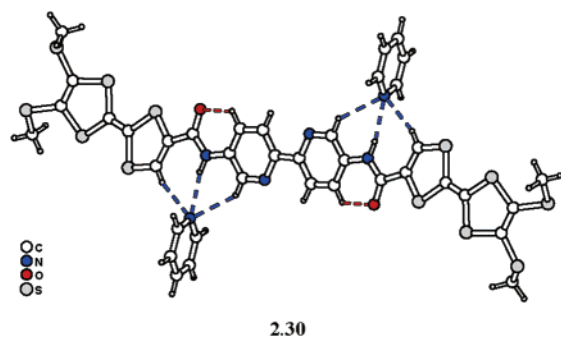
A very similar organization is found in the bis-(methylthio) analogue, (MeS)<sub>2</sub>TTF-CONH-(*m*-pyridine) while no N-H...O or N-H...N hydrogen bonds are identified in its *para* isomer. However, as stated by Desiraju and Steiner,<sup>24</sup> these *intramolecular* short contacts could be only a fortuitous result of stronger intermolecular effects and not a true hydrogen bond interaction, albeit the C-H moiety engaged in this C-H...O interaction is most probably strongly activated by the neighboring sp<sup>2</sup> nitrogen atom. A singular feature of this planar, extended TTF finds its origin in the singular arrangement within the dyads found in the (*a*, *c*) plane (2.28). An inversion-centered motif, stabilized by charge transfer π-π donor-acceptor interactions, forces the outer double bonds of the TTF core to lie above each other at the short separation of 3.51 Å, allowing for a [2 + 2] cyclodimerization to proceed readily upon UV irradiation, an efficient single crystal-to-single-crystal stereospecific reaction with 100% yield.<sup>66</sup>



Three bipyridine amide derivatives are described (Chart 4),<sup>65</sup> with one TTF moiety as in EDT-TTF-CONH-(*m*-bipy) and (MeS)<sub>2</sub>TTF-CONH-(*m*-bipy). In the former, the amidic N-H moiety is now hydrogen bonded to the two nitrogen atoms of the bipyridine fragment and also imposes an orthogonal orientation of two donor molecules, while, in the latter (2.29), an included MeOH molecule interferes in the hydrogen bond network, acting as donor toward the nitrogen pyridine atoms and as acceptor for the amidic N-H.

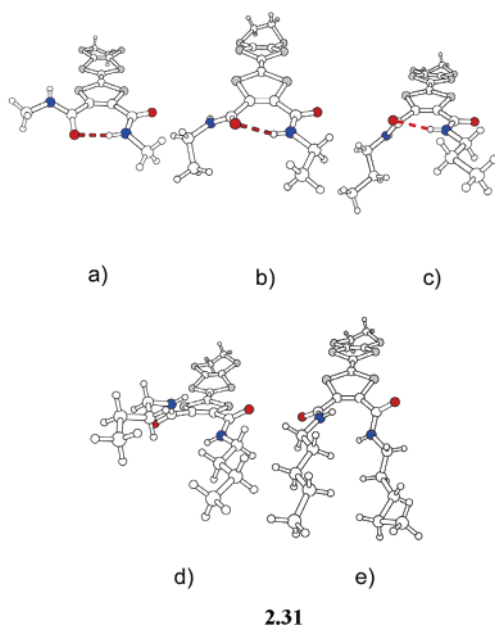


Finally, in [(MeS)<sub>2</sub>TTFCONH]<sub>2</sub>-*m*-2,2'-bipy, one 2,2'-bipyridine linked to two tetrathiafulvalenyl units in the 4,4' positions through amide linkages<sup>65</sup> co-crystallizes with two pyridine molecules to form a trimolecular inversion-centered motif shown in 2.30, where the amidic N-H and both C<sub>bipy</sub>-H and C<sub>ortho</sub>-H donors are hydrogen bonded to the included pyridine molecules. These six examples of tetrathiafulvalenyl amide including pyridine or bipyridine rings present some remarkable features, among them the apparent systematic absence of hydrogen-bonding acceptor character of the carbonyl oxygen atom. However, as shown in the three figures above, in every



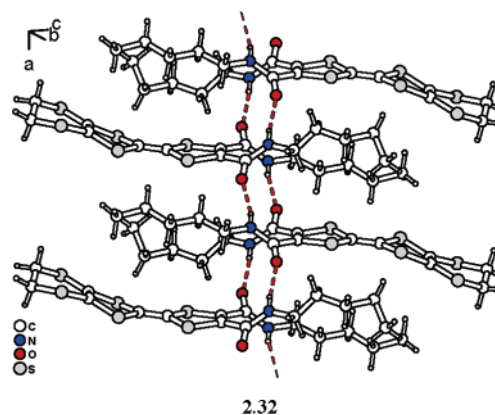
case, the pyridyl ring is found to be constrained to coplanarity with the amidic linkage by a short *intramolecular* C—H...O=C interaction with a C—H group of the pyridine ring, systematically located *ortho* or *para* to the pyridyl nitrogen atom. This intramolecular hydrogen bond, generating six-membered rings, is probably energetically favored despite the acute C—H...O angle observed in every case (Table 5). As a consequence of the carbonyl unavailability, the pyridine or bipyridine nitrogen atoms compete with solvent molecules (MeOH, pyridine) as hydrogen bond acceptors, demonstrating that the former are relatively weak acceptors in that respect, either because of deactivation by the electron-withdrawing amidic substituent or because of steric constraints.

The extensive series of secondary *ortho*-bis(amides) EDT-TTF(CONHR)<sub>2</sub> with R = Me, Et, Pr, Bu, Pent, Hex, and Bz were recently described and characterized.<sup>67</sup> In the neutral monomolecular solids, an intramolecular N—H...O hydrogen bond seals a constrained seven-membered ring for R = Me, Et, Pr (**2.31a–c**), and Bz, which is disrupted, however,



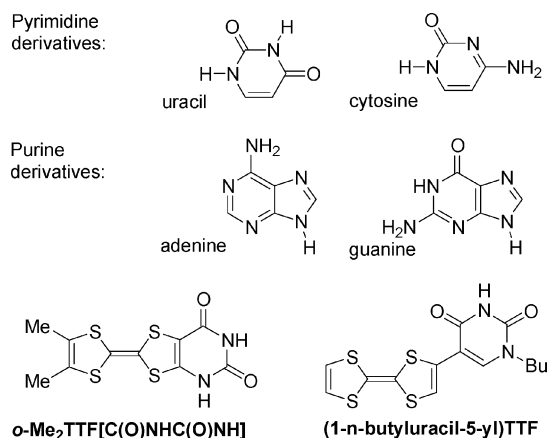
in the case of the pentyl and butyl derivatives (**2.31d–e**) in favor of an antiparallel ladder at the expense of any intramolecular hydrogen bond. A recent Cambridge Structural Database (CSD) search has shown that this kind of intramolecular ring is much less probable than five- or six-membered

rings,<sup>68</sup> mainly because it is constrained and also when the two amides are conjugated through a C=C double bond. The lengthening of the alkyl chain induces the rotation of the carbonyl groups away from the constrained intramolecular seven-membered ring up to the point where the ring is disrupted for the butyl and pentyl derivatives. Hence, within these series, the hydrogen-bonded ring motif proved to be highly sensitive to crystal packing as the decoration with increasingly larger side chains in the neutral solids sacrifices its conformational uniqueness. The open and closed forms of these flexible conjugated secondary *ortho*-diamides are in equilibrium in solution, as demonstrated by NMR experiments, but the possibility that the two forms would crystallize out of the solution as concomitant polymorphs has not been observed. [EDT-TTF(CONHMe)<sub>2</sub>]<sub>2</sub>X salts, X = ClO<sub>4</sub><sup>−</sup> and ReO<sub>4</sub><sup>−</sup>, have vastly different architectures, dimensionalities, and electronic structures, a consequence of the presence of the closed or open structural isomer in one or the other, as described below in section 2.2.2.. Considering now the solid-state organization of the EDT-TTF cores, slightly dimerized stacks are observed with EDT-TTF(CONHMe)<sub>2</sub>, uniform stacks with the ethyl derivative, and stacking, inversion-centered dyads in the propyl and benzyl diamides, stabilized through intradyad hydrogen bonds, while the longer chain butyl and pentyl derivatives (**2.32**) are characterized by a segregation of the EDT-TTF cores and alkyl chains on the one hand and the amidic function on the other hand. Here again, such recurrent one-dimensional structures are far from usual in neutral TTF molecules and demonstrate the efficiency of hydrogen-bonding interactions to cooperate and direct the formation of robust patterns in the solid state.

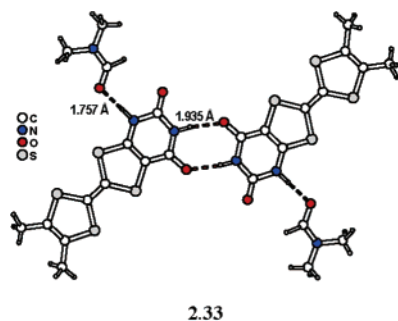


As constituents of the nucleic acids, the four bases derived from purine and pyrimidine, that is, uracil, guanine, cytosine, and adenine, are conjugated planar systems (Chart 5). As a consequence, the exocyclic C=O and NH<sub>2</sub> groups exhibit geometrical characteristics indicating partial double bond character, and specifically, the exocyclic NH<sub>2</sub> groups are never acting as hydrogen bond acceptors. Because of this aromatic character, however,  $\pi$ -bond cooperativity enhances hydrogen-bonding forces and leads to cyclic or chain motifs similar to those observed with secondary amides.

## Chart 5

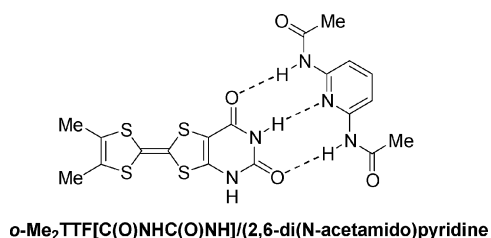


Two tetrathiafulvalenes bearing an uracil moiety have been described (Chart 5), either fused on the TTF core as in  $o$ -Me<sub>2</sub>TTF[C(=O)NHC(=O)NH]<sup>69</sup> or linked to the TTF core as in (1-*n*-butyluracil-5-yl)-TTF.<sup>70</sup> In the former, of the two N–H available for hydrogen bonding, one engages into the dimeric eight-membered cyclic motif while the other interacts strongly with a DMF solvate molecule, as shown in **2.33**.



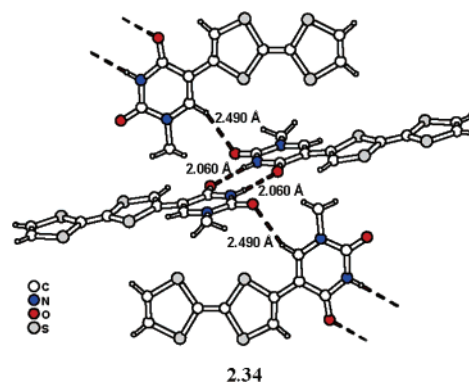
The very low solubility of this singular electron-donating molecule has yet precluded the isolation of oxidation products, either chemically or electrochemically. Notice, however, that addition of the complementary 2,6-di(*N*-acetamido)pyridine (Chart 6) in

## Chart 6

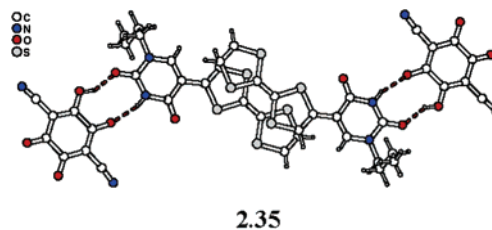


solutions of  $o$ -Me<sub>2</sub>TTF[C(=O)NHC(=O)NH] produces a positive shift of the  $E_{1/2}$ <sup>1</sup> redox potential of the TTF core of 30 mV,<sup>71</sup> a likely consequence of the efficient recognition process.

A more soluble derivative was found by Morita in (1-*n*-butyluracil-5-yl)-TTF (Chart 5), a consequence of the presence of one butyl group, which also leaves one N–H group only for hydrogen bonding. As a consequence, a single homo inversion-centered dimer is formed. Notice in **2.34** that the “uncomplexed” carbonyl group is in fact engaged in a C–H···O

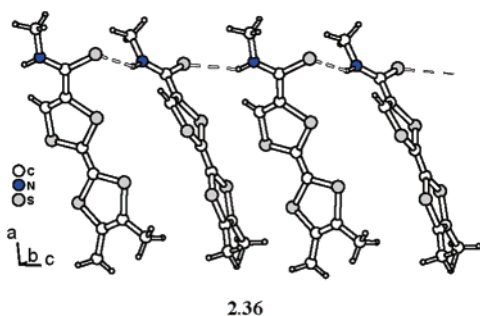


hydrogen bond with the free C–H group of the uracil function, thus orienting the dimer pairs perpendicular to each other. The structure of one salt of (1-*n*-butyluracil-5-yl)-TTF with the cyananilate anion (**2.32**) is available and will be described here to allow an immediate comparison with that of the neutral donor molecule. It combines the requirements of both the overlap of open-shell TTF<sup>+</sup> moieties and hydrogen bonding of the uracil group with the complementary cyananilate anion. As shown in **2.35**, two TTF<sup>+</sup> moieties are associated into a ring-over-ring dicationic motif with a short interplanar distance (3.56 Å), hence the insulating character of the salt, while each uracil moiety is hydrogen bonded to an cyananilate anion through strong N–H···O and O–H···O interactions (see Table 5).



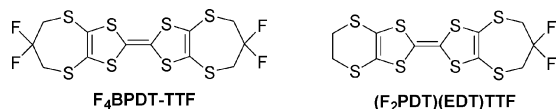
The hydrogen bond acceptor character of the thiocarbonyl function in thioamides is weaker than that of C=O in classical amides.<sup>24</sup> Thereby, the cyclic eight-membered dimer motif found with amides is usually also observed in thioamides with an increase of the hydrogen bond length by up to 0.5 Å. Also, a sharper, more directional O(N)–H···S=C hydrogen bond occurs toward lone pairs with a preference for H···S=C angles around 110°, rather than 120–130° with amides. None of the four neutral TTF thioamides described by Bryce adopt the cyclic eight-membered dimer motif, but they rather adopt the chain motif shown in **2.36** for  $o$ -Me<sub>2</sub>TTF–C(S)NHMe, where hydrogen bond distances<sup>72</sup> (Table 5) compare with the mean geometries determined from statistical studies [(N–)H···S(=C) = 2.51(1) Å, N···S(=C) = 3.43(1) Å, N–H···S = 134(1)°].<sup>73</sup> A very similar organization is found for TTF–C(S)NHMe<sup>74</sup> and Me<sub>3</sub>TTF–C(S)NHMe<sup>72</sup> but with much weaker interactions. In the three compounds, the TTF moieties arrange into face-to-face dimers, further packed into a  $\kappa$  fashion, a very rare arrangement among crystalline neutral TTF derivatives.<sup>75,76</sup> On the other hand, in the aniline derivative,<sup>77</sup> TTF–C(S)NH–Ph, molecules typically stack on top of each other in a head-to-tail fashion.



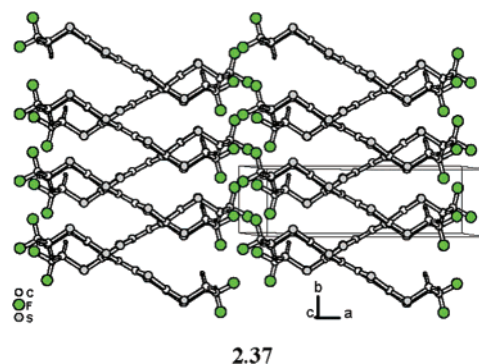


Several observations emerge from the analysis of the 23 different structures of neutral primary and secondary amides described above. First of all, in most instances, directional hydrogen bonding is established whose geometrical characteristics compare well with the literature data. In other words, tetrathiafulvalenyl amides are amides in their own right. Also, the hydrogen bond network involves almost invariably all available donor and acceptor functionalities, exemplifying the synergistic effect of packing and hydrogen bonding underlined by Hagler and Leiserowitz.<sup>78</sup> Indeed, among the several possible packing arrangements, the one chosen corresponds to a situation where all the donor and acceptor functionalities are satisfied. Such synergistic hydrogen bond associations effectively direct the way these functionalized TTFs organize in the solid state. Recall in that respect that tetrathiafulvalene derivatives often crystallize into a herringbone fashion or into a herringbone arrangement of face-to-face dimers. Clearly, here, one observes recurrent low-dimensional structures such as stacks or  $\beta'$  or  $\kappa$  slabs (see Scheme 2 in section 1.3 for definitions), typically found in radical cation salts instead. Similar effects were already observed in the hydroxyl derivatives described in section 4.1.2, indicating a probable common origin. The van der Waals interaction energy is the change in self-energy of two atoms as a function of their separation. Van der Waals forces are sensitive to interfacial geometry and curvature and play a major role at the mesoscopic length scale in the dynamics of small, self-assembled confining systems.<sup>79–81</sup> Therefore, molecular similarity is an important factor in the dynamics of the complex process which directs intermolecular interactions and achieves solid-state architectures. Hence, introduction of increments of dissimilarity—such as the hydrophilic  $\text{CH}_2\text{OH}$  or  $\text{C}(=\text{O})\text{NHR}$  moieties on an otherwise sulfur-rich core—is likely to perturb the molecular recognition and generate interfaces where hydrophilic–hydrophobic segregation effects play a significant role. The herringbone pattern of association, which in essence is of three-dimensional character, does not easily allow for such segregation, contrary to the one- or two-dimensional structures observed above. Similar effects were identified in a series of fluorinated tetrathiafulvalenes<sup>76</sup> (Chart 7) where the van der Waals balance between the lipophilic sulfur-

Chart 7

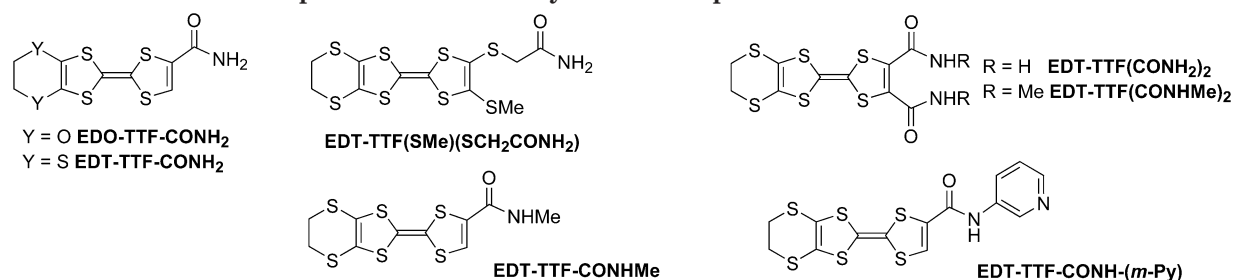


rich TTF core and super-lipophilic  $\text{CF}_2$  moieties also constrains the structures to adopt layered architectures, such as the parallel uniform stacks with  $\text{F}_4\text{BPDT-TTF}$  shown in **2.34** or  $\kappa$ -type slabs with  $(\text{F}_2\text{PDT})(\text{EDT})\text{TTF}$ , with a strong, efficient segregation of antagonist molecular fragments. These observations also demonstrate that the introduction on the TTF core of ancillary groups able to discriminate the space through hydrophilic–lipophilic interactions is a highly efficient tool for enforcing  $\pi$ – $\pi$  stacking between *neutral* TTF moieties, at the expense of the usual three-dimensional herringbone pattern, a result of strong interest in the design of crystalline thin films for transistor devices.<sup>82</sup> A systematic investigation of the interplanar distances should allow for a selection of the best candidates for producing high quality thin films with high intralayer mobilities.



### 2.2.2. Radical Cation Salts of Amide and Thioamide Tetrathiafulvalenes

Textbook examples of the complex interdependence between (i) the templating effect of the anions, (ii) the competing hydrogen-bonding interactions, (iii) the overlap interactions of the open-shell species, and (iv) the redox tuning of the activation–deactivation of the hydrogen-bonding capabilities of the functionalized TTF cores are provided by the two salts  $[\text{EDT-TTF-CONH}_2]_6\text{AsF}_6$  and  $[\text{EDT-TTF-CONH}_2]_2\text{ReO}_4$ .<sup>83</sup> Consider first the structure of the 6:1  $[\text{EDT-TTF-CONH}_2]_6\text{AsF}_6$  salt, shown in **2.38** and **2.39**. Three crystallographically independent donor molecules form singly oxidized  $(\text{BCA}^+\text{ACB})^+$  centrosymmetrical hexameric units, found to cluster around two independent threefold symmetry sites both occupied by  $\text{AsF}_6^-$  anions. Note that the two  $\text{AsF}_6^-$  are selectively encapsulated either by hydrophobic  $\text{CH}_2\text{CH}_2$  groups or by hydrophilic  $\text{CONH}_2$  functions, an illustration of the templating effect of the octahedral anion and the ambivalent character of fluorides, which adjust to both environments. On the basis of the evolution of intramolecular bond lengths in the TTF core, molecules **B** and **C** are identified as neutral while **A** is partially oxidized, hence the  $(\text{A}_2)^+(\text{B}^0)_2(\text{C}^0)_2(\text{AsF}_6^-)$  formulation. Focus now on **2.39** on the hydrophilic pocket and its network of donor–anion  $\text{N-H}\cdots\text{F}$  hydrogen bonds complemented by donor–donor  $\text{N-H}\cdots\text{O}$  hydrogen bonds (Table 6). While the carbonyl groups of the neutral molecules **B** and **C** act as hydrogen bond acceptors to form the seven-membered cyclic motif involving both  $\text{N-H}$  and  $\text{C}_{\text{ortho}}\text{-H}$  moieties, the carbonyl function of the par-

**Table 6. Structural Characteristics of Hydrogen Bonds in Radical Cation Salts of Tetrathiafulvalenyl Amides Together with the Room Temperature Conductivity and Its Temperature Behavior<sup>a</sup>**

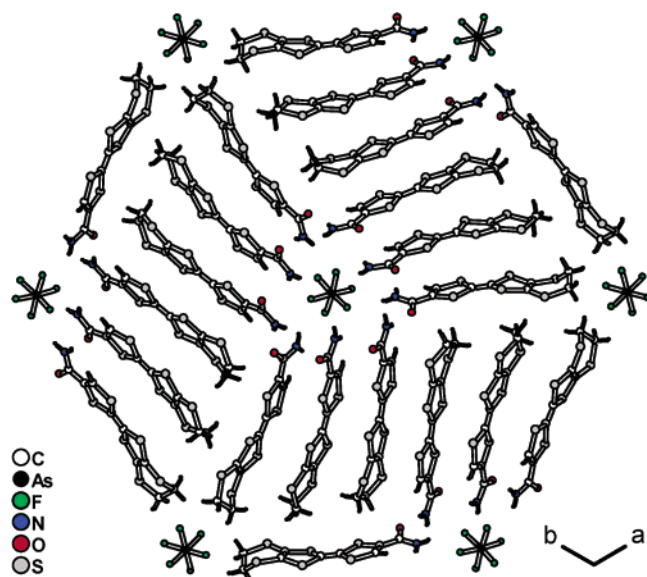
salt	H...X (Å)	N...X (Å)	N-H...X (deg)	$\sigma_{RT}^b$ (S cm <sup>-1</sup> )	ref
(EDT-TTF-CONH <sub>2</sub> ) <sub>6</sub> AsF <sub>6</sub> A <sup>+0.5</sup>	2.06 (O <sub>B</sub> ) 2.61 (O <sub>B</sub> )	2.78 (O <sub>B</sub> ) 3.47 (O <sub>B</sub> )	155 155	(insul)	83
B <sup>0</sup>	2.08 (O <sub>C</sub> ) 2.37 (O <sub>C</sub> )	2.93 (O <sub>C</sub> ) 3.18 (O <sub>C</sub> )	172 146		
C <sup>0</sup>	2.71 (F) 2.41 (F) 2.29 (F) 2.35 (F)	3.16 (F) 3.25 (F) 3.08 (F) 2.97 (F)	114 166 152 130		
(EDT-TTF-CONHMe) <sub>6</sub> [Re <sub>6</sub> Se <sub>8</sub> (CN) <sub>6</sub> ] A <sup>+</sup>	2.63 (O <sub>A</sub> )	3.38 (O <sub>A</sub> )	139	(insul)	84
B <sup>+</sup>	2.05 (N) 2.40 (N)	2.87 (N) 3.29 (N)	158 160		
C <sup>0</sup>	2.27 (O <sub>C</sub> ) 2.20 (O <sub>C</sub> ) 2.31 (N) 2.52 (N)	3.14 (O <sub>C</sub> ) 3.07 (O <sub>C</sub> ) 3.16 (N) 3.43 (N)	170 154 168 165		
(EDT-TTF-CONH <sub>2</sub> ) <sub>2</sub> ReO <sub>4</sub> A <sup>+0.5</sup>	2.09 (ReO <sub>4</sub> ) 2.36 (ReO <sub>4</sub> ) 2.76 (ReO <sub>4</sub> )	2.95 (ReO <sub>4</sub> ) 3.06 (ReO <sub>4</sub> ) 3.64 (ReO <sub>4</sub> )	171 138 158	14 (metal, T <sub>MI</sub> = 200 K)	83
B <sup>+0.5</sup>	2.23 (ReO <sub>4</sub> ) 2.07 (ReO <sub>4</sub> ) 2.52 (ReO <sub>4</sub> )	3.02 (ReO <sub>4</sub> ) 2.91 (ReO <sub>4</sub> ) 3.41 (ReO <sub>4</sub> )	153 166 158		
[EDT-TTF(SMe)(SCH <sub>2</sub> CONH <sub>2</sub> )] (BF <sub>4</sub> )	2.26 (F) 2.40 (F)	3.19 (F) 3.27 (F)	164 156	10 <sup>-7</sup>	89
(EDT-TTF-CONHMe) <sub>2</sub> Cl·H <sub>2</sub> O	2.48 (Cl/O <sub>w</sub> ) 2.52 (Cl/O <sub>w</sub> )	3.32 (Cl/O <sub>w</sub> ) 3.42 (Cl/O <sub>w</sub> )	168 176	120 (metal down to 0.47 K)	87
[TTF-C(=S)NHMe]Br	2.37 (Br) 2.90 (Br)	3.21 (Br) 3.67 (Br)	163 156	5 × 10 <sup>-5</sup>	72
[EDT-TTF-CONH-( <i>m</i> -py)]PF <sub>6</sub> ·THF	2.03 (O <sub>THF</sub> ) 2.33 (O <sub>THF</sub> ) 2.20 (O <sub>intra</sub> )	2.82 (O <sub>THF</sub> ) 3.13 (O <sub>THF</sub> ) 2.83 (O <sub>intra</sub> )	153 143 126		65
<i>ortho</i> -diamide salts: [EDT-TTF(CONH <sub>2</sub> ) <sub>2</sub> ](ClO <sub>4</sub> )	1.98 (intra) 2.09 2.00 2.18 1.97 (intra) 2.19 2.14 2.20 (ClO <sub>4</sub> )	2.79 (intra) 2.92 2.85 2.97 2.76 (intra) 3.03 2.99 2.99 (ClO <sub>4</sub> )	155 164 169 151 153 166 167 153	0.15 (E <sub>a</sub> = 0.14 eV)	61
[EDT-TTF(CONH <sub>2</sub> ) <sub>2</sub> ](HSO <sub>4</sub> )	1.94 (intra) 2.07 2.98 2.31 1.96 (intra) 2.27 2.20 2.09 (HSO <sub>4</sub> )	2.76 (intra) 2.91 2.84 3.04 2.76 (intra) 3.12 3.04 2.88 (HSO <sub>4</sub> )	158 167 172 143 153 170 165 153		61
[EDT-TTF(CONH <sub>2</sub> ) <sub>2</sub> ](Mo <sub>6</sub> Cl <sub>14</sub> )	2.31 1.98 2.56 (Cl) 2.55 (Cl)	2.99 2.79 3.40 (Cl) 3.29 (Cl)	135 157 165 143		
[EDT-TTF(CONHMe) <sub>2</sub> ] <sub>2</sub> ClO <sub>4</sub> A	2.12 2.43	2.96 2.91	165 116	3 × 10 <sup>-2</sup> (E <sub>a</sub> = 0.14 eV)	67
B	2.00 2.21 (ClO <sub>4</sub> )	2.81 2.97 (ClO <sub>4</sub> )	158 157		
[EDT-TTF(CONHMe) <sub>2</sub> ] <sub>2</sub> ReO <sub>4</sub> A	1.86 (intra)	2.67 (intra)	158	8.5 (E <sub>a</sub> = 50 meV)	67
B	2.35 1.86 (intra) 2.07 (ReO <sub>4</sub> ) 2.05 (ReO <sub>4</sub> )	3.00 2.68 (intra) 2.76 (ReO <sub>4</sub> ) 2.86 (ReO <sub>4</sub> )	133 159 137 156		

Table 6 (Continued)

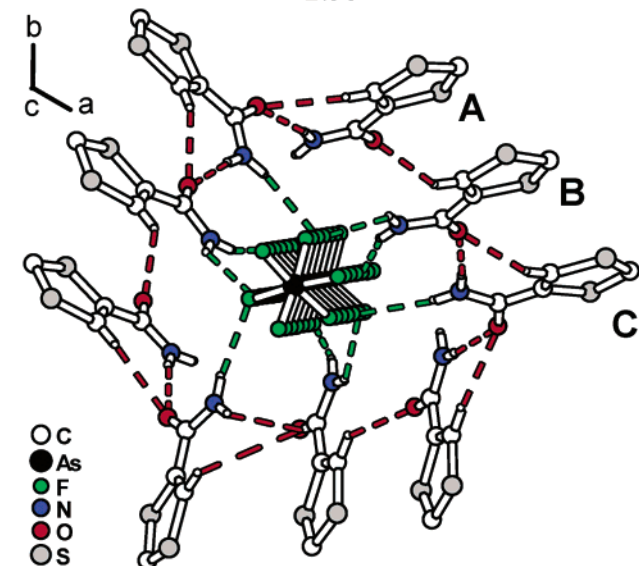
salt	H...X (Å)	N...X (Å)	N-H...X (deg)	$\sigma_{RT}^b$ (S cm <sup>-1</sup> )	ref
TCNQ(F <sub>4</sub> ) salts:					
[ <i>o</i> -(MeS) <sub>2</sub> TTF-CSNHMe]	2.24 (NC)	3.01 (NC)	167	5 × 10 <sup>-6</sup>	72
(TCNQ)	2.47 (NC)	3.35 (NC)	157		
(EDO-TTF-CONH <sub>2</sub> )(TCNQF <sub>4</sub> )	2.07 (OC)	2.89 (OC)	160	3 × 10 <sup>-3</sup>	88
	2.03 (NC)	3.08 (NC)	151		
	2.46 (N=C)	3.32 (N=C)	153		
(EDT-TTF-CONH <sub>2</sub> ) <sub>2</sub> (TCNQF <sub>4</sub> )	2.06 (OC)	2.91 (OC)	174	1.4 × 10 <sup>-5</sup>	89
	2.31 (NC)	3.13 (NC)	161		
	2.59 (NC)	3.40 (NC)	147		
[EDT-TTF(SMe)(SCH <sub>2</sub> CONH <sub>2</sub> )] (TCNQF <sub>4</sub> )		2.94 (O=C)			
		3.02 (N=C)			

<sup>a</sup> C-H...X hydrogen bonds are given in italics. <sup>b</sup>  $T_{MI}$  = metal-insulator transition temperature;  $E_a$  = activation energy in the semiconducting regime.

tially oxidized molecule  $A^{+0.5}$  only accepts a weak C-H...O interaction.



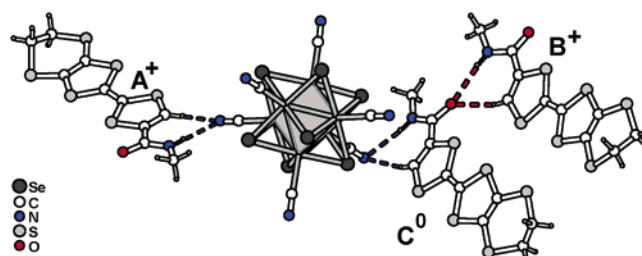
2.38



2.39

This salient, clear-cut deactivation of the hydrogen bond acceptor capability of the carbonyl function upon TTF oxidation was nicely demonstrated in another 6:1 salt,<sup>84</sup> formulated as (EDT-TTF-

CONHMe)<sub>6</sub>[Re<sub>6</sub>Se<sub>8</sub>(CN)<sub>6</sub>](CH<sub>3</sub>CN)<sub>2</sub>(CH<sub>2</sub>Cl<sub>2</sub>)<sub>2</sub> (**2.40**), where now two fully oxidized ( $A^{+}$  and  $B^{+}$ ) and one neutral ( $C^0$ ) secondary amides are hydrogen bonded to the cluster anion [Re<sub>6</sub>Se<sub>8</sub>(CN)<sub>6</sub>]<sup>4-</sup>, hence the formulation [( $A^{+}$ )<sub>2</sub>( $B^{+}$ )<sub>2</sub>( $C^0$ )<sub>2</sub>][Re<sub>6</sub>Se<sub>8</sub>(CN)<sub>6</sub>]<sup>4-</sup>. Both N-H...N and C-H...N hydrogen bonds are shorter with  $A^{+}$  than with  $C^0$  (Table 6), indicating that the hydrogen bond donor character for  $A^{+}$  is stronger than that for  $C^0$ . Meanwhile, it is remarkable that the C=O's of  $A^{+}$  and  $B^{+}$  are not involved in any hydrogen bond while the C=O of  $C^0$  is grasped in the seven-membered cyclic motif.

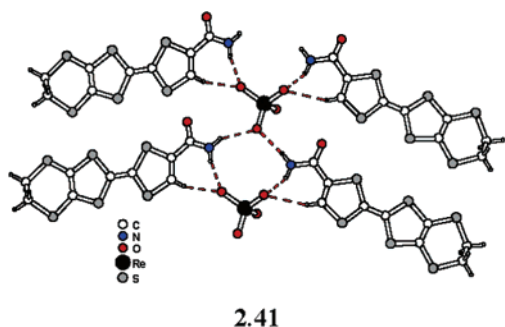


2.40

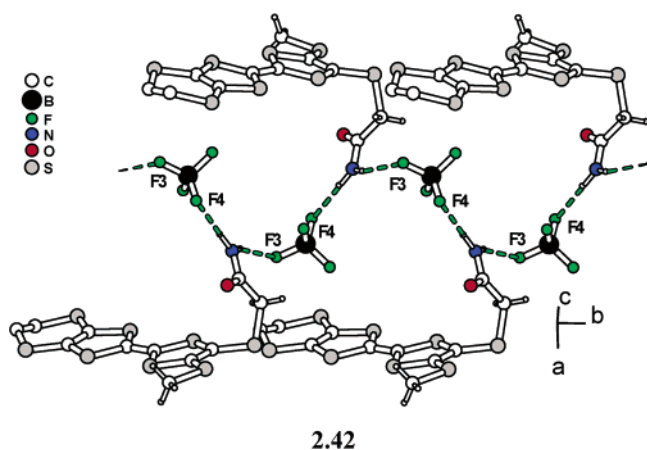
Thus, upon one-electron oxidation, an activation of the N-H and C<sub>ortho</sub>-H donor ability of the conjugated tetrathiafulvalenyl amide system is coupled to a deactivation of the hydrogen bond acceptor character of the oxygen carbonyl atom, as confirmed by calculations of electrostatic potential surfaces for both  $A^{+}$  and  $C^0$ . This redox modulation of the hydrogen bond donor-acceptor character has to be distinguished from situations of charge-assisted hydrogen bonding,<sup>85</sup> where enhanced interactions result from the presence of point charges localized on the hydrogen-bonded atoms (ammoniums, carboxylates).

A very different structure is obtained for (EDT-TTF-CONH<sub>2</sub>)<sub>2</sub>ReO<sub>4</sub>.<sup>83</sup> Each partially oxidized molecule is hydrogen bonded through the seven-membered cyclic motif to the ReO<sub>4</sub><sup>-</sup> anion (**2.41**), which appears as a stronger hydrogen bond acceptor than the carbonyl function, which in effect turns out to be fully deactivated here. The partially oxidized donor molecules then adopt a layered,  $\beta$ -type structure which exhibits metallic conductivity down to 200 K, where a weak localization leads to a semiconducting behavior with a very small activation energy (0.3 meV). These striking differences of stoichiometries and structures between the AsF<sub>6</sub><sup>-</sup> and ReO<sub>4</sub><sup>-</sup> salts

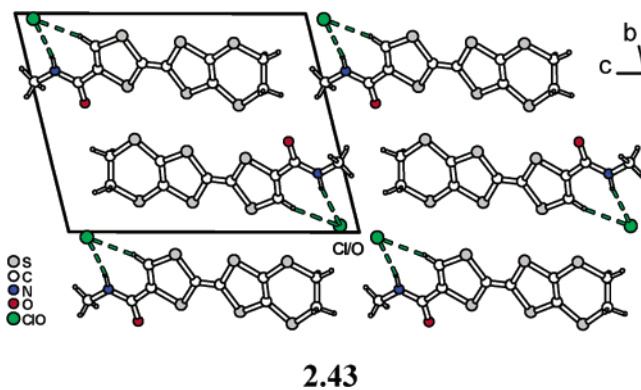
of EDT-TTF-CONH<sub>2</sub> demonstrate the rather acute efficiency of hydrogen-bonding interactions at distinguishing between otherwise isosteric anions, which typically affords isostructural salts with TMTTF or TMTSF, for example.<sup>86</sup>



In the 1:1 BF<sub>4</sub><sup>-</sup> salt of the primary amide EDT-TTF(SMe)(SCH<sub>2</sub>CONH<sub>2</sub>), oxidized molecules are associated into dicationic dyads (2.42). N-H...F hydrogen bonds are identified (Table 6) and form an helical motif along the 2<sub>1</sub> screw axis along *b* (space group P2<sub>1</sub>/a).

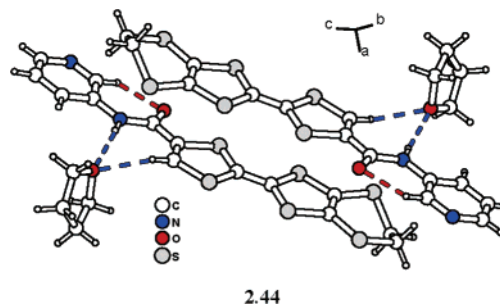


Another striking example of the efficiency of the pair of NH/CH hydrogen bond tweezers to generate the seven-membered cyclic motif is found in the halide salts of secondary amides or thioamides. In the 2:1 (EDT-TTF-CONHMe)<sub>2</sub>Cl·H<sub>2</sub>O salt,<sup>87</sup> a chloride anion and water molecule are disordered on the same site, and they are coordinated to the π-donor molecule by two strong N-H...Cl/OH<sub>2</sub> and C-H...Cl/OH<sub>2</sub> hydrogen bonds (Table 6), as shown in 2.43. The short separation between the inversion-related Cl/OH<sub>2</sub> sites (3.09 Å) falls in the reported range for Cl...O distances between water or alcohol molecules hydrogen bonded to Cl<sup>-</sup>,<sup>23</sup> as seen, for example, in [BEDT-TTF(CH<sub>2</sub>OH)]<sub>2</sub>Cl (vide supra, section 2.1.3), where O...Cl distances amount to 3.12–3.16 Å. (EDT-TTF-CONHMe)<sub>2</sub>Cl·H<sub>2</sub>O adopts a layered β'-type structure with a pronounced two-dimensional character of the calculated Fermi surface. The EPR Dysonian line observed below 120 K indicates a highly conducting system, confirmed by a room-temperature conductivity of 120 S cm<sup>-1</sup> and metallic behavior down to 0.47 K, but no indication of a transition to a superconducting state, a likely consequence of the Cl/H<sub>2</sub>O disorder.



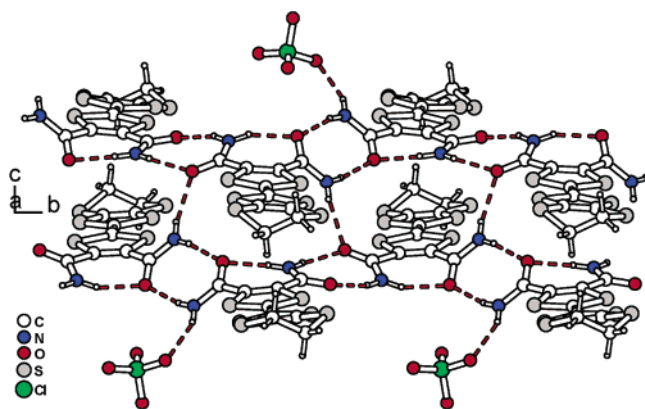
A similar motif is observed with the secondary thioamide TTF-C(=S)NHMe in [TTF-C(=S)NHMe]·Br.<sup>72</sup> Notice that this efficient anion recognition effect is also observed in solution, as demonstrated by <sup>1</sup>H NMR downfield shifts of both the N-H and C-H hydrogen atom resonances, as well as by a cathodic shift of the oxidation potential of EDT-TTF-CONHMe upon complexation by Cl<sup>-</sup>.<sup>87</sup> It is then likely that the actual electrocrystallized species is the negatively charged, solvated chloride complex, (EDT-TTF-CONHMe)(Cl<sup>-</sup>)(H<sub>2</sub>O)<sub>n</sub> rather than the free amide. This situation is probably general among functionalized TTFs and, specifically, among amides, which calls for a systematic investigation of their complexation ability and selectivity with various anions.

Among the six neutral TTF amides bearing a pyridine or bipyridine substituent (see section 2.2.1 above), only EDT-TTF-CONH-(*m*-Py) was described in a 1:1 radical cation salt with PF<sub>6</sub><sup>-</sup>, as a THF solvate.<sup>65</sup> As shown in 2.44, the radical cation, planarized through the intramolecular C-H...O hydrogen bond, associates into inversion-centered dicationic dyads through a strong SOMO-SOMO overlap interaction. As a consequence, the two TTF moieties now face each other, in sharp contrast with the structure of the neutral molecule (see 2.28), where a large longitudinal shift allowed for π-π interactions between the electron-rich TTF and electron-poor pyridylamide moieties.



Electrocrystallization of the neutral primary *ortho*-diamide EDT-TTF(CONH<sub>2</sub>)<sub>2</sub> in the presence of ClO<sub>4</sub><sup>-</sup>, ReO<sub>4</sub><sup>-</sup>, HSO<sub>4</sub><sup>-</sup>, and AsF<sub>6</sub><sup>-</sup> produces a series of isostructural 2:1 salts,<sup>61</sup> in sharp contrast with the case of the corresponding *monoamide* EDT-TTF-CONH<sub>2</sub>, where two different salts were isolated with ReO<sub>4</sub><sup>-</sup> and AsF<sub>6</sub><sup>-</sup> (see above).<sup>83</sup> The oxidized molecule adopts the closed conformation revealed in the structure of the neutral donor (see above section 2.2.1). The molecules then assemble into infinite puckered rib-

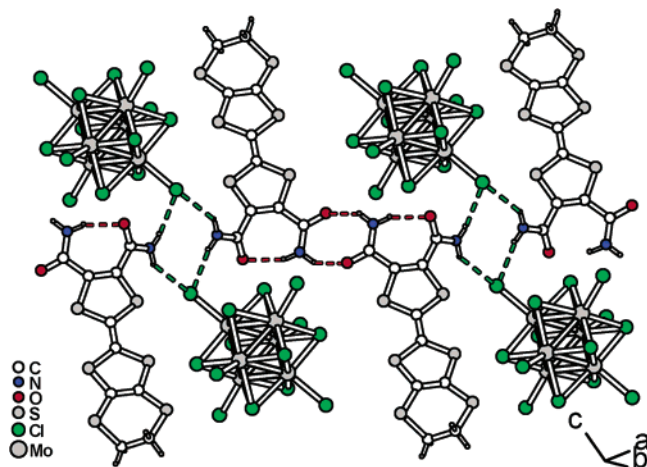
bonds running along *b* and developing out of self-complementary and centrosymmetrical eight-membered cyclic motifs (**2.45**). Of the two N–H protruding



2.45

from the ribbons, one is hydrogen bonded to the disordered counterion while the other connects two ribbons. The absence of a structural directing effect of the anion in these series demonstrates the pre-eminence of the amide...amide hydrogen-bonded network. The segregation of the EDT-TTF cores and the hydrophilic amidic moieties lead to the formation of donor slabs of  $\beta'$ -type. The  $\text{HSO}_4^-$  salt is virtually structurally indistinguishable, yet minute modulations of the ribbons' curvature and shape throughout the series have been shown to correlate to very remarkable differences in the intrastack  $\beta_{\text{HOMO-HOMO}}$  interaction energies and changes in the density of states at the Fermi level and to important differences of spin (Pauli) susceptibility behavior in a system where electron correlations are significant.

Another salt with  $\text{EDT-TTF}(\text{CONH}_2)_2$  was also obtained with the dianionic  $\text{Mo}_6\text{Cl}_{14}^{2-}$  cluster. The

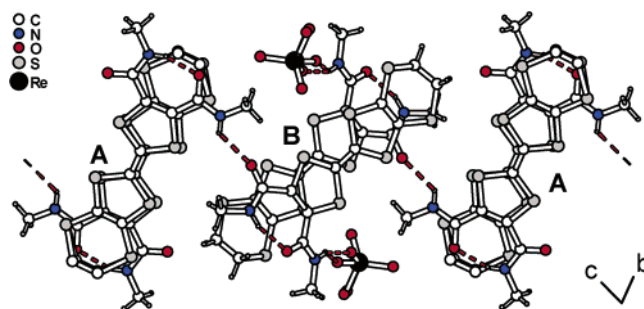


2.46

fully oxidized donor molecules arrange into discrete dicationic dyads through  $\text{HOMO}\cdots\text{HOMO}$  overlap. The hydrogen bond network shown in **2.46** is again characterized by the intramolecular motif, complemented by the recurrent dimeric association through the eight-membered centrosymmetrical cyclic motif. The resulting bimolecular entity interacts with the hydrogen bond acceptor terminal chloride ligands of

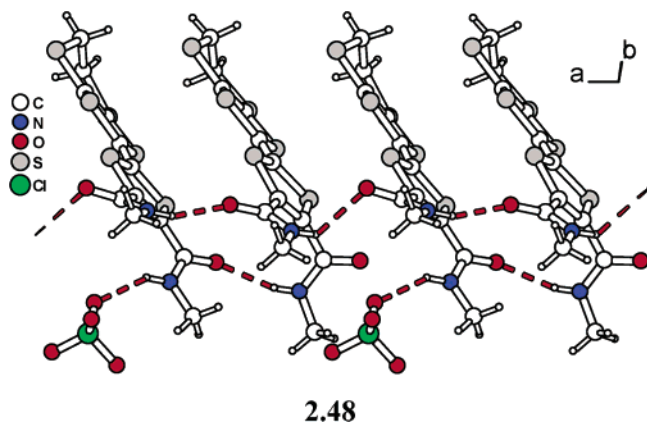
$(\text{Mo}_6\text{Cl}_{14})^{2-}$ , forming a symmetrical cyclic motif involving four N–H and two Cl fragments.

The gradually evolving molecular conformations of the neutral secondary *ortho*-diamides  $\text{EDT-TTF}(\text{CONHR})_2$  described in section 2.2.1., from the closed form stabilized by an intramolecular hydrogen bond ( $\text{R} = \text{Me}, \text{Et}, n\text{Pr}, \text{Bz}$ ) to the antiparallel ladders built out of open molecules ( $\text{R} = n\text{Bu}, n\text{Pent}, n\text{Hex}$ ), pave the route for the possible observation of both closed and open conformers of one given molecule, under different structural constraints. This assumption turned out to be verified in the radical cation salts of the methyl derivative,  $\text{EDT-TTF}(\text{CONHMe})_2$ . Salts with either  $\text{ReO}_4^-$  or  $\text{ClO}_4^-$ , two similar tetrahedral anions, have vastly different architectures, dimensionality, and electronic structures, a consequence of the presence of the closed or open structural isomers in one or the other. In  $[\text{EDT-TTF}(\text{CONHMe})_2]_2\text{ReO}_4$ , the mixed-valence donor molecules are in the closed conformation. Two crystallographically independent molecules **A** and **B** stack along *a* to form two well separated columns (**2.47**). The infinite hydrogen-bonded chain motif present in the neutral molecule is not present in its  $\text{ReO}_4^-$  salts, where one oxygen atom of the anion competes favorably with the neighboring molecule carbonyl oxygen atom for the available single N–H donor. This is another manifestation of the weaker hydrogen bond acceptor character of the amide carbonyl oxygen atom in such radical cation forms.



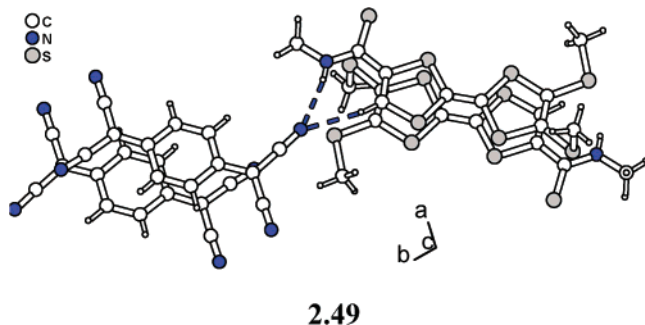
2.47

The structure of TTF-based materials is usually not affected upon substitution of  $\text{ReO}_4^-$  for the smaller  $\text{ClO}_4^-$ . Here, however, both salts are not isostructural. In  $[\text{EDT-TTF}(\text{CONHMe})_2]_2\text{ClO}_4$ , the two donor molecules **A** and **B** are in the open conformation and the two pairs of C=O and N–H functionalities available for hydrogen bonding combine as shown in **2.48**. The  $\beta''$  donor layer of  $[\text{EDT-TTF}(\text{CONHMe})_2]_2\text{ClO}_4$  leads to a two-dimensional Fermi surface, the characteristics of which would indicate a metallic behavior, in contradiction with the observed semiconducting behavior with  $\sigma_{\text{RT}} = 3 \times 10^{-2} \text{ S cm}^{-1}$  and an activation energy of 0.14 eV. This observation of structural isomerism in the radical cation salts of  $\text{EDT-TTF}(\text{CONHMe})_2$  is seen as a direct manifestation in the solid state of a fine sensitivity of the constrained seven-membered ring to the change of internal chemical pressure exerted by either  $\text{ReO}_4^-$  or  $\text{ClO}_4^-$ , two anions of different volumes and otherwise identical charge and symmetry. These are valuable observations in the field



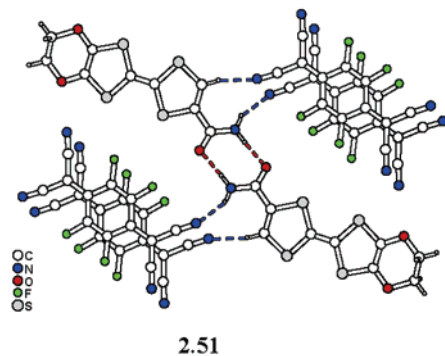
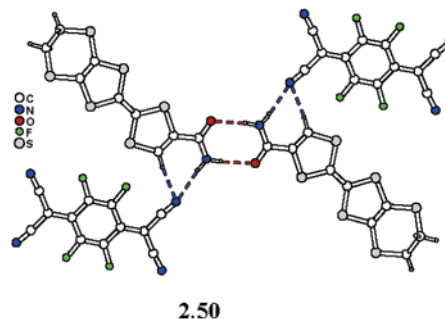
of crystal engineering, where the flexibility conferred to the molecule becomes a key parameter in the a priori prediction of crystal structures. These results demonstrate that the Coulomb energy, intermolecular  $p_\pi-p_\pi$  overlap interactions, and bandwidth of electronic molecular materials may be manipulated by creation of structural isomers of radical cation salts upon tuning of their internal chemical pressure.

Different amides or thioamides have also been engaged in charge-transfer salts with TCNQ or the stronger oxidizer TCNQF<sub>4</sub>. In the 1:1 TCNQ salt [*o*-(MeS)<sub>2</sub>TTF-C(=S)NHMe](TCNQ),<sup>72</sup> mixed-valence donor and acceptor dyads stack along the *c*-axis (**2.49**). These (DD)<sup>+0.5</sup>(AA)<sup>-0.5</sup>(DD)<sup>+0.5</sup> chains are connected to each other through N-H⋯N<sub>TCNQ</sub> and C-H⋯N<sub>TCNQ</sub> hydrogen bonds, forming the cyclic characteristic seven-membered motif.

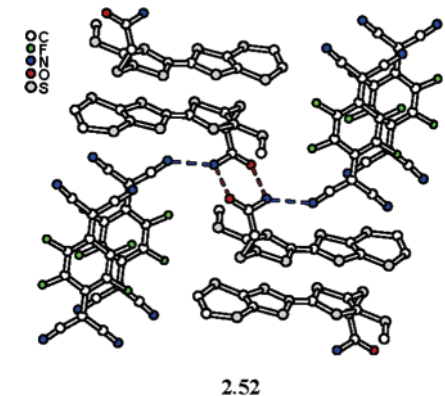


On the other hand, full charge transfer onto the acceptor moiety is observed with the stronger oxidizer TCNQF<sub>4</sub> in the two salts described with the primary amides EDO-TTF-CONH<sub>2</sub> and EDT-TTF-CONH<sub>2</sub>.<sup>88</sup> In the 1:1 (EDO-TTF-CONH<sub>2</sub>)(TCNQF<sub>4</sub>) salt (**2.50**), donor and acceptor (EDO-TTF-CONH<sub>2</sub>)<sub>2</sub><sup>2+</sup> and (TCNQF<sub>4</sub>)<sub>2</sub><sup>2-</sup> face-to-face dyads alternate, giving rise to a fully ionic, rock-salt structure, while, in the 2:1 (EDT-TTF-CONH<sub>2</sub>)<sub>2</sub>(TCNQF<sub>4</sub>) salt (**2.51**), parallel chains of alternating (EDT-TTF-CONH<sub>2</sub>)<sub>2</sub><sup>+</sup> dyads and singly reduced TCNQF<sub>4</sub><sup>-</sup> anions develop along *b*. In both salts, the robust, recurrent centrosymmetric eight-membered cyclic hydrogen bond dimer motif, common to a great many primary amides, is identified. The remaining N-H group, assisted by a C<sub>ortho</sub>-H group, reaches out for the nitrile hydrogen bond acceptor moiety of the reduced TCNQF<sub>4</sub> to form the equivalently robust, recurrent seven-membered cyclic motif in (EDT-TTF-CONH<sub>2</sub>)<sub>2</sub>(TCNQF<sub>4</sub>) (**2.50**) while, in the 1:1 (EDO-TTF-CONH<sub>2</sub>)(TCNQF<sub>4</sub>) salt, the

N-H and C-H groups are hydrogen bonded to the nitrile group of two different TCNQF<sub>4</sub><sup>-</sup> anions (**2.51**).



Finally, in the 1:1 [EDT-TTF(SMe)(SCH<sub>2</sub>CONH<sub>2</sub>)]-(TCNQF<sub>4</sub>) salt,<sup>89</sup> inversion-centered dicationic donor dyads alternate with inversion-centered (TCNQF<sub>4</sub>)<sub>2</sub><sup>2-</sup> dianions within the rock-salt structure shown in **2.52**. As observed above, the donor dyads are connected to each other through the cyclic eight-membered motif while the remaining N-H group is hydrogen bonded to a nitrile of the TCNQF<sub>4</sub><sup>-</sup> anion.

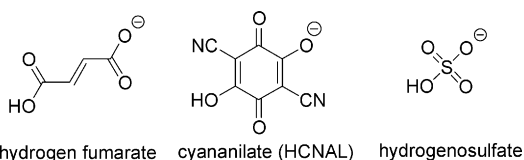


### 2.3. Hydrogen Bonding in the Anionic Network

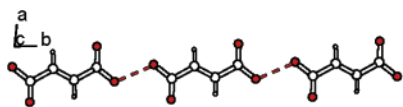
There are two ways to make use of intermolecular hydrogen-bonding interactions to direct the topology of crystalline molecular conductors. One consists in engaging anions able to act both as hydrogen bond donor and acceptor; another is to try and introduce in the salt formulation a third neutral component which acts as a hydrogen bond donor toward the functional hydrogen bond donor/acceptor anion. Only a few examples of the former, "self-sufficient anion" approach have been reported. Introduction of a third neutral component in ternary systems has been, however, the subject of several systematic investigations aimed at understanding the structural and

electronic modifications caused by the presence of neutral, structure-directing molecules deliberately introduced in the (anionic) lattice. Note finally the special case of water inclusion, found in more than 70 salts of TTF derivatives reported in the CSD, where the H<sub>2</sub>O molecules, acting both as hydrogen bond donor and acceptor, play a strongly structuring role in the anionic layers, particularly with the smallest halide anions. We will restrict ourselves here to the analysis of the few examples involving "self-sufficient" anions, since, in most other cases, solvent or water molecules were not introduced purposely for hydrogen-bonding interactions. Self-sufficient anions are found among partially neutralized di- or polyacids, be they organic, such as the hydrogenofumarate or the cyananilate (HCNAL) anions, or inorganic, such as HSO<sub>4</sub><sup>-</sup> (Chart 8).

### Chart 8



In the 2:1 BEDT-TTF salt of the hydrogenofumarate anion,<sup>90</sup> infinite chains running along *b* (**2.53**) are formed via O–H···O–C hydrogen bonds with a short O···O distance (2.48 Å), characteristic of strong hydrogen bonds between hydroxyl and negatively charged oxygen atoms.<sup>91</sup> Since the hydrogen atoms could not be identified in Fourier-difference maps, the question remains whether this hydrogen bond is symmetrical, as often observed in strong hydrogen bonds, or unsymmetrical.



2.53

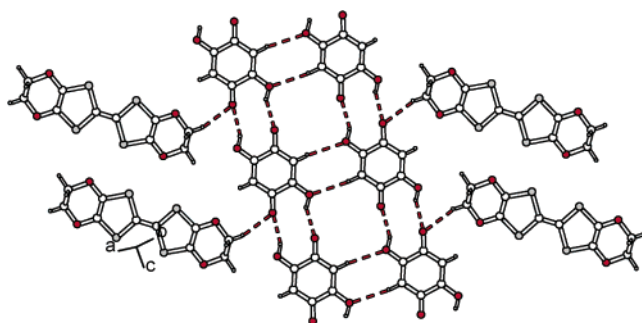
The 2:1 BEDT-TTF salt of the cyananilate anion, (BEDT-TTF)<sub>2</sub>(HCNAL), produces also an infinite hydrogen-bonded ribbon along *a* (**2.54**) with a intermolecular O···O distance of 3.027(6) Å.<sup>92</sup> Other salts of the cyananilate anion have also been reported with various donor molecules such as TMTTF<sup>93</sup> or octamethylenetetrafulvalene<sup>94</sup> (OMTTF) with a similar disorder of the H atom on two symmetrical positions.



2.54

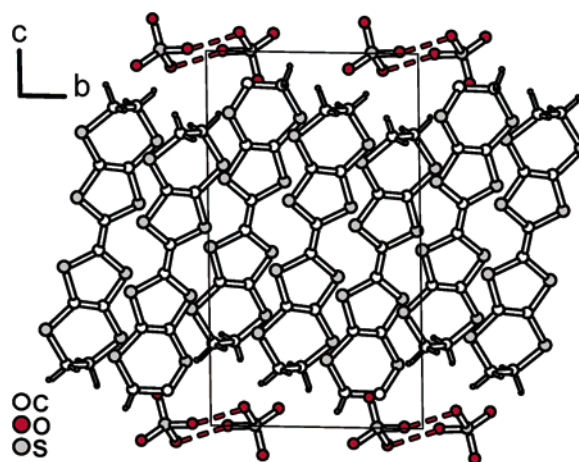
A 1:2 molecular neutral complex of BEDO-TTF with 2,5-dihydroxy-*p*-quinone forms alternated stacks of one donor and two quinones. Perpendicular to the stacking direction, O–H···O=C hydrogen bonds develop between the quinones, giving rise to a chain system (**2.55**) further linked to a neighboring chain

through C<sub>sp</sub><sup>2</sup>–H···O hydrogen bonds to the hydroxyl oxygen atoms as well as to BEDO-TTF molecules through C<sub>sp</sub><sup>3</sup>–H···O=C interactions.



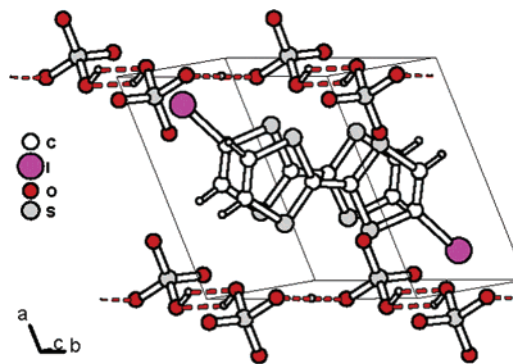
2.55

Upon monodeprotonation, the inorganic diacid H<sub>2</sub>SO<sub>4</sub> generates a hydrogenosulfate anion HSO<sub>4</sub><sup>-</sup> able to act as both hydrogen bond donor and acceptor, as indeed observed in the two examples reported in the CSD, that is (BEDT-TTF)<sub>3</sub>(HSO<sub>4</sub>)<sub>2</sub> and (TTF-I)(HSO<sub>4</sub>). In the former, the anions form inversion-centered eight-membered cyclic motifs shown in **2.56**.<sup>96</sup>



2.56

In (TTF-I)(HSO<sub>4</sub>),<sup>97</sup> a chain of HSO<sub>4</sub><sup>-</sup> anions runs along *b*, linked by two strong O–H···O hydrogen bonds (Table 7). Both are crystallographically centrosymmetric. One hydrogen atom was found disordered on two positions while the other could only be located on the inversion center, implying a truly symmetrical bond. Notice in **2.57** the strong associa-



2.57

**Table 7. Structural Characteristics of the Hydrogen Bond Network Found in the Anionic Part of Selected Radical Cation Salts<sup>a</sup>**

salt	H···O (Å)	O···O (Å)	O–H···O (deg)	$\rho$	$\sigma_{\text{RT}}^b$ (S cm <sup>-1</sup> )	ref
(BEDT-TTF) <sub>2</sub> (Hfum)	<i>2.40</i> <i>2.47</i>	2.48 (sym) 3.30 3.33	180 160 153	1/2	3 ( $E_a = 0.2$ eV)	90
(BEDT-TTF) <sub>2</sub> (HCNAL)	2.14	3.03	159	1/2	0.2–0.8 ( $E_a = 0.15$ eV)	92
(TMTTF) <sub>2</sub> (HCNAL)		2.81		1/2	$3 \times 10^{-2}$ ( $E_a = 52$ meV)	93
(OMTTF) <sub>3</sub> (HCNAL) <sub>2</sub> (BEDO-TTF) <sub>2</sub> [Q(OH) <sub>2</sub> ]	2.04 2.75 2.44	2.84 2.80 3.70 3.31	149 165 157	2/3 1	$3 \times 10^{-8}$	94 95
(TTF–I)(HSO <sub>4</sub> )	1.86	2.63 (sym) 2.56 (dissym)	180 139	1		97
(BEDT-TTF) <sub>3</sub> (HSO <sub>4</sub> ) <sub>2</sub>		2.61		2/3		96

<sup>a</sup> C–H···O hydrogen bonds are in italics. <sup>b</sup>  $E_a$  = activation energy in semiconductors.

tion of the two TTF–I<sup>+</sup> radical cations into a diamagnetic dicationic (TTF–I)<sub>2</sub><sup>2+</sup> dyad with a short plane-to-plane distance (3.33 Å) through a SOMO···SOMO overlap interaction.

### 3. C–H···O(N, Hal) Hydrogen Bonds

Between the “normal” hydrogen bond interactions based on OH or NH donor groups described above in section 2 and the weak C–H···X interactions systematically observed, for example between the S–CH<sub>2</sub>CH<sub>2</sub>–S group of BEDT-TTF and the anionic network, a number of stronger C–H···X hydrogen bonds have been identified in the structures of the primary and secondary amides deciphered earlier (section 2.2.). Such weak hydrogen bonds have been the subject of much debate but are now generally recognized to have an important role in influencing, moderating, or complementing stronger forces, to the point where they have been shown in several instances to direct the formation of structural patterns.<sup>24</sup> In their 1982 paper, Taylor and Kennard used a strict cutoff for the H···O distance (2.4 Å) below which the denomination of the C–H···O hydrogen bond may apply.<sup>98</sup> Larger values were considered as van der Waals interactions. This criterion was reevaluated on the basis of extensive statistical studies performed by analyzing a great quantity of structural data,<sup>99,100</sup> with, for example, C···O distances between 3.0 and 4.0 Å or H···O distances between 2.0 and 3.0 Å. Nevertheless, as stated by Desiraju, “the greatest weight should be given to those contacts wherein short H···O separations (2.0 <  $d$  < 2.3 Å) are accompanied by large hydrogen bond angles (150 <  $\theta$  < 180°).”<sup>24</sup> These C–H···X hydrogen bonds are essentially observed with X = O, N, and Hal, and characteristic distances for different substitution patterns (Table 8) have been collected by Steiner<sup>101</sup> as reference data for further comparison. As with normal hydrogen bonds, their strength is related to the H···X and C(–H)···X distances, with the same directionality preferences: on the C–H side, with 150 < C–H···X angles < 180°; on the acceptor side, with a preference for interaction with lone pairs. As seen in Table 8, the C–H···X strength critically depends on the nature of the carbon atom bearing the hydrogen atom. Note that the strongest

**Table 8. Mean  $d(\text{H}\cdots\text{X})$  Distances on Hydrogen Bonds of Different C–H Donor Molecules to the Acceptors O, N, and Cl<sup>–</sup> (Ref 101)**

H donor	O acceptor (Å)	N acceptor (Å)	Cl <sup>–</sup> acceptor (Å)
Cl <sub>3</sub> C–H	2.31(2)	2.37(3)	2.38(3)
C≡C–H	2.40(2)	2.40(6)	2.56(4)
Cl <sub>2</sub> CH <sub>2</sub>	2.492(8)	2.53(2)	2.59(3)
NC–CH <sub>3</sub>	2.567(9)	2.59(1)	2.72(3)
MeSO <sub>2</sub> CH <sub>3</sub>	2.56(1)	2.65(2)	2.94
Me(CO)CH <sub>3</sub>	2.60(1)	2.64(3)	2.98

hydrogen bond donors are provided by alkynes’ C<sub>sp</sub>–H, allowing for very strong interactions:<sup>102</sup> C<sub>sp</sub>–H > C<sub>sp<sup>2</sup></sub>–H > C<sub>sp<sup>3</sup></sub>–H. Furthermore, the presence of electron-withdrawing groups (EWGs) on that carbon atom enhances the hydrogen acidity and its propensity to engage in C–H···X hydrogen bonds. When it comes to assess the existence and role of C–H···X hydrogen bonds in radical cation salts of TTF and derivatives, one can therefore sort them out with the nature of the carbon atom hybridization, that is in only two categories, C<sub>sp<sup>2</sup></sub>–H and C<sub>sp<sup>3</sup></sub>–H, since no TTF alkyne derivative has been structurally characterized so far. Furthermore, activation of a C–H···X hydrogen bond will depend essentially on the presence of neighboring electron-withdrawing groups. Note also that only those examples where the distance and directionality criteria are both fulfilled will be singled out, since numerous, and in that respect essentially meaningless, C–H···X interactions may be virtually denoted in any salt.

#### 3.1. Hydrogen Bonding with C<sub>sp<sup>2</sup></sub>–H Groups

The earliest report (see section 1.4) on the importance of C–H···O hydrogen bonds in a TTF complex was one made as early as 1981 when the X-ray crystal structure of TTF–chloranil described two years before<sup>103</sup> was analyzed<sup>8</sup> in the light of the discovery of the structural transition accompanying the neutral-to-ionic transition.<sup>9</sup> In TTF–chloranil as well as in several TTF complexes with other quinones (benzoquinone,<sup>104</sup> fluoranil,<sup>103</sup> bromanil, tetraazidoquinone<sup>105</sup>) or analogues (pyrromellitic dianhydride),<sup>106</sup> mixed stacks of neutral donor and acceptor are observed, the consequence of electrostatic  $\pi$ – $\pi$  quadrupolar interactions.<sup>107</sup> As shown in **3.1**, each TTF molecule is surrounded by quinones of neighbor-

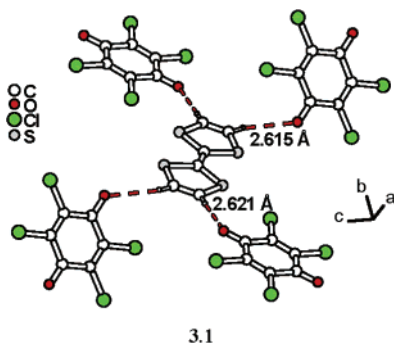


**Table 9. Structural Characteristics of the C–H···X Hydrogen Bonds in TTF–Acceptor Complexes**

compound	H···O (Å)	C···O (Å)	C–H···O (deg)	H···O=C (deg)	ref
TTF–benzoquinone	2.39	3.37	165	118	104
TTF–fluoranil	2.89	3.70	162	123	103
TTF–chloranil	2.61	3.36	143	126	103
	2.62	3.44	178	138	
( <i>E</i> -Me <sub>2</sub> TTF)–chloranil	<i>a</i>	3.42	<i>a</i>		108
( <i>E</i> -Me <sub>2</sub> TTF)–(Br <sub>2</sub> Cl <sub>2</sub> Q)	<i>a</i>	3.42	<i>a</i>		108
( <i>E</i> -Me <sub>2</sub> TTF)–bromanil	<i>a</i>	3.48	<i>a</i>		108
TTF–[(N <sub>3</sub> ) <sub>4</sub> Q]	2.33	3.33	170	167	105
TTF–pyrromellitic dianhydride	2.24 (pyrro)	3.29 (pyrro)	160	152	106
	2.20 (pyrro)	3.30 (pyrro)	169	160	
	2.52 (TTF)	3.59 (TTF)	165	105	
	2.54 (TTF)	3.21 (TTF)	117	158	
[TTF] <sub>2</sub> [TTF(CO <sub>2</sub> H) <sub>2</sub> (CO <sub>2</sub> ) <sub>2</sub> ]	2.35	3.07	130	138	32
	2.50	3.40	157	165	
	2.76	3.33	118	128	
	2.58	3.21	123	149	
	2.24	3.20	172	109	

<sup>a</sup> The atomic coordinates of hydrogen atoms were not reported, but the structures show unambiguously the short and directional C–H···O interactions.

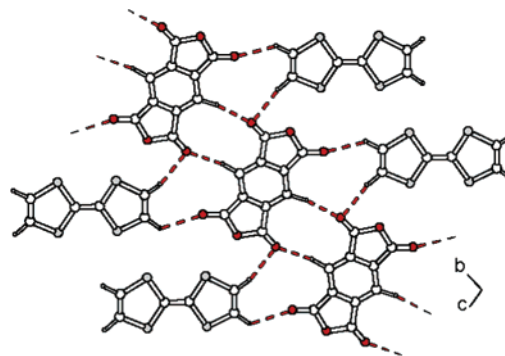
ing stacks and connected to the carbonyl groups of these quinones by short C–H···O interactions whose



structural characteristics are collected in Table 9. Note the directionality of these hydrogen bonds ( $160 < \text{C–H}\cdots\text{O} < 180^\circ$ ) as well as their tendency to interact with the oxygen lone pair, as shown by the  $\text{H}\cdots\text{O}=\text{C}$  angles close to  $120^\circ$ . Of particular interest in TTF–chloranil is the evolution of those interactions below the neutral–ionic transition temperature ( $T_{\text{NI}} = 84 \text{ K}$ ). The temperature dependence of the thermal expansion tensor determined from powder diffraction data around the transition temperature indicates two strikingly different behaviors.<sup>8</sup> Above  $T_{\text{NI}}$ , the lattice contraction is almost entirely along the stacking axis while, below  $T_{\text{NI}}$ , it occurs in a plane that makes an angle of  $44^\circ$  with the stacking axis. Careful examination of the room-temperature X-ray crystal structure reveals that this plane coincides with the mean plane defined by the network of C–H···O hydrogen bonds, a signature of enhanced interactions between the activated C–H groups of the oxidized TTF and the oxygen atoms of the quinone radical anion. Similar C–H···O hydrogen bonds are also present in the *E*-Me<sub>2</sub>TTF complexes of chloranil,

dibromodichloroquinone, or bromanil,<sup>108</sup> where each C–H group of *E*-Me<sub>2</sub>TTF is coordinated to the oxygen atom of a quinone.

In the TTF–pyrromellitic dianhydride neutral complex, columns are also observed where donor and acceptor molecules alternate along *a*. In the *bc* plane shown in **3.2**, we do not observe the usual chessboardlike motif but rather C<sub>pyrro</sub>–H···O hydrogen-bonded chains of pyrromellitic dianhydride running along *b* and laterally connected to the neutral TTF moieties through weaker C<sub>TTF</sub>–H···O hydrogen bonds.

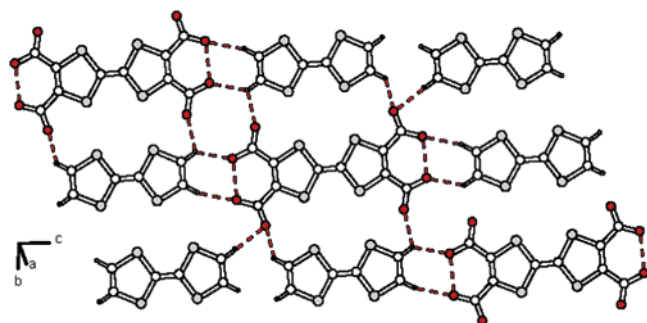
**3.2**

The partially neutralized tetrathiafulvalene tetracarboxylic acid,<sup>32</sup> TTF(CO<sub>2</sub>H)<sub>2</sub>(CO<sub>2</sub><sup>−</sup>)<sub>2</sub>, where two strong, intramolecular OH···O=C hydrogen bonds leave the dianion as a sole potential acceptor (see section 2.1.1), can be considered as a dianionic analogue of the pyrromellitic anhydride. In its TTF-based composite salt shown in **3.3**, (TTF<sup>•+</sup>)<sub>2</sub>[TTF(COOH)<sub>2</sub>(COO<sup>−</sup>)<sub>2</sub>], all four of TTF's C<sub>sp<sup>2</sup></sub>–H hydrogen bond donors are engaged with the oxygen atoms of the TTF dicarboxylatediacid to develop the six-point,

**Table 10. Bond Distances (Å) and Angles (deg) of the C–H···N≡C– Hydrogen Bonds in TTF–Acceptor Complexes**

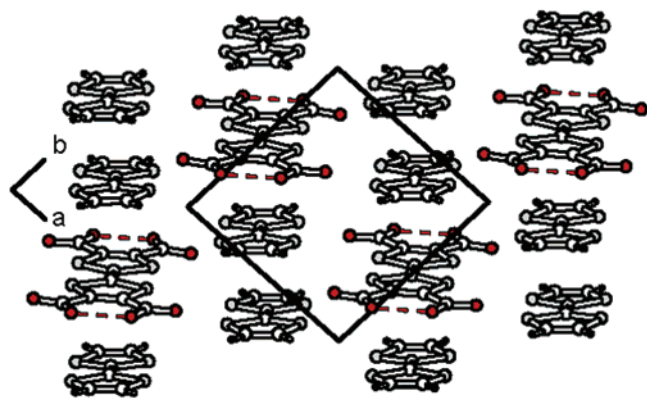
compound	$\rho$	H···N	C···N	C–H···N	H···N≡C	ref
Alternated stacks:						
TTF–(Bz <sub>2</sub> TCNQ)	0	2.52 2.59	3.45 3.23	167 120	170 144	110
TTF–DMDCNQI	0	2.65 2.79	3.36 3.50	119 147	126 135	112
TTF–[(CH <sub>2</sub> ) <sub>4</sub> DCNQI]	0	2.57 2.63	3.40 3.26	148 126	141 156	113
Segregated stacks:						
TTF–TCNQ	0.59	2.59	3.45	152	132	109
TTF–DCNQI–(H <sub>2</sub> O) <sub>2</sub>	0.48	2.56	3.48	160	103	111
TTF–(NaphtDCNQI)	?	2.45	3.35	163	119	114
Oxidized dimers:						
TTF–(MeClDCNQI)	1	2.43	3.35	159	121	115

two-dimensional charged organic hydrogen-bonded polymer.



3.3

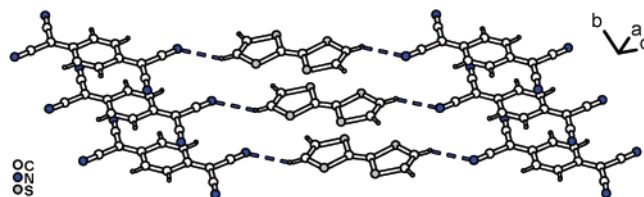
An added dimension to this remarkable achievement is the occurrence of an unprecedented (TTF)<sub>2</sub><sup>cation</sup>–TTF<sup>(anion)</sup>, β-like hybrid topology, shown in 3.4, within which fully oxidized TTF dimers are interspersed between dianions.



3.4

Clearly then, hydrogen bonds stand out as a characteristic feature of complexes or salts with

quinones, pyromellitic anhydride, or TTF carboxylate complexes. It is not the case, however, for the prototypical charge-transfer complexes between TTF and stronger acceptors such as TCNQ or DCNQI. One plausible C–H···N interaction connecting the TTF and TCNQ stacks running along *b* can be identified in the structure of TTF–TCNQ (3.5);<sup>109</sup> its geometrical characteristics do not point, however, to “strong C–H···N” hydrogen bonds (Table 10), and other TTF salts of substituted TCNQ do not exhibit specific interactions.<sup>110</sup>



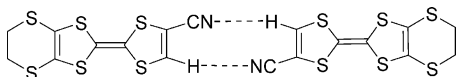
3.5

The dicyanoquinone diimines (DCNQIs) are another class of acceptor molecules recently investigated. C–H···N interactions can be identified between TTF and DCNQI,<sup>111</sup> DMDCNQI,<sup>112</sup> and derivatives,<sup>113,114,115</sup> but no pronounced preference for the CN lone pair occurs (Table 10). This absence of sizable C–H···N interactions, when compared with C–H···O=C interactions, might be related to the properties of the nitrile group as well as to the nature of the LUMOs of those acceptor molecules. Indeed, as pointed by Steiner on the basis of statistical studies,<sup>101</sup> N atoms appear to be weaker hydrogen bond acceptors than oxygen atoms in C–H···X interactions, and the sp<sup>2</sup> hybridized N atoms appear to be even weaker hydrogen bond acceptors than the sp<sup>2</sup> N atoms of pyridines. Furthermore, in the context of charged molecules as for the radical anions, TCNQ<sup>•-</sup> or DCNQI<sup>•-</sup>, one should not expect enhanced interactions, since their LUMOs are distributed over the whole molecules with little contribution of the

nitrile groups. The opposite situation is indeed observed in quinones, the LUMOs of which exhibit large coefficients on the oxygen atoms.

We have seen above that the hydrogen atoms of TTF itself, in its neutral form and even more so in its oxidized state, were activated enough to engage in C–H···X hydrogen bonds. We know by now that the introduction of an electron-withdrawing group (EWG) on the TTF core, even if it raises its oxidation potential, will also activate the neighboring  $sp^2$  hydrogen atom. The case of TTF amides and thioamides has been evoked in section 2.2: the  $sp^2$  hydrogen atom located  $\alpha$  to the amido or thioamide group is systematically engaged in cyclic hydrogen bond motifs together with the NH groups, in the neutral molecules as well as in their salts. Among the few other TTF derivatives bearing an EWG such as an ester or a nitrile group characterized,<sup>116</sup> the (EDT-TTF–CN)<sub>n</sub>(I<sub>3</sub>) ( $n = 1, 2$ ) series stands out because the hydrogen atom  $\alpha$  to the CN group is engaged in a C–H···N hydrogen bond with the CN group of a neighboring molecule to form a cyclic, inversion-centered motif identified previously in various benzonitrile derivatives (Chart 9).<sup>117,118</sup>

Chart 9



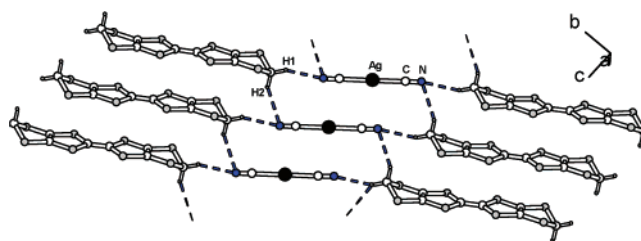
### 3.2. Hydrogen Bonding with $sp^3$ -CH<sub>2</sub> Groups

The salient examples of  $C_{sp^3}$ –H···X hydrogen bonds concern those structures where the methylenic moiety is flanked by a sulfur atom and another EWG such as another sulfur atom,<sup>119–121</sup> a carbonyl,<sup>121</sup> or a difluoromethylene<sup>122</sup> fragment, as shown in the chart in Table 11. One typical case is that of the fully oxidized radical cation salts of bis(methylenedithio)tetrathiafulvalene, such as (BMDT-TTF)[Ag(CN)<sub>2</sub>]

**Table 11. Structural Characteristics of the C–H···X Interactions Encountered with Activated  $sp^3$  CH<sub>2</sub> Groups**

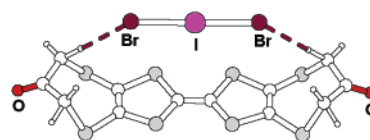
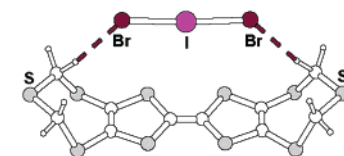
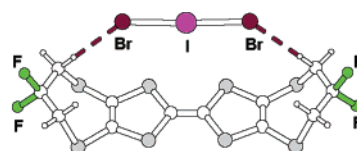
compound	(C–)H···X (Å)	C(–H)···X (Å)	C–H···X (deg)	ref
(BMDT-TTF)SbF <sub>6</sub>	2.50 (F)	3.32	142	119
	2.54 (F)	3.23	132 (bif)	
	2.58 (F)	3.22	127 (bif)	
(BMDT-TTF)[Ag(CN) <sub>2</sub> ]	2.45 (N)	3.38	156	120
	2.70 (N)	3.61	151	
	2.67 (Cl)	3.62	166	
(CF <sub>2</sub> ) <sub>2</sub> (Mo <sub>6</sub> Cl <sub>14</sub> )	2.68 (Cl)	3.56	152	122
	2.69 (Cl)	3.58	153	
	2.80 (Cl)	3.65	148	
	2.96 (Cl)	3.67	131	
(S)(IBr <sub>2</sub> )	2.64 (Br)	3.65	152	121
(C=O)(IBr <sub>2</sub> )	2.72 (Br)	3.84	174	121
(CF <sub>2</sub> ) <sub>2</sub> (IBr <sub>2</sub> )	2.69 (Br)	3.64	166	122
(CF <sub>2</sub> ) <sub>2</sub> (I <sub>2</sub> Br)	2.74 (I, Br)	3.69	166	122

with its neat complex network of C–H···N interactions involving both hydrogen atoms of the methylenic moiety shown in **3.6**.



3.6

It is of interest to note that only two of the eight hydrogen atoms in the bis(propylenedithio)tetrathiafulvalene derivatives labeled **S**, **CF<sub>2</sub>**, and **C=O** in Table 11 are engaged in a C–H···Br hydrogen bond in their 1:1 salts with IBr<sub>2</sub><sup>–</sup>. Remarkably, the very same motif shown in **3.7** is observed for all three salts, with the anion precisely anchored by two C–H···Br hydrogen bonds protruding out of the same TTF side. The structural characteristics of these



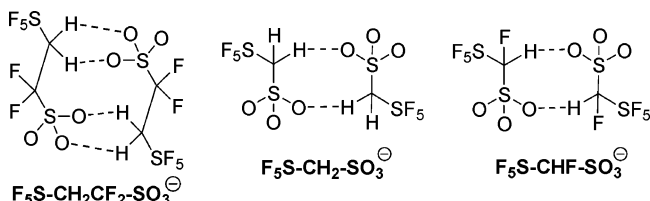
3.7

hydrogen bonds are collected in Table 11. The same principle apply for the Mo<sub>6</sub>Cl<sub>14</sub><sup>2–</sup> salt of **CF<sub>2</sub>**,<sup>122</sup> (CF<sub>2</sub>)<sub>2</sub>(Mo<sub>6</sub>Cl<sub>14</sub>), where two one-electron oxidized molecules now sandwich the metal cluster dianion to afford a robust trimolecular motif which further associates through overlap interaction into infinite alternated chains ... (CF<sub>2</sub>)<sub>2</sub>(Mo<sub>6</sub>Cl<sub>14</sub>)(CF<sub>2</sub>)<sub>2</sub>(Mo<sub>6</sub>Cl<sub>14</sub>).... In these salts, there is an interest in sorting the weight of the redox modulation of the TTF core out of the net hydrogen-bonding interaction. One way to reach a deeper insight on that matter would be to cocrystallize the neutral donor molecules **S**, **C=O**, or **CF<sub>2</sub>** with the same anions without oxidizing the donor molecules. This would demonstrate whether the radical cation TTF<sup>•+</sup> plays a significant role in the formation of such C–H···Hal bonded complexes.

### 3.3. C–H···O Hydrogen Bonding within the Anionic Network

Other examples of activated  $C_{sp^3}$ –H groups engaged in C–H···O hydrogen bonds were also found in the case of organic anions layers. For example, in their extensive series of BEDT-TTF salts based on sulfonate anions such as  $F_5S-CH_2-SO_3^-$ ,<sup>123</sup>  $F_5S-CHF-SO_3^-$ ,<sup>123</sup>  $F_5S-CH_2CF_2-SO_3^-$ ,<sup>124</sup> and  $F_5S-CHFCH_2-SO_3^-$ ,<sup>125</sup> Geiser and Schlueter observed the recurrent formation of C–H···O hydrogen bonds between anions,<sup>126</sup> giving rise to cyclic dianionic species as shown in Table 12.

**Table 12. Structural Characteristics of the C–H···O Hydrogen Bonds Observed in Sulfonated Anions**



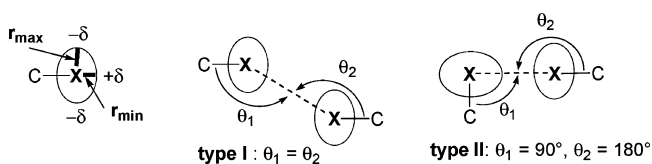
compound	(C–)H···X dist	C(–H)···X dist	C–H···X angle	ref
(ET) <sub>2</sub> (F <sub>5</sub> S–CH <sub>2</sub> CF <sub>2</sub> –SO <sub>3</sub> )	2.50	3.24	136	124
(ET) <sub>2</sub> (F <sub>5</sub> S–CH <sub>2</sub> –SO <sub>3</sub> )	2.61	3.33	132	123
(ET) <sub>2</sub> (F <sub>5</sub> S–CHF–SO <sub>3</sub> )	2.28	3.25	173	123
(ET) <sub>2</sub> (F <sub>5</sub> S–CHF–SO <sub>3</sub> )	2.21	3.19	174	123

## 4. Halogen Bonding

### 4.1. Halogen Bonding in the Solid State

The molecular interaction which occurs in the system X–Hal···B when a halogen atom approaches a Lewis base B has been the object of much investigation since the work of Guthrie, Remsen, and Norris.<sup>127</sup> The term halogen bonding was first introduced by Dumas et al.,<sup>128</sup> and their geometrical characteristics, established by Legon<sup>129</sup> in the gas phase in inorganic dihalogen complexes, have been recently investigated in detail in the solid state<sup>130</sup> and were found to also apply to organic halogens.<sup>21</sup> This interaction has been recently extensively used for the elaboration of extended networks based on halogenated molecules activated by fluorine atoms such as 1,2-diiodotetrafluoroethane or 1,4-diodo-2,3,5,6-tetrafluorobenzene, interacting with various amines (pyrazine, 4,4'-bipyridine, ...).<sup>131,132</sup> The halogen bonding interaction is essentially electrostatic in nature, the polarization, charge-transfer, and dispersion contributions notwithstanding.<sup>21</sup> These effects find their origin in the anisotropy of the electron density around the halogen nucleus, which leads to a smaller effective atomic radius along the extended C–Hal bond axis than that in the direction perpendicular to this axis. As exemplified in Chart 10, the latter is

**Chart 10**



represented by an ellipsoid elongated in the direction across the bonding axis, a feature called polar flattening. Thus, the electron-deficient region in the vicinity of the halogen atom is the direction of maximum attractive electrostatic interaction toward electron-rich (lone pairs) regions of Lewis bases.

Halogen bonding is characterized by (i) a Hal···B distance shorter than the sum of the van der Waals radii, (ii) a strong linearity of the C–Hal···B bond, in fact much stronger than that with hydrogen bonds, (iii) a preferred orientation of the C–Hal bond in the plane of the lone pair of B with a preference for the lone pair direction within that plane, and (iv) a tendency for stronger halogen bonding in the order  $I > Br > Cl$ .

These characteristics demonstrate that halogen bonding can be as effective as hydrogen bonding for driving highly specific crystal packing motifs, as investigated recently in competitive experiments where amines were faced with both C–I and C–OH groups, demonstrating even a preference for halogen bonding versus hydrogen bonding in the specific examples described.<sup>133</sup> Important Lewis bases to be considered are –O– and C=O groups as well as the corresponding sulfur and selenium analogues, amines ( $sp^3$  or  $sp^2$  as in pyridines), and NC– groups, in addition to halogen atoms themselves. Indeed, on the basis of statistical studies,<sup>134</sup> Desiraju and Parthasarathy have shown that Hal···Hal interactions can be divided into two groups according to their geometrical features. While both are characterized by Hal···Hal distances significantly shorter than the sum of the van der Waals radii of the contacting atoms, the shortest distances were found with the geometries described in Chart 10 with  $\theta_1 \approx 90^\circ$  and  $\theta_2 \approx 180^\circ$  (type II) while weaker interactions were characterized with the  $\theta_1 = \theta_2$  motif (type I). The type II motif corresponds to the halogen bonding described above, with these geometrical preferences originating from the electrostatic forces and repulsion anisotropy arising from the lone pair electron density of the halogen atom, with the equatorial electron-rich region of the electronic density interacting with the polar, electron-poor region.<sup>135</sup>

The comparison of observed contacts with the sum of van der Waals radii, albeit the most obvious way of elucidating specific interactions, crucially depends on the correct choice of these radii. The hard sphere models developed by Pauling,<sup>136</sup> and further by Bondi,<sup>137</sup> are based on the assumption that those radii are (i) additive and (ii) not affected by the nature of the other atom(s) to which the atom of interest is bonded or by the nature of the chemical bond(s) involved. Recent statistical approaches have shown that it might be still true for O and N but not for highly polarizable atoms that exhibit a strongly anisotropic shape (polar flattening) when forming a covalent bond.<sup>138</sup> Each atom (X) can thus be characterized by two effective radii: the shortest one ( $r_{min}$ ) in the prolongation of the C–X bond and the longer one ( $r_{max}$ ), close to Pauling/Bondi values, perpendicular to the C–X bond. As a consequence, the definition of close contacts for C–Hal···B interactions will strongly depend on the geometry (type I, type II) of

the interaction. For example, the I $\cdots$ Br distance in a C–I $\cdots$ Br interaction will be compared to the sum [ $r_{\max}(\text{I}) + r_{\max}(\text{Br})$ ] for a type I interaction, while the contact distance in the type II geometry will be [ $r_{\min}(\text{I}) + r_{\max}(\text{Br})$ ] (Chart 10). These contact distances, abbreviated as  $D_{\text{anis}}$  in the following, have been calculated on the basis of the  $r_{\max}/r_{\min}$  sets of values reported by Nyburg<sup>138</sup> and collected in Table 13 for the interactions of interest in this article.

**Table 13. Contact Distances Predicted by the Anisotropic Model<sup>138</sup>**

interaction	$D_{\text{anis}}$ (type I) (Å)	$D_{\text{anis}}$ (type II) (Å)
C–Cl $\cdots$ Cl	3.56	3.36
C–Br $\cdots$ Br	3.68	3.38
C–Br $\cdots$ I	3.97	3.67
C–I $\cdots$ Cl	3.91	3.54
C–I $\cdots$ Br	3.97	3.60
C–I $\cdots$ I	4.26	3.89
C–Cl $\cdots$ N		3.18
C–Br $\cdots$ N		3.14
C–I $\cdots$ N		3.36
C–I $\cdots$ O	3.67	3.30
C–I $\cdots$ S	4.16	3.79

Strong halogen bonding will then be considered to occur for Hal $\cdots$ B distances shorter than the  $D_{\text{anis}}$  value.

This interaction has been introduced very successfully in 1995 in the field of molecular conductors by Imakubo and Kato for controlling the solid-state organization of radical cation salts of iodotetrathiafulvalenes such as EDT-TTF–I with counterions of Lewis base character (Br $^-$ , Ag(CN) $_2^-$ ).<sup>139</sup> Halogen bonding interactions have been observed incidentally in neutral halogenated tetrathiafulvalenes while they have been purposely investigated as their radical cation salts. In the following section we will first describe the structures derived from a variety of

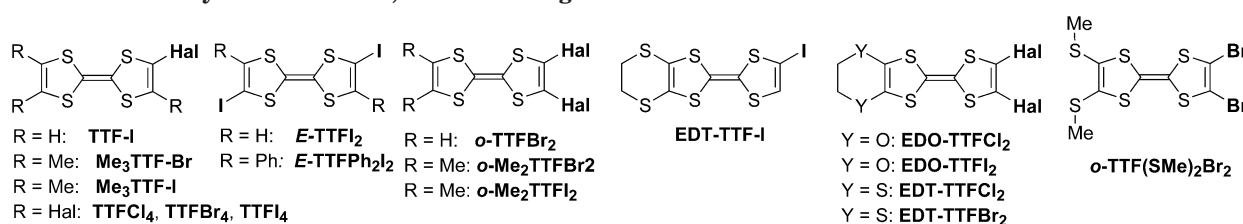
neutral halogenated TTFs and then investigate how these interactions are modified in their radical cation salts, particularly when oxidized halogenated TTFs are associated with counterions with Lewis base character.

## 4.2. Neutral Halogenated Tetrathiafulvalenes

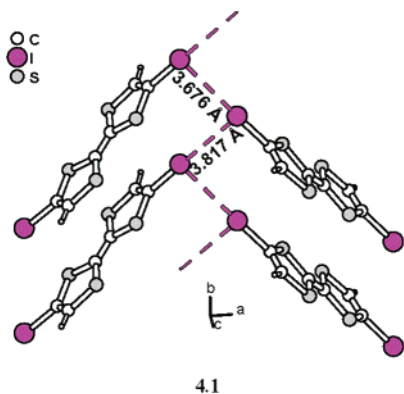
Among the numerous halogenated tetrathiafulvalenes the synthesis of which has been described so far, only a few have been crystallographically characterized. They are collected in Table 14. No specific Hal $\cdots$ Hal interactions are observed in tetrathiafulvalenes bearing only one halogen atom (Me $_3$ TTF–Br,<sup>140</sup> TTF–I,<sup>141</sup> Me $_3$ TTF–I,<sup>140</sup> EDT-TTF–I),<sup>142</sup> where most often the halogen atom is typically found to be disordered over several positions. Two examples of short type II contacts stand out, however, for *E*-TTFI $_2$  and *E*-TTFPh $_2$ I $_2$ . While *E*-TTFPh $_2$ I $_2$  is characterized<sup>143</sup> with longer I $\cdots$ I intermolecular distances (4.12(2) Å) and a type I motif ( $\theta_1 = \theta_2 = 120^\circ$ ), *E*-TTFI $_2$  exhibits much shorter I $\cdots$ I distances with the type II motifs shown in 4.1 (I $\cdots$ I = 3.676(3) Å,  $\theta_1 = 88.7(6)^\circ$ ,  $\theta_2 = 175.9(5)^\circ$  and I $\cdots$ I = 3.817(3) Å,  $\theta_1 = 87.7(5)^\circ$ ,  $\theta_2 = 175.9(6)^\circ$ ),<sup>141</sup> the signature of strong I $\cdots$ I halogen bonding.

Surprisingly, *ortho*-dihalo derivatives (*o*-Me $_2$ -TTFCl $_2$ ,<sup>144</sup> EDO-TTFCl $_2$ ,<sup>145</sup> EDT-TTFCl $_2$ ,<sup>146</sup> EDT-TTFBr $_2$ ,<sup>146</sup> *o*-TTFBr $_2$ ,<sup>147</sup> *o*-TTF(SMe) $_2$ Br $_2$ ,<sup>148</sup> *o*-Me $_2$ -TTFI $_2$ ,<sup>144</sup> EDO-TTFI $_2$ )<sup>145</sup> do not show any sizable Hal $\cdots$ Hal interactions but are organized instead into inversion-centered dyads, a recurrent feature for neutral TTF derivatives,<sup>149</sup> a likely manifestation of the large number of S $\cdots$ S van der Waals contacts which effectively overcome Hal $\cdots$ Hal interactions. Only in *o*-TTFBr $_2$  is a type I (Br $\cdots$ Br = 3.70 Å,  $D_{\text{anis}}$  = 3.68 Å) interaction identified,<sup>147</sup> note also that, in *o*-TTF(S(CH $_2$ ) $_2$ CN) $_2$ Br $_2$ ,<sup>140</sup> the Br $\cdots$ Br interaction ex-

**Table 14. Structurally Characterized, Neutral Halogenated TTF Derivatives**

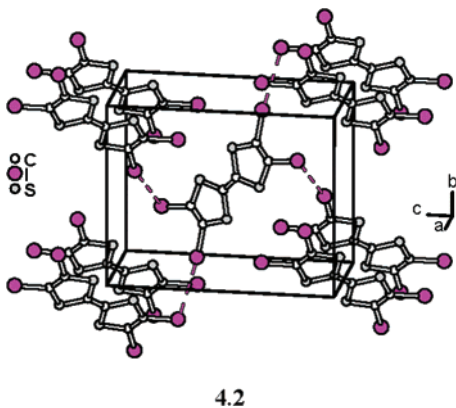


compound	structural characteristics	ref
Me $_3$ TTF–Br	disordered Br atom, isostructural with TMTTF	140
TTF–I	large lateral and longitudinal shift within stacks	141
Me $_3$ TTF–I	disordered I atom	140
EDT-TTF–I	inversion-centered dyads, S $\cdots$ S interactions	142
<i>E</i> -TTFI $_2$	I $\cdots$ I short contacts with type II motif	141
<i>E</i> -TTFPh $_2$ I $_2$	I $\cdots$ I contacts with type I motif	143
<i>o</i> -Me $_2$ TTFCl $_2$	disordered Cl atom, isostructural with TMTTF	144
EDO-TTFCl $_2$	Cl $\cdots$ Cl contacts with type I motif	145
EDT-TTFCl $_2$	inversion-centered dyads, S $\cdots$ S interactions	146
EDT-TTFBr $_2$	inversion-centered dyads, S $\cdots$ S interactions	146
<i>o</i> -TTFBr $_2$	large lateral shift within stacks	147
<i>o</i> -TTF(SMe) $_2$ Br $_2$	inversion-centered dyads, S $\cdots$ S interactions	148
<i>o</i> -TTFBr $_2$ (S(CH $_2$ ) $_2$ CN) $_2$	Br $\cdots$ Br contacts with type II motif	140
<i>o</i> -Me $_2$ TTFI $_2$	inversion-centered dyads	144
EDO-TTFI $_2$	inversion-centered dyads	145
TTFCl $_4$	Cl $\cdots$ Cl contacts with type I motif	144
TTFBr $_4$	isostructural with TTFCl $_4$	150
TTFI $_4$	I $\cdots$ I 3.85, 3.99 Å contacts with type II motif	140



hibits type II characteristics ( $\text{Br}\cdots\text{Br} = 3.57 \text{ \AA}$ ,  $\theta_1 = 97^\circ$ ,  $\theta_2 = 167^\circ$ ), albeit with a long  $\text{Br}\cdots\text{Br}$  distance ( $D_{\text{anis}} = 3.38 \text{ \AA}$ ).

Tetrasubstituted tetrathiafulvalenes proved to be an interesting playground for evaluating the evolution of  $\text{Hal}\cdots\text{Hal}$  interactions in the Cl/Br/I series. In  $\text{TTFCl}_4$ ,<sup>144</sup> numerous type I  $\text{Cl}\cdots\text{Cl}$  contacts are observed to be larger than  $3.63 \text{ \AA}$  with essentially a type I motif, indicating closed-packed rather than strong, directional  $\text{Cl}\cdots\text{Cl}$  interactions. The two shortest contacts, however, seem to indicate a tendency toward type II motifs with the following characteristics:  $3.63 \text{ \AA}$ ,  $\theta_1 = 86^\circ$ ,  $\theta_2 = 150^\circ$  and  $3.68 \text{ \AA}$ ,  $\theta_1 = 85^\circ$ ,  $\theta_2 = 149^\circ$ .  $\text{TTFBr}_4$  proved to be isostructural with  $\text{TTFCl}_4$ .<sup>150</sup> In  $\text{TTFI}_4$ ,<sup>140</sup> two symmetrically nonequivalent molecules (A and B), both possessing crystallographic inversion centers, segregate into homostacks AAA and BBB. Intrastack contacts ( $4.17\text{--}4.19 \text{ \AA}$ ) are closed-packed interactions with a type I motif while the two shorter interstack contacts shown in **4.2** ( $3.85 \text{ \AA}$ ,  $\theta_1 = 87^\circ$ ,  $\theta_2 = 166^\circ$  and  $3.99 \text{ \AA}$ ,  $\theta_1 = 101^\circ$ ,  $\theta_2 = 174^\circ$ ) are consistent with an attractive, type II motif, interaction.



Thus, by and large, halogen bonding in neutral TTF molecules is not efficient at controlling the solid-state organization and most often competes with the overall  $\text{S}\cdots\text{Hal}$  and  $\text{S}\cdots\text{S}$  van der Waals interactions. The latter are well-known to stabilize the formation of inversion-centered TTF face-to-face dyads,<sup>149</sup> the recurrent motif observed with *o*-dihalotetrathiafulvalenes while monosubstituted molecules are disordered in the solid state. On the other hand, the steric congestion introduced by four halogen atoms hinders the formation of the dyadic motif and favors close-

packed interactions in  $\text{TTFX}_4$  molecules with  $\text{X} = \text{Cl}$ ,  $\text{Br}$ , or  $\text{I}$ .

### 4.3. Radical Cation Salts of Halogenated Tetrathiafulvalenes

A distinction will be made among the various salts of halogenated tetrathiafulvalenes between (i) those incorporating halogenated anions ( $\text{Br}^-$ ,  $\text{IBr}_2^-$ ,  $\text{I}_3^-$ ), where  $\text{Hal}\cdots\text{Hal}$  interactions were expected, and (ii) those incorporating other heteroatoms as Lewis bases for  $\text{Hal}\cdots\text{B}$  interactions, essentially organic and inorganic nitriles where  $\text{Hal}\cdots\text{N}\equiv\text{C}$  interactions were anticipated.

#### 4.3.1. C–Hal $\cdots$ Hal<sub>anion</sub> Interactions

Crystals of neutral, chlorinated tetrathiafulvalenes exhibit at best close-packed  $\text{Cl}\cdots\text{Cl}$  interactions. Because of the strong electronegative character of the chlorine atom, Cl-substituted TTFs oxidize at higher potentials than the bromo or iodo derivatives<sup>151</sup> and their radical cation salts have not been investigated to any extent. A 2:1 salt of EDT- $\text{TTFCl}_2$  has been obtained by chemical oxidation with the strong TCNQF<sub>4</sub> oxidant,<sup>152</sup> while electrocrystallization experiments afforded a 1:1 salt with  $\text{ClO}_4^-$ , (EDT- $\text{TTFCl}_2$ )-( $\text{ClO}_4$ ), and with EDO- $\text{TTFCl}_2$  and (*n*-Bu<sub>4</sub>NPF<sub>6</sub>), a 2:1 salt formulated as (EDO- $\text{TTFCl}_2$ )<sub>2</sub>(PF<sub>6</sub>) was obtained.<sup>153</sup> Short type I  $\text{Cl}\cdots\text{Cl}$  contacts were only observed in (EDT- $\text{TTFCl}_2$ )<sub>2</sub>(TCNQF<sub>4</sub>) with  $\text{Cl}\cdots\text{Cl} = 3.42 \text{ \AA}$  and  $\theta_1 = \theta_2 = 126^\circ$ . Note also that a shorter type I contact ( $3.38 \text{ \AA}$ ,  $\theta_1 = \theta_2 = 146^\circ$ ) was observed in neutral EDO- $\text{TTFCl}_2$ .<sup>145</sup>

On the other hand, several salts of *o*-dibromotetrathiafulvalene derivatives have been synthesized, essentially with inorganic polyhalides such as  $\text{I}_3^-$  or  $\text{IBr}_2^-$  with the objective to promote cation $\cdots$ anion,  $\text{Br}\cdots\text{Br}$ , or  $\text{Br}\cdots\text{I}$  interactions. And indeed, such interactions have been clearly observed while they were essentially absent in the neutral donor molecules. For example, in the 1:1 [*o*-TTF(SMe)<sub>2</sub>Br<sub>2</sub>]- $\text{I}_3^-$  salt shown in **4.3**,<sup>140,148</sup> the shortest  $\text{Br}\cdots\text{I}$  ( $3.63 \text{ \AA}$ ,  $\theta_1 = 72^\circ$ ,  $\theta_2 = 164^\circ$ ) contact involves the terminal iodine atom of  $\text{I}_3^-$  ( $d_1$  in **4.3**). The  $\text{I}_3^-$  anion thus bridges two adjacent cations through  $\text{I}_3\cdots\text{Br}$  and  $\text{I}_3\cdots\text{S}$  ( $d_2$ ) contacts while a  $\text{I}_3\cdots\text{Br}$  ( $3.85 \text{ \AA}$ ,  $\theta_1 = 72^\circ$ ,  $\theta_2 = 164^\circ$ ) contact ( $d_3$ ) with a neighboring donor molecule along *c* results in the formation of an extended two-dimensional network.

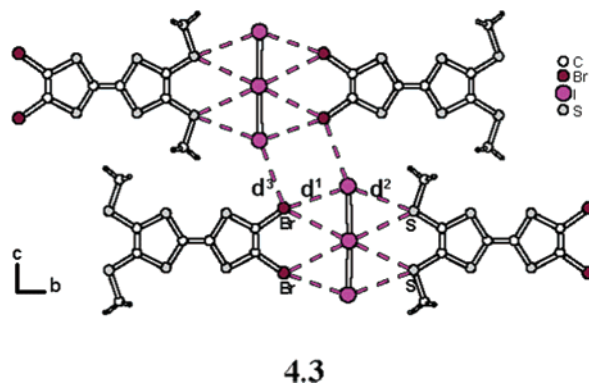
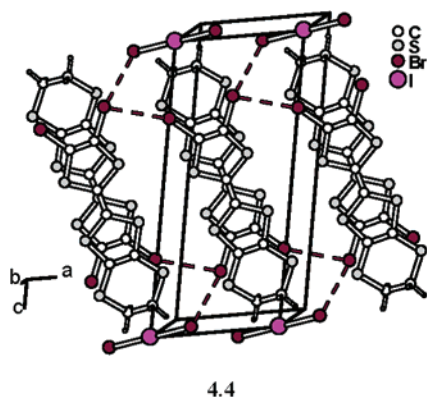


**Table 15. Structurally Characterized Radical Cation Salts of Halogenated TTFs with Hal...Hal Interactions<sup>a</sup>**

compound	$\rho$	Hal...Hal interactions	$\sigma_{RT}^b$ (S cm <sup>-1</sup> )	ref
(EDT-TTFCl <sub>2</sub> ) <sub>2</sub> (TCNQF <sub>4</sub> )	1/2	Cl...Cl 3.42 Å (type I)	1 (semicond)	152
(EDT-TTFCl <sub>2</sub> )(ClO <sub>4</sub> )	1	no	2 × 10 <sup>-3</sup> (semicond)	152
(EDO-TTFCl <sub>2</sub> ) <sub>2</sub> (PF <sub>6</sub> )	1/2	no	170 (metal, $T_{MI}$ = 262 K)	153
(EDO-TTFBr <sub>2</sub> ) <sub>3</sub> (I <sub>3</sub> )	1/3	Br...I 4.06 Å	10 (metal, $T_{MI}$ = 180 K)	153
[TTF(SMe) <sub>2</sub> Br <sub>2</sub> ]I <sub>3</sub>	1	<b>Br...I 3.63 Å (type II)</b> Br...I 3.85 Å (type II)	(2–8) × 10 <sup>-3</sup> (semicond)	140, 148
(EDT-TTFBr <sub>2</sub> ) <sub>2</sub> (IBr <sub>2</sub> )	1/2	Br...Br 3.46 Å (type II) Br...Br 3.42 Å (type II)	1 (semicond)	154
(EDT-TTFBr <sub>2</sub> ) <sub>2</sub> I <sub>3</sub>	1/2	Br...Br 3.51 Å (type II) <b>Br...I 3.51 Å (type II)</b>	0.5 (semicond)	154
(Me <sub>3</sub> TTF-I) <sub>2</sub> (I <sub>3</sub> ) <sub>2</sub> -(I <sub>2</sub> )	1	disordered I atom	10 <sup>-6</sup>	140
(EDT-TTF-I) <sub>2</sub> (Br)	1/2	<b>I...Br 3.21 Å (type II)</b>	1 (semicond)	139
(EDO-TTFI <sub>2</sub> ) <sub>2</sub> (I <sub>2</sub> )(I <sub>2</sub> )	1	<b>I...I 3.40 Å (type II)</b>	2 × 10 <sup>-3</sup> (semicond)	155
(EDT-TTFI <sub>2</sub> ) <sub>2</sub> I <sub>3</sub>	1/2	<b>I...I 3.60 Å (type II)</b> <b>I...I 3.55 Å (type II)</b>	10 (semicond)	154
(EDT-TTFI <sub>2</sub> ) <sub>2</sub> (Pb <sub>5/6</sub> I <sub>2</sub> ) <sub>3</sub>	1/2	I...I 3.81–4.09 Å	2.5 (metal, $T_{MI}$ = 70 K)	158
(EDT-TTFI <sub>2</sub> ) <sub>2</sub> (Pb <sub>2/3+x</sub> Ag <sub>1/3-2x</sub> O <sub>x</sub> I <sub>2</sub> ) <sub>3</sub>	1/2	I...I 3.81–4.09 Å	110 (metal, $T_{MI}$ = 70 K)	158
(EDT-TTFI <sub>2</sub> ) <sub>2</sub> (PbI <sub>3</sub> )	1/2	<b>I...I 3.57–3.71 Å (type II)</b>	20 (metal, $T_{MI}$ = 150 K)	157
(TTFI <sub>4</sub> )I	1	<b>I...I 3.37, 3.42 Å</b>	insulator	156

<sup>a</sup> In bold are indicated those Hal...Hal distances markedly shorter than the  $D_{anis}$  distances (see text for definition and Table 13 for corresponding values). <sup>b</sup>  $T_{MI}$  = metal–insulator transition temperature.

In the 2:1 I<sub>3</sub><sup>-</sup> and IBr<sub>2</sub><sup>-</sup> salts of EDT-TTFBr<sub>2</sub>,<sup>154</sup> organic slabs adopt the so-called  $\beta'$  structure of BEDT-TTF salts. Two short Hal...Hal contacts shown in 4.4 are identified, one between donor molecules (Br...Br = 3.46 Å,  $\theta_1 = 97^\circ$ ,  $\theta_2 = 152^\circ$  in the IBr<sub>2</sub><sup>-</sup> salt, Br...Br = 3.51 Å,  $\theta_1 = 98^\circ$ ,  $\theta_2 = 150^\circ$  in the I<sub>3</sub><sup>-</sup> salt) and one between EDT-TTFBr<sub>2</sub> and the terminal atom of either (Br–I–Br)<sup>-</sup> (Br...Br<sub>anion</sub> = 3.42 Å,  $\theta_1 = 109^\circ$ ,  $\theta_2 = 165^\circ$ ) or I<sub>3</sub><sup>-</sup> (Br...I<sub>anion</sub> = 3.51 Å,  $\theta_1 = 110^\circ$ ,  $\theta_2 = 165^\circ$ ) anion, with both having the characteristics of a strong, type II halogen bond. Moreover,

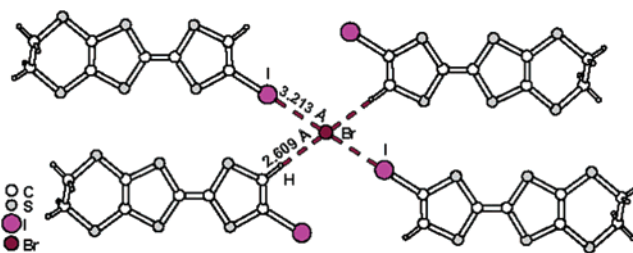


4.4

it was shown that the presence of Hal...Hal interactions between the partially oxidized molecules contributes not only to the structural stabilization but also to the electronic delocalization. Indeed, the presence of nonzero atomic coefficients on the halogen atoms in the HOMO of EDT-TTFBr<sub>2</sub> or EDT-TTFI<sub>2</sub>, together with the short Hal...Hal contacts, leads to a sizable increase of the band dispersion and stabilizes a rare  $\beta'$  structure through the side-by-side arrangement of the inversion-centered dyads connected by Hal...Hal interactions. Both salts are semiconductors with room-temperature conductivities around 1 S cm<sup>-1</sup>, a large value when compared with other  $\beta'$  structures such as  $\beta'$ -(BEDT-TTF)<sub>2</sub>(ICl<sub>2</sub>) (see Table 15).

(EDT-TTF-I)<sub>2</sub>Br, reported in 1995 by Imakubo and Kato, is the first, seminal, and elegant example of

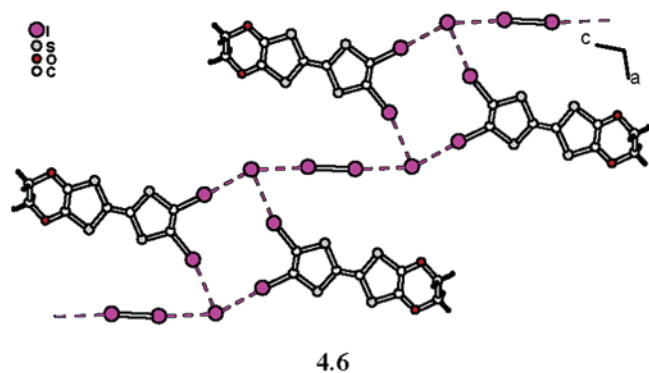
halogen bonding in tetrathiafulvalene salts.<sup>139</sup> As exemplified in 4.5, two partially oxidized EDT-TTF-I molecules are linked to the bromide anion via a perfectly linear and very short (3.21 Å,  $D_{anis} = 3.60$  Å) I...Br contact. Note also the stabilizing contribution of two C–H...Br<sup>-</sup> hydrogen bonds from two neighboring donor molecules, whose structural characteristics (H...Br = 2.61 Å, C–H...Br = 177°) are well in the range described in section 3 for such interactions. As a consequence of both halogen and hydrogen bonding, all four molecules and bromide anion are fully coplanar. The salt is a semiconductor with  $\sigma_{RT} = 1$  S cm<sup>-1</sup> and an activation energy of 51 meV.



4.5

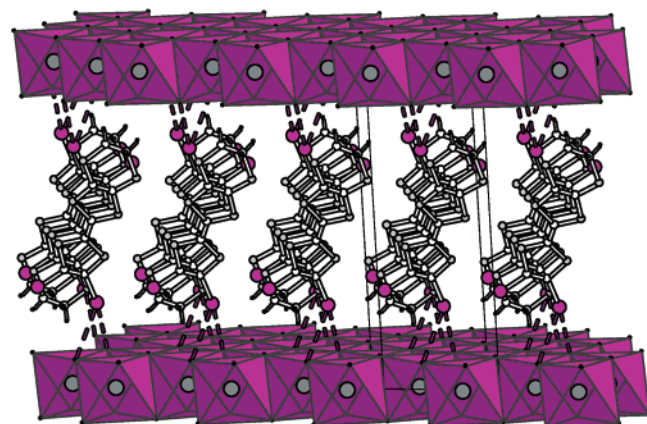
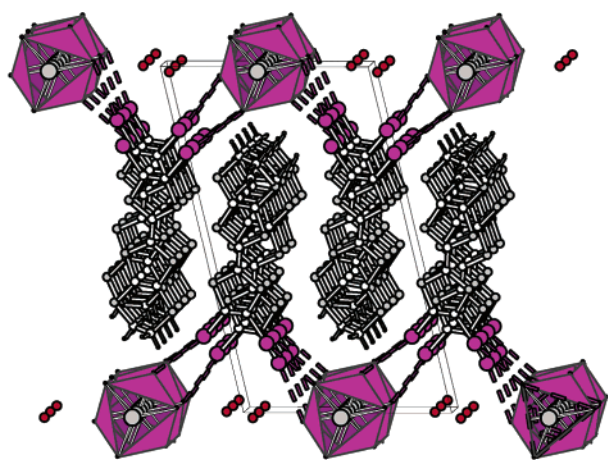
Other examples of strong I...I interactions are found in the 1:1 salt<sup>155</sup> (EDO-TTFI<sub>2</sub>)<sub>2</sub>(I<sub>2</sub>)·(I<sub>2</sub>), where two donor molecules are linked to two I<sup>-</sup> anions through the short and linear contacts (3.40 Å,  $\theta_2 = 163^\circ$ ,  $173^\circ$ ) shown in 4.6. Further interaction of I<sup>-</sup> with a diiodine molecule (I...I = 3.40 Å) actually generates I<sub>4</sub><sup>2-</sup> species and an extended halogen bonded network running along  $a + c$ . Finally, very short I...I<sup>-</sup> halogen bonds (3.37 Å, 3.41 Å) afford a three-dimensional structure also in the 1:1 iodide salt of TTFI<sub>4</sub>, (TTFI<sub>4</sub>)I.<sup>156</sup>

These salts clearly emphasize that oxidation of EDT-TTF-I, EDT-TTFI<sub>2</sub>, or TTFI<sub>4</sub> into a radical cation increases the electron-deficient character of the polar region of the electronic cloud of the iodine atoms for an enhanced electrostatic interaction with



the negatively charged anions, since such interactions were not observed in the different neutral molecules. The observations that the strongest interactions are found in fully oxidized salts ( $\rho = 1$ ) and with the monatomic anions ( $\text{Br}^-$ ,  $\text{I}^-$ ) confirm, if necessary, the electrostatic character of the interaction.

This last point is illustrated by the superb structures of two salts of EDT-TTFI<sub>2</sub> with the polymeric 1D  $\text{PbI}_3^-$  and 2D  $(\text{Pb}_{5/6}\square_{1/6}\text{I}_2)_3^-$  anions ( $\square =$  lead vacancy) where shorter  $\text{C-I}\cdots\text{I}_{\text{anion}}$  contacts are observed with the linear  $\text{PbI}_3^-$  chains (4.7)<sup>157</sup> with a charge per iodine atom of  $-0.33$ , when compared with the two-dimensional  $(\text{Pb}_{5/6}\square_{1/6}\text{I}_2)_3^-$  layers<sup>158</sup> shown in 4.8, where the charge per iodine atom amounts to  $-0.17$  for the same oxidation state of EDT-TTFI<sub>2</sub> ( $\rho$



$= 0.5$ ). In the latter, the inorganic layers exhibit the  $\text{CdI}_2$  structure type, as observed in the neutral, layered hexagonal  $\text{PbI}_2$ ,<sup>159</sup> thus providing the first and long awaited example of crystal structures of  $\text{PbI}_2$  intercalation compounds. The exact negative charge of the layer is governed by the presence of a specific number of lead vacancies. The shortest  $\text{I}_{\text{donor}}\cdots\text{I}_{\text{anion}}$  distances (3.81, 4.09 Å; see 4.8), albeit longer than those in the other salts described above, are still much shorter than the  $\text{I}\cdots\text{I}$  separation across the van der Waals gap in  $2H\text{-PbI}_2$  (4.95 Å). Attempts to fill the vacancies of the inorganic  $(\text{Pb}_{5/6}\square_{1/6}\text{I}_2)_3^-$  layers and manipulate the electronic properties by alloying the metal site with monovalent  $\text{Ag}^+$  cations afforded a lead-silver alloy, formulated as  $(\text{EDT-TTFI-I})_2\text{-}(\text{Pb}_{2/3+x}\text{Ag}_{1/3-2x}\square_x\text{I}_2)_3$ ,  $x \approx 0.05$ , with the same mixed-valence state for the donor molecules ( $\rho = 1/2$ ). Both salts exhibit a metallic behavior at room temperature ( $\text{Pb}$ :  $\sigma_{\text{RT}} = 2.5 \text{ S cm}^{-1}$ ,  $T_{\text{MI}} = 70 \text{ K}$ .  $\text{Pb-Ag}$ :  $\sigma_{\text{RT}} = 110 \text{ S cm}^{-1}$ ,  $T_{\text{MI}} = 70 \text{ K}$ ) associated with a  $\beta$ -type organization of the EDT-TTFI-I<sub>2</sub> in the organic slabs despite their pseudo-1D electronic structure. On the other hand,  $(\text{EDT-TTFI}_2)(\text{PbI}_3)$  adopts a  $\beta'$  structure and exhibits metallic conductivity ( $\sigma_{\text{RT}} = 20 \text{ S cm}^{-1}$ ) down to 70 K.<sup>157</sup>

Finally, it should be stressed here that most of the mixed valence salts described above exhibit, together with halogen bonding at the organic-inorganic interface, the typical pseudo-1D or -2D organization of the organic part, with their associated Fermi surfaces and highly conducting behavior. In other words, halogen bonding and band formation are able to express themselves in unison, with the added value of the involvement of the halogen atom in the band dispersion.

#### 4.3.2. $\text{C-Hal}\cdots\text{O}, \text{S}_{\text{anion}}$ Interactions

Besides the  $\text{C-Hal}\cdots\text{Hal}$  interactions described above, there are a few examples of well characterized  $\text{C-Hal}\cdots\text{O}$  or  $\text{C-Hal}\cdots\text{S}$  interactions in TTF radical cation salts (Table 16). For example, in  $(\text{EDO-TTFI}_2)_2\text{-}(\text{ClO}_4)$ ,<sup>155</sup> one iodine atom of each of the two crystallographically independent EDO-TTFI<sub>2</sub> molecules is engaged in a  $\text{C-I}\cdots\text{O}$  interaction with the oxygen atom of the ethylenedioxy moiety of neighboring

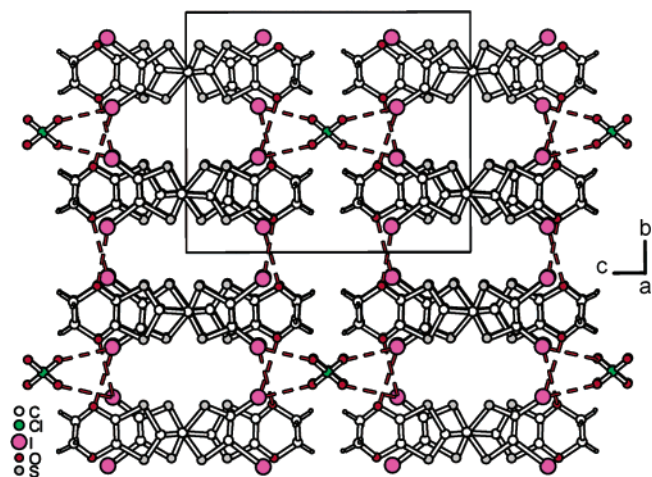




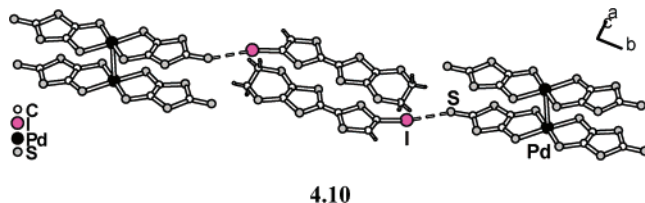
**Table 16. Structurally Characterized Radical Cation Salts of Halogenated TTFs with Hal...O or Hal...S Interactions<sup>a</sup>**

compound	I...O(S)	C-I...O(S)	I...O(S)-X	$\nu_{\text{RT}}$ (S cm <sup>-1</sup> )	ref
(EDO-TTFI <sub>2</sub> ) <sub>2</sub> (ClO <sub>4</sub> )	3.20 (ClO <sub>4</sub> )	153	151	70 (metal, $T_{\text{MI}} = 50$ K)	155
	3.43 (O)	141	151		
	3.24 (ClO <sub>4</sub> )	151			
	3.28 (O)	141			
	3.42(O)	142			
	3.32 (O)	137			
(TTF-I)-[ <i>p</i> -C <sub>6</sub> H <sub>4</sub> (NO <sub>2</sub> ) <sub>2</sub> ]	3.19 Å (O)	161	107	neutral complex	160
(TTF-I)(HSO <sub>4</sub> )	2.92 Å (O)	167	127	$5 \times 10^{-7}$	97
(EDT-TTF-I)[Pd(dmit) <sub>2</sub> ]	3.31 Å (S)	166	128	300 (metal to 4.2 K)	161

<sup>a</sup> Bond distances are in angstroms; bond angles are in degrees.

molecules along *b* while the other iodine atom is linked through two C-I...O interactions to both a donor molecule and the ClO<sub>4</sub><sup>-</sup> anion (**4.9**).

Two iodotetrathiafulvalene (TTF-I) derivatives have been described: (i) (TTF-I)·[*p*-C<sub>6</sub>H<sub>4</sub>(NO<sub>2</sub>)<sub>2</sub>] with alternating stacks of neutral donor and *p*-dinitrobenzene acceptor<sup>160</sup> and (ii) (TTF-I)(HSO<sub>4</sub>) with dyads of fully oxidized (TTF-I)<sup>+</sup> radical cation with HSO<sub>4</sub><sup>-</sup> as counterion.<sup>97</sup> In both derivatives, a type II geometry characterizes the C-I...O interaction, with the I...O-N(S) angle close to 120°, an indication of a preferred orientation of the C-I bond toward the lone pairs of the oxygen atom. The lone pair orientation effect is more clearly evidenced in (EDT-TTF-I)[Pd(dmit)<sub>2</sub>] shown in **4.10**, where inversion-centered (EDT-TTF-I)<sub>2</sub><sup>2+</sup> dyads are linked to [Pd(dmit)<sub>2</sub>]<sub>2</sub><sup>2-</sup> dyads stabilized through a Pd-Pd interaction.<sup>161</sup>



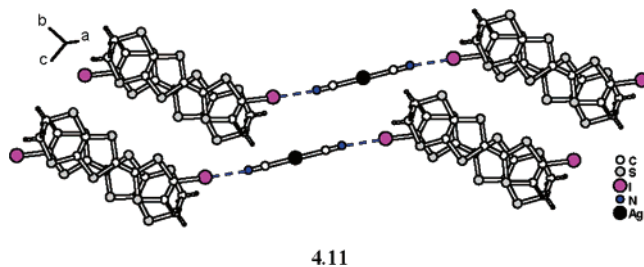
4.10

### 4.3.3. C-Hal...N Interactions

The first and most striking example of an Hal...N≡C interaction in radical cation salts of halogenated TTF's was reported by Imakubo and Kato in (EDT-TTF-I)<sub>2</sub>[Ag(CN)<sub>2</sub>].<sup>139</sup> Other systems have been described later with such complex cyanide anions, either square planar [Pt(CN)<sub>4</sub>]<sup>2-</sup>, [Au(CN)<sub>4</sub>]<sup>-</sup> or octahedral [Cr(CN)<sub>6</sub>]<sup>3-</sup>,<sup>162</sup> [Fe(CN)<sub>5</sub>(NO)]<sup>2-</sup><sup>163</sup> metal complexes. They will be described first, followed by those examples described with *organic* nitriles, such as dithiolene complexes with CN substituents (Table 17).

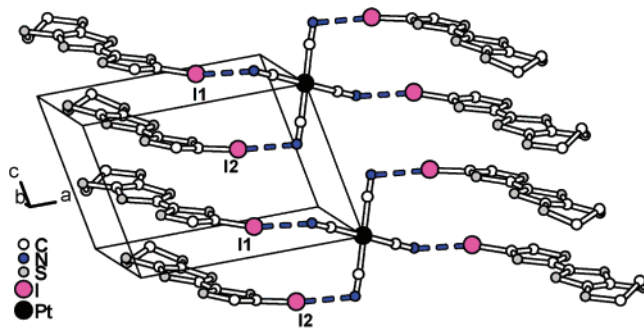
In (EDT-TTF-I)<sub>2</sub>[Ag(CN)<sub>2</sub>], a very short (2.88 Å,  $D_{\text{anis}} = 3.36$  Å) and linear interaction shown in **4.11** joins together two EDT-TTF-I molecules around a Ag(CN)<sub>2</sub><sup>-</sup> anion.<sup>139</sup> Note also the perfect match between the number of iodine and nitrogen atoms, which allows all halogen bonding interactions to be fulfilled in the present 2:1 stoichiometry.

Similarly, in the isostructural 4:1 (EDT-TTF-I)<sub>4</sub>[Pt(CN)<sub>4</sub>] and (EDT-TTF-I)<sub>4</sub>[Pd(CN)<sub>4</sub>] salts shown in **4.12**,<sup>164</sup> dimerized stacks of mixed-valence EDT-



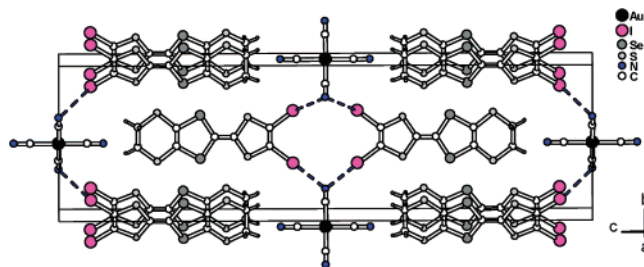
4.11

TTF-I molecules are connected through the M(CN)<sub>4</sub><sup>2-</sup> anion with an exact match between the number of available iodine and nitrogen atoms.

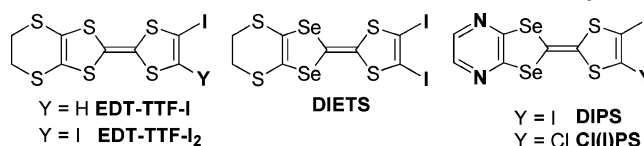


4.12

*o*-Diodotetrathiafulvalene donor molecules such as DIEST or EDT-TTFI<sub>2</sub> afforded several mixed valence salts with either [Ni(CN)<sub>4</sub>]<sup>2-</sup>,<sup>165</sup> [Pt(CN)<sub>4</sub>]<sup>2-</sup>,<sup>165</sup> [Pd(CN)<sub>4</sub>]<sup>2-</sup>,<sup>165</sup> [Au(CN)<sub>4</sub>]<sup>-</sup>,<sup>166</sup> [Cr(CN)<sub>6</sub>]<sup>3-</sup>,<sup>162</sup> or [Fe(CN)<sub>5</sub>(NO)]<sup>2-</sup>.<sup>163</sup> They all exhibit short I...N≡C interactions, most of them bifurcated, that is, with two iodine atoms linked to one NC group, as shown in **4.13** for *θ*-(DIEST)<sub>2</sub>-[Au(CN)<sub>4</sub>]. As a consequence, the halogen bond is no



4.13

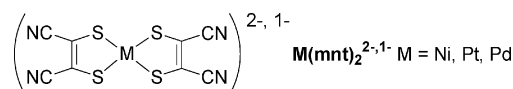
**Table 17. Structurally Characterized Radical Cation Salts of Iodo TTFs with Cyano Anions<sup>a</sup>**

compound	I···N(≡C) distance	C–I···N and I···N≡C angles <sup>b</sup> (deg)	$\sigma_{\text{RT}}^c$ (S cm <sup>-1</sup> )	ref
(EDT-TTF–I) <sub>2</sub> [Ag <sub>2</sub> (CN) <sub>2</sub> ]	<b>2.88 Å</b>	<b>177, 153</b>	semicond	139
(EDT-TTF–I) <sub>4</sub> [Pt(CN) <sub>4</sub> ]	3.07 Å	173, 98	semicond	164
	3.14 Å	167, 119		
(EDT-TTF–I) <sub>4</sub> [Pd(CN) <sub>4</sub> ]	3.07 Å	173, 98	metal ( $T_{\text{MI}} = 130$ K)	164
	3.14 Å	167, 119		
(DIETS) <sub>4</sub> [Pd(CN) <sub>4</sub> ]	2.95 Å	171, 143 (bif)	$2 \times 10^2$	165
	3.11 Å	174, 107 (bif)	(metal, $T_{\text{MI}} = 100$ K)	
$\theta$ -(DIETS) <sub>2</sub> [Au(CN) <sub>4</sub> ]	3.02 Å	174, 131 (bif)	5 (metal, $T_{\text{MI}} = 226$ K)	166
			$T_c = 8.6$ K @ 10 kbar/c)	
(DIETS) <sub>8</sub> (Cl) <sub>2</sub> (Cr(CN) <sub>6</sub> ) <sub>2.3</sub>	2.72 Å		1 ( $E_a = 65$ meV)	162
(DIETS) <sub>3</sub> (Et <sub>4</sub> N)(Cr(CN) <sub>6</sub> )	3.50 Å		0.2 ( $E_a = 175$ meV)	162
(EDT-TTF–I) <sub>3</sub> [Fe(CN) <sub>5</sub> NO]	2.93 Å	177, 102 (bif)	5 ( $E_a = 30$ meV)	163
(DIETS) <sub>4</sub> [Fe(CN) <sub>5</sub> NO]	3.07 Å	172, 117 (bif)	$2 \times 10^{-2}$ ( $E_a = 60$ meV)	163
	3.07 Å	169, 120 (bif)		
	<b>3.10 Å</b>	<b>167, 159</b> (bif)		
	3.25 Å	165, 101 (bif)		
(EDT-TTFI <sub>2</sub> ) <sub>4</sub> [Fe(CN) <sub>5</sub> NO]	3.08 Å	172, 117 (bif)	$10^{-6}$	163
	3.08 Å	170, 114 (bif)		
	<b>3.11 Å</b>	<b>168, 157</b> (bif)		
	3.25 Å	166, 100 (bif)		
(TTF–I) <sub>2</sub> [Pd(mnt) <sub>2</sub> ]	<b>3.04 Å</b>	<b>175, 173</b>	$2 \times 10^{-6}$	97
(EDO-TTFI <sub>2</sub> ) <sub>2</sub> [Ni(mnt) <sub>2</sub> ]	<b>3.04 Å</b>	<b>169, 165</b>	110 (metal, $T_{\text{MI}} = 110$ K)	169
(EDO-TTFI <sub>2</sub> ) <sub>2</sub> [Pt(mnt) <sub>2</sub> ]	<b>3.05 Å</b>	<b>169, 167</b>	170 (metal, $T_{\text{MI}} = 110$ K)	169
(EDT-TTF–I) <sub>2</sub> [Ni(mnt) <sub>2</sub> ]	<b>2.93 Å</b>	<b>178, 172</b>		142
(EDT-TTFI <sub>2</sub> ) <sub>2</sub> [Ni(mnt) <sub>2</sub> ]	<b>2.95 Å</b>	<b>177, 172</b>	$6 \times 10^{-3}$ ( $E_a = 140$ meV)	142
(EDO-TTF–I)–TCNQ	3.07 Å	173, 141		
(DIPS) <sub>3</sub> (PF <sub>6</sub> )–(PhCl) <sub>1.15</sub>	<b>2.88 Å</b>	<b>178</b>	10 ( $E_a = 50$ meV)	170
(DIPS) <sub>3</sub> (PF <sub>6</sub> )–(CH <sub>2</sub> Cl) <sub>1.66</sub>	<b>2.87 Å</b>	<b>178</b>	10 ( $E_a = 50$ meV)	170
(DIPS) <sub>3</sub> (PF <sub>6</sub> )–(C <sub>2</sub> H <sub>3</sub> Cl <sub>3</sub> ) <sub>1.3</sub>	<b>2.84 Å</b>	<b>178</b>	10 ( $E_a = 50$ meV)	170

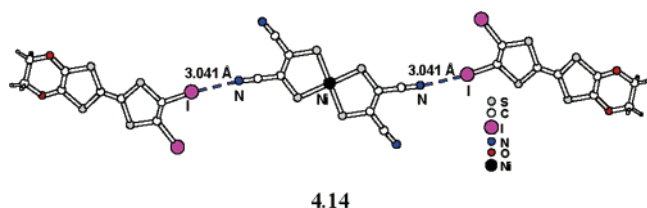
<sup>a</sup> In bold are indicated those I···N≡C distances markedly shorter than the  $D_{\text{anis}}$  distance, here 3.36 Å. <sup>b</sup> bif = bifurcated halogen bond C–Hal···N···Hal–C. <sup>c</sup>  $T_{\text{MI}}$  = metal-to-insulator transition temperature;  $T_c$  = superconducting transition temperature;  $E_a$  = activation energy at room temperature in the semiconducting regime.

longer fully linear but the I···N≡C angle is now close to 120°. As often observed with hydrogen bonds, the presence of such bifurcated halogen bonds finds its origin in the number of halogen bond acceptors (here the CN groups), largely exceeding the number of available iodine atoms. Among those salts,  $\theta$ -(DIEST)<sub>2</sub>–[Au(CN)<sub>4</sub>] exhibits a peculiar electronic behavior.<sup>167</sup> Under hydrostatic pressure, the sharp (semi)metal–insulator transition observed at 226 K was gradually suppressed but still present under 18 kbar. However, when applying a uniaxial strain along *c*, the (semi)metal–insulator transition around 226 K was mostly suppressed at 5 kbar while a superconducting transition ( $T_c = 8.6$  K) was observed at 10 kbar. As stated by Imakubo, the large anisotropy of the pressure effect (superconductivity is not observed with uniaxial strain along *a* or *b*) could be related to the presence of strong halogen bonding. While electrocrystallization experiments with [Cr(CN)<sub>6</sub>]<sup>3-</sup> afforded complex salts,<sup>162</sup> the analogous nitroprusside salts with EDT-TTF–I,<sup>142</sup> EDT-TTFI<sub>2</sub>, and DIEST were prepared<sup>163</sup> as an approach for possible photochromic organic conductors. The changes in geometry of the excited states of the nitroprusside anion are expected to affect the conducting properties more efficiently through the strong donor···anion halogen bonding interactions. All three salts exhibit bifurcated halogen bonds and a semiconducting behavior.

Salts of halogenated tetrathiafulvalenes—essentially iodo derivatives—are also described with dithiolene complexes of the 1,2-dicyanoethylene dithiolate (mnt) ligand. They are particularly attractive, since they can combine the conductive behavior of the organic slabs with the magnetic ( $S = 1/2$ ) properties of the [M(mnt)<sub>2</sub>]<sup>-</sup> (M = Ni, Pt, Pd) dithiolene complexes (Chart 11).<sup>168</sup>

**Chart 11**

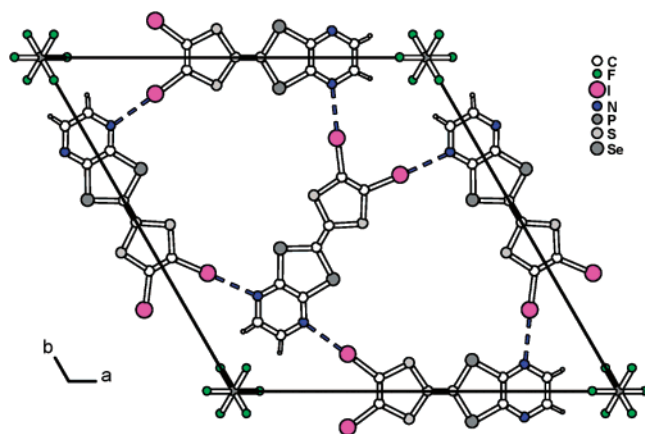
In every M(mnt)<sub>2</sub><sup>2-, 1-</sup> salt reported with either TTF–I,<sup>97</sup> EDT-TTF–I,<sup>142</sup> EDO-TTFI<sub>2</sub>, or<sup>169</sup> EDT-TTFI<sub>2</sub>,<sup>142</sup> short and strongly linear interactions are observed, as shown in 4.14 for (EDO-TTFI<sub>2</sub>)<sub>2</sub>[Ni(mnt)<sub>2</sub>];<sup>169</sup> that is, not only the C–Hal···N but also the Hal···N≡C angles are close to 180°, indicating an enhanced directionality of the lone pair of the sp N atom in these organic CN groups, when compared with inorganic complexes of the CN<sup>-</sup> ligand. However, those dithiolene complexes have been stabilized for different oxidation states, and a given salt such as (TTF–I)<sub>2</sub>[Pd(mnt)<sub>2</sub>] can be alternatively formulated as a mixed valence (TTF–I)<sub>2</sub><sup>1+</sup>[Pd(mnt)<sub>2</sub>]<sup>1-</sup> salt of the paramagnetic [Pd(mnt)<sub>2</sub>]<sup>1-</sup> anion or a



4.14

(TTF-I)<sup>•+</sup> salt of the dianionic, diamagnetic [Pd(mnt)<sub>2</sub>]<sup>2-</sup>. The latter, electronically silent situation was identified indeed in (TTF-I)<sub>2</sub>[Pd(mnt)<sub>2</sub>] and (EDT-TTF-I)[Ni(mnt)<sub>2</sub>] while mixed-valence salts were found in (EDO-TTFI<sub>2</sub>)[Ni(mnt)<sub>2</sub>], (EDO-TTFI<sub>2</sub>)[Pt(mnt)<sub>2</sub>], and (EDT-TTFI<sub>2</sub>)[Ni(mnt)<sub>2</sub>]. In EDO-TTFI<sub>2</sub> salts,<sup>169</sup> segregated stacks of donor and dithiolene complexes are connected through the halogen bonds. The metallic behavior of the conductivity originates from the EDO-TTFI<sub>2</sub> stacks with the <sup>3</sup>/<sub>4</sub> filled state while the magnetic contribution of the *S* = 1/2 [M(mnt)<sub>2</sub>]<sup>-</sup> anions is well fitted with a one-dimensional ferromagnetic chain model. The electronic coupling between both systems, eventually through the halogen bonds, is further demonstrated by the observation of a single broad ESR signal.

Another striking example of halogen bonding in TTF-based conducting systems is provided by the PF<sub>6</sub><sup>-</sup> salts of the DIPS molecule (see scheme in Table 17).<sup>170</sup> This donor bears not only two iodine atoms but also two sp<sup>2</sup> nitrogen atoms incorporated in a fused pyrazine ring. Electrocrystallization in the presence of PF<sub>6</sub><sup>-</sup> anions afforded 3:1 salts incorporating solvent molecules, which crystallize in a hexagonal *P6<sub>3</sub>/mcm* space group, as shown in 4.15, where the solvent molecules (PhCl, CH<sub>2</sub>Cl<sub>2</sub>, C<sub>2</sub>H<sub>3</sub>Cl<sub>3</sub>) have been omitted for clarity. Donor molecules are orga-



4.15

nized into triangular motifs stabilized by a strong and directional C-I...N interaction (2.84–2.88 Å, *D*<sub>anis</sub> = 3.36 Å), among the shortest described in this review. The rigidity of this triangular motif allows for the formation of channels, occupied by the solvent molecules, a very promising example of an “organic zeolite”. To evaluate the evolution within the Cl/Br/I series, the heterohalogenated chloro/iodo I(Cl)PS molecule (see chart in Table 17) was also prepared, and its structure,<sup>171</sup> in the neutral state,

confirms indeed the stronger affinity of the nitrogen atom for the iodine rather than for the chlorine atom with a sizable C-I...N interaction (3.08 Å, *D*<sub>anis</sub> = 3.36 Å), albeit longer than that in the salts of DIPS for example, in accordance with the general observation that the stronger is the charge, the stronger is the interaction.

#### 4.3.4. Evolution of Halogen Bonding in TTF Salts

Several questions have arisen in the course of the cross-examination of the crystal structures of the different donor molecules and those of their salts: (i) how much are the crystallographic and electronic structures of the salts modified/influenced by the presence of halogen bonding, and (ii) how much is halogen bonding itself modified/influenced in these radical cation salts?

The first point is that the presence of halogen bonding interactions in TTF salts does not hinder the formation of the characteristic one-dimensional or two-dimensional structures found with nonfunctionalized donor molecules such as TMTTF, TMTSF, BEDT-TTF, or EDT-TTF. Thus, sizable overlap between partially oxidized molecules allows for the formation of conduction bands whose dispersion is large enough to allow for a metallic behavior. Also, and contrariwise to the effect of hydrogen-bonding groups, the halogen atoms, directly linked to the TTF π system, contribute significantly to the HOMO of the donor molecules and therefore also to the dispersion of the bands deriving from that HOMO. It is therefore tempting to take advantage of this interaction to electronically connect the conducting 1D or 2D organic system with an anionic network blessed with another functionality (magnetism, photochromism, chirality, ...). First attempts along those lines (paramagnetic M(mnt)<sub>2</sub><sup>-</sup> dithiolene complexes, photochromic nitroprusside anions, luminescent PbI<sub>2</sub> layers) are very promising for the elaboration of multifunctional systems. On the other hand, the absence of any superconducting systems among those salts can be surprising. While studying in detail the organic–inorganic interface in BEDT-TTF salts with IBr<sub>2</sub><sup>-</sup>, AuI<sub>2</sub><sup>-</sup>, and I<sub>3</sub><sup>-</sup> anions, Whangbo<sup>172</sup> postulated that superconductivity was in fact related to the presence of a low-frequency phonon spectrum, attributable to translational and/or librational modes of vibration of BEDT-TTF molecules. This softness of the phonon spectrum would be correlated to weak C-H...Hal hydrogen bonds at the organic–inorganic interface which reach maximum strength for the most polarizable atoms. In that respect, the occurrence of strong hydrogen or halogen bond links between the conducting and anionic subnetworks may turn out to be a *cul-de-sac* with respect to the quest for superconductivity.

Concerning halogen bonding itself, the strongest interactions described so far in the literature are indeed found here, in the radical cation salts of halogenated TTF, where the electrostatic component of the interaction is strongly enhanced. All C-I...N contacts described in Table 10 are much shorter than the prototypical C-I...N interaction found in *p*-iodobenzonitrile (3.13 Å),<sup>173</sup> where the iodine atom

**Table 18. Inventory of the Available Structures of Radical Cation Halides with an Additional Neutral Iodinated Molecule Incorporated into the Anionic Network<sup>a</sup>**

compound	$\rho$	Hal...Hal interactions	state	ref
(ET) <sub>2</sub> Cl(DIA)	1/2	C-I...Cl <sup>-</sup> 3.04 Å	metal down to 1.6 K	178
(ET) <sub>3</sub> Cl( <i>p</i> BIB)	1/3	C-I...Cl <sup>-</sup> 3.11 Å	metal down to 1.6 K	179
(ET) <sub>3</sub> Cl(DFBIB)	1/3	C-I...Cl <sup>-</sup> 3.13 Å	metal down to 1.6 K	180
(ET) <sub>3</sub> Cl( <i>p</i> BIB- <i>d</i> <sub>4</sub> )	1/3	C-I...Cl <sup>-</sup> 3.15 Å	metal down to 1.6 K	180
(ET) <sub>2</sub> Cl <sub>2</sub> (DIA)(TIE)	1	C-I...Cl <sup>-</sup> 3.09 (DIA) C-I...Cl <sup>-</sup> 3.24, 3.34 Å (TIE)	semiconductor	179
(ET) <sub>2</sub> Br(DIA)	1/2	C-I...Br <sup>-</sup> 3.16 Å	metal down to 1.6 K	178
(ET) <sub>3</sub> Br(DFBIB)	1/3	C-I...Br <sup>-</sup> 3.27 Å	metal down to 1.6 K	180
(ET) <sub>3</sub> Br( <i>p</i> BIB- <i>d</i> <sub>4</sub> )	1/3	C-I...Br <sup>-</sup> 3.25 Å	metal down to 1.6 K	180
(ET) <sub>3</sub> Br(TFBIB)	1/3	C-I...Br <sup>-</sup> 3.13 Å	metal down to 1.6 K	180
(ET) <sub>2</sub> Br <sub>2</sub> (DIA)(TIE)	1	C-I...Br <sup>-</sup> 3.19 (DIA) C-I...Br <sup>-</sup> 3.33, 3.40 Å (TIE)	semiconductor	179
(ET) <sub>6</sub> (AuBr <sub>2</sub> ) <sub>6</sub> Br(TIE) <sub>3</sub>	7/6	C-I...Br <sup>-</sup> 3.23 Å C-I...BrAuBr <sup>-</sup> 3.27, 3.37 Å	weak metal, $T_{MI} = 50$ K	179
(EDT-TTF) <sub>4</sub> Br <sub>2</sub> I <sub>3</sub> (TIE)	3/4	C-I...Br <sup>-</sup> 3.22, 3.26 Å	semiconductor	179
(EDT-TTF) <sub>4</sub> BrI <sub>2</sub> (TIE) <sub>5</sub>	3/4	C-I...Br <sup>-</sup> 3.71 Å C-I...I <sup>-</sup> 3.45, 3.74 Å	semiconductor	179
(ET) <sub>3</sub> Br(DFTIB)	1/3	C-I...Br <sup>-</sup> 3.25, 3.33 Å	semiconductor	181
(ET) <sub>2</sub> Br <sub>2</sub> (DFTIB)	1	C-I...Br <sup>-</sup> 3.31, 3.31 Å	semiconductor	181
(ET) <sub>2</sub> Br <sub>2</sub> (DFTIB) <sub>3</sub> (PhCl) <sub>x</sub>	1	C-I...Br <sup>-</sup> 3.39, 3.63, 3.35, 3.30 Å	semiconductor	181

<sup>a</sup>  $D_{anis}(C-I...Cl) = 3.54$  Å;  $D_{anis}(C-I...Br) = 3.60$  Å.

is already activated by the *para* effect of the electron-withdrawing CN group. The pyrazine derivatives (DIPS) exhibit the shortest I...N distances (2.84–2.88 Å), comparable to those observed in neutral, binary systems which involve the cocrystallization of activated iodo compounds such as I–CF<sub>2</sub>CF<sub>2</sub>–I with aliphatic or aromatic amines.<sup>174</sup>

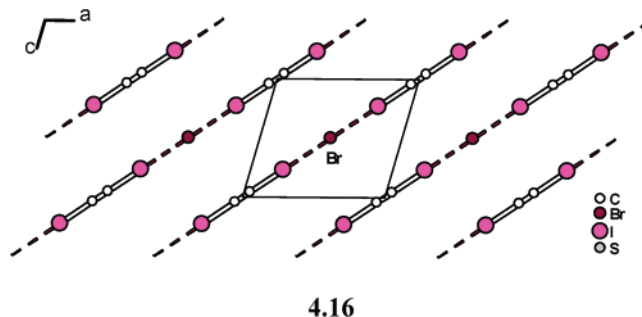
A neat, negative counter-manifestation of these electrostatic effects is illustrated by the opposite situation, where the Lewis base is now attached on the tetrathiafulvalene core, as in EDT-TTF–CN.<sup>116</sup> In the six examples described so far where (EDT-TTF–CN)<sup>+</sup> is engaged with the halogenated ions I<sub>3</sub><sup>-</sup>, FeBr<sub>4</sub><sup>-</sup>, InBr<sub>4</sub><sup>-</sup>, AuBr<sub>4</sub><sup>-</sup>, Mo<sub>6</sub>Br<sub>14</sub><sup>2-</sup>, and Mo<sub>6</sub>Cl<sub>8</sub>Br<sub>6</sub><sup>2-</sup>, no CN...Hal interaction occurs. One C<sub>sp<sup>2</sup></sub>–H...N hydrogen bond only is identified, involving the hydrogen atom *ortho* to the CN group (see Chart 10 in section 3.1).

Turning our attention back to the molecule DIPS shown in 4.15, one can note that, in every solid-state construct described above, the nitrogen lone pair oriented at 60° off the C–I bond axis directs a threefold symmetry structure with inherent cavities filled with various solvent molecules. This combination of a predetermined molecular orientation with a strongly directional interaction delivers building units for zeolite-like systems and paves the way for the preparation of other ternary systems. Such systems, where different solvent molecules can be introduced in a tailored hole within the structure, have attracted much attention because the third (neutral) component (solvent molecule) affects the details of the electronic structure and thus tunes its physical properties.<sup>175,176</sup> To get more control of the formation of such ternary systems, Yamamoto and Kato took advantage of halogen bonding to stabilize

binary anionic networks in ternary BEDT-TTF salts, as described below.

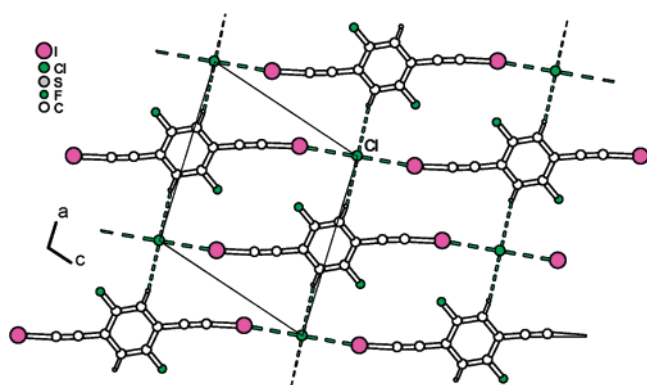
#### 4.4. Halogen Bonding Interactions in the Anionic Network

The observation<sup>177</sup> that cocrystallization of diiodoacetylene (DIA) with PPh<sub>4</sub>Cl, PPh<sub>4</sub>Br, or PPh<sub>4</sub>I generates two-dimensional networks with I–C≡C–I...Hal interactions prompted the electrocrystallization of BEDT-TTF with DIA and PPh<sub>4</sub>Cl or PPh<sub>4</sub>Br, affording the metallic (BEDT-TTF)<sub>2</sub>X(DIA) (X = Cl, Br) series,<sup>178</sup> where the halide anions are interspersed with DIA molecules within the one-dimensional chains shown in 4.16 with short intermolecular distances (C–I...Cl: 3.04 Å,  $D_{anis} = 3.54$  Å. C–I...Br: 3.15 Å,  $D_{anis} = 3.60$  Å) qualifying strong halogen bonding. This concept has been successfully extended to other neutral molecules such as *p*-bis(iodoethynyl)benzene<sup>179</sup> and the substituted derivatives<sup>180</sup> tetraiodoethylene<sup>179</sup> and difluorotetraiodobenzene (see Table 18).<sup>181</sup>



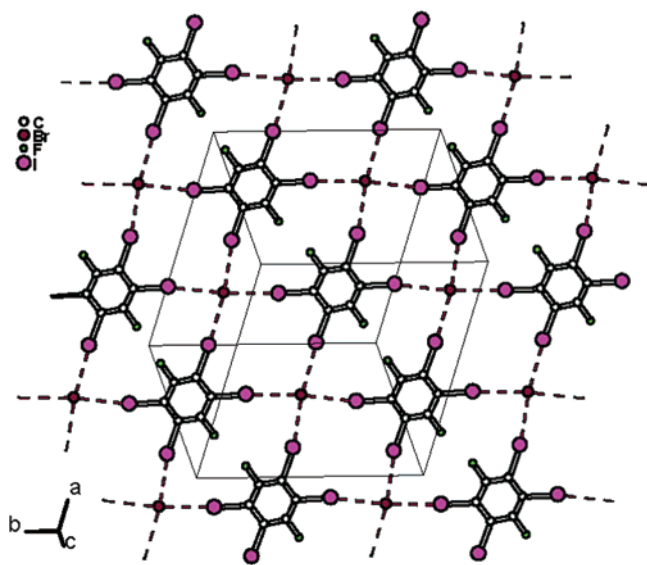
For example, in (BEDT-TTF)<sub>2</sub>Cl(DFBIB),<sup>180</sup> the coordination of the chloride by two 2,5-difluoro-1,4-

bis(iodoethynyl)benzene (DFBIB) molecules is complemented by two weak C–H···Cl interactions ( $H\cdots Cl = 2.85 \text{ \AA}$ ,  $C-H\cdots Cl = 171^\circ$ ) shown in **4.17**.



4.17

These systems concern not only iodoacetylene derivatives but also iodo aromatics such as 1,4-difluorotetraiodobenzene (DFTIB), as observed in **4.18** for  $(BEDT-TTF)_3Br(DFTIB)$ , where the bromide anion is coordinated by four iodine atoms. Notice the presence of the two fluorine atoms on the aromatic core, which are expected to enhance the “electrophilic” character of the iodine atoms, a strategy recently popularized by Resnati and Metrangolo in an extensive series of neutral binary systems built from fluorinated iodo derivatives and diamines.<sup>174</sup> In these salts, the halide anion ( $Cl^-$ ,  $Br^-$ ) is “coordinated” by two, three, four, six, or eight iodine atoms of neutral iodinated molecules. One observes that larger  $(C^-)I\cdots X$  ( $X = Cl, Br$ ) distances are found with higher coordination numbers, which is the consequence of a reduced negative charge on the halide atom upon coordination.



4.18

## 5. Concluding Remarks

From the early indications singled out in the introduction of the significance of weak  $C_{sp^2}-H\cdots O_{\text{quinone}}$ ,  $C_{sp^3}-H\cdots X^-$ , and  $C_{sp^3}-H\cdots O_{\text{Keggin anion}}$  hydrogen bond

interactions in TTF-based conductors to the present outpost established after traveling all the way over the topology of intermolecular patterns of hydrogen and halogen bond interactions across 164 crystal structures, much understanding has been gained by using the crystal engineering approach, principles, and concepts developed in the past 20 years to decipher the complex, entangled issues raised by the subtle interplay of stoichiometry, redox state, hydrogen-bonding, and overlap interactions in determining the structure and transport properties of molecular materials. In the field of crystalline molecular conductors under review, the deliberate choice of engaging tetrathiafulvalene precursors functionalized by strong hydrogen bond donor/acceptor groups, such as  $-(CH_2-OH)_n$ ,  $-CO_2H$ ,  $-PO_3H$ ,  $-CO(S)NH_2$ ,  $-CO(S)NHR$ , and *ortho*-bis(amide) linkages  $-(CONHR)_2$ , is one which delivered remarkable architectures which are now manipulated with a significant degree of prediction. It is likely this will serve as an incentive to pursue a creative quest for new systems engaging tetrathiafulvalene or its multistage extended, fused variants or related oligomers even, appended with even more complex, self-complementary functionalities, such as the purine or pyrimidine base pairs, for example.

A second of the review's themes, that is the cross-examination of how intermolecular hydrogen-bonding patterns of interactions in the parent, neutral solid constructs are transformed in the structure of their radical cation children, has outlined the evolving picture of an activation of  $C_{sp^2}-H$  and  $N-H$  donors coupled to a deactivation of  $O=C$  acceptors and shined a light on a dynamic interdependence of redox state, hydrogen bonding, anion recognition, and charge partition in crystalline radical cation salts in a way which confers to the hydrogen bond network the character of an amplifier converting the local conjugation and charge modulation into a comparatively huge macroscopic electronic response.

Furthermore, a salient outcome of the parallel, complementary survey proposed in the review of the nature and efficiency of electrostatic, strongly directional hydrogen and halogen bonding interactions in crystalline molecular conductors is the compelling evidence of their similarity and equally powerful ability at directing molecular orientations. One common feature worthy of reiteration is, here again, their activated nature, defined as the rather magnificent, enhanced response of both the  $C_{sp^2}-H\cdots$ acceptor and  $C_{sp^2}-Hal\cdots$ acceptor interactions upon electron transfer when the halogen atom is attached directly to the radical cation core. Perhaps the most obvious benefit of this observation is the variety of constructs made accessible by taking along neutral molecular spacers of diverse shape, length, symmetry, and so forth in the design of charge-diluted, ternary molecular systems.

Thus, molecular metals' architecture and their collective electronic response may be governed by hydrogen or halogen bonds, and there is a bewildering choice of combinations yet to be fashioned and explored. But then, our ability to predict with confidence that their structures are to meet the needs of

low dimensional physics expectations and crystalline devices fabrication remains to grow further out of its present, however promising, infancy: there is plenty of room for future creative developments in the chemistry and physics of hydrogen and halogen bond interactions in crystalline molecular systems.

## 6. Acknowledgments

The authors would like to thank the following current and former co-workers for their contribution to the work on many of the issues discussed in this article, Narcis Avarvari, Stéphane Baudron, Josep N. Bertran, Kamal Boubekeur, André Deluzet, Thomas Devic, Anne Dolbecq, Benoît Domercq, Aude Guirauden, Karine Heuzé, and Cécile Mézière, as well as their collaborators from diverse walks of materials chemistry and physics, Alain Gorgues, Marc Sallé, Philippe Blanchard, Philippe Molinié, Enric Canadell, Carme Rovira, and the groups of Denis Jérôme and Pascale Auban-Senzier, and Claude Coulon and Rodolphe Clérac. We also thank R. Kato, J. Nishijo, and M. Iyoda for providing us with unpublished X-ray data.

## 7. References

- Guru Row, T. N.; Parthasarathy, R. *J. Am. Chem. Soc.* **1981**, *103*, 477.
- Desiraju, G. R.; Gavezotti, A. *J. Chem. Soc., Chem. Commun.* **1989**, 621.
- Ellern, A.; Bernstein, J.; Becker, J. Y.; Zamir, S.; Shahal, L.; Cohen, S. *Chem. Mater.* **1994**, *6*, 1378.
- Cooper, W. F.; Edmonds, J. W.; Wudl, F.; Coppens, P. *Cryst. Struct. Commun.* **1974**, *3*, 23.
- Novoa, J. J.; Tarron, B.; Whangbo, M.-H.; Williams, J. M. *J. Chem. Phys.* **1991**, *95*, 5179.
- Novoa, J. J.; Rovira, M. C.; Rovira, C.; Veciana, J.; Tarrés, J. *Adv. Mater.* **1995**, *7*, 233.
- (a) Mori, T. *Bull. Chem. Soc. Jpn.* **1998**, *71*, 2509. (b) Mori, T.; Mori, H.; Tanaka, S. *Bull. Chem. Soc. Jpn.* **1999**, *72*, 179. (c) Mori, T. *Bull. Chem. Soc. Jpn.* **1999**, *72*, 2011.
- Batail, P.; LaPlaca, S. J.; Mayerle, J. J.; Torrance, J. B. *J. Am. Chem. Soc.* **1981**, *103*, 951.
- Torrance, J. B.; Girlando, A.; Mayerle, J. J.; Crowley, J. I.; Lee, V. Y.; Batail, P.; LaPlaca, S. *J. Phys. Rev. B* **1981**, *47*, 1747.
- Whangbo, M.-H.; Williams, J. M.; Schultz, A. J.; Emge, T. J.; Beno, M. A. *J. Am. Chem. Soc.* **1987**, *109*, 90.
- (a) Batail, P.; Ouahab, L. CNRS French patent 2565978, 1984. (b) Ouahab, L.; Batail, P.; Perrin, A.; Garrigou-Lagrange, C. *Mater. Res. Bull.* **1986**, *21*, 1223. (c) Batail P.; Ouahab, L.; Pénicaud, A.; Lenoir, C.; Perrin, A. *C. R. Acad. Sci., Ser. II* **1987**, *304*, 1111. (d) Batail, P.; Boubekeur, K.; Fourmigué, M.; Dolbecq, A.; Gabriel, J.-C.; Guirauden, A.; Livage, K.; Uriel, S. *New J. Chem.* **1994**, *18*, 999.
- Davidson, A.; Boubekeur, K.; Pénicaud, A.; Auban, P.; Lenoir, C.; Batail, P.; Hervé, G. *J. Chem. Soc., Chem. Commun.* **1989**, 1373.
- Coronado, E.; Gomez-Garcia, C. *J. Chem. Rev.* **1998**, *98*, 273.
- Bryce, M. R. *J. Mater. Chem.* **1995**, *5*, 1481.
- Nakasuji, K.; Sugiura, K.; Kitagawa, T.; Toyoda, J.; Okamoto, H.; Okaniwa, K.; Mitani, T.; Yamamoto, H.; Murata, I.; Kawamoto, A.; Tanaka, J. *J. Am. Chem. Soc.* **1991**, *113*, 1862.
- Desiraju, G. R. *Angew. Chem., Int. Ed. Engl.* **1995**, *34*, 2311.
- Desiraju, G. R. In *Crystal Engineering: The Design of Organic Solids*; Elsevier: Amsterdam, 1989.
- Atwood, J. L.; Lehn, J.-M.; Davies, J. E. D.; MacNicol, D. D.; Vogtle, F. *Comprehensive Supramolecular Chemistry*; Pergamon Press: New York, 1996; 11-volume set.
- (a) Tsoucaris, G., Ed. *Crystallography of Supramolecular Compounds*; NATO ASI Series, Series C; 1996. (b) Tsoucaris, G.; Atwood, J. L.; Lipkowski, J. *Crystallography of Supramolecular Compounds*; Kluwer, New York, 1996.
- Jeffrey, G. A.; Saenger, W. *Hydrogen Bonding in Biological Structures*; Springer: Berlin, 1991.
- Lommerse, J. P. M.; Stone, A. J.; Taylor, R.; Allen, F. H. *J. Am. Chem. Soc.* **1996**, *118*, 3108.
- Valerio, G.; Raos, G.; Meille, S. V.; Metrangolo, P.; Resnati, G. *J. Phys. Chem. A* **2000**, *104*, 1617.
- Steiner, T. *Angew. Chem., Int. Ed.* **2002**, *41*, 48.
- Desiraju, G. R.; Steiner, T. *The Weak Hydrogen Bond*; Oxford University Press: Oxford, New York, 1991.
- Sheldrick, G. M. *SHELXL-97—Crystal Structure Refinement*, WinGX Version 97-2.
- Mézière, C.; Fourmigué, M.; Fabre, J.-M. *C. R. Acad. Sci., Ser. IIc* **2000**, *3*, 387.
- Heuzé, K.; Fourmigué, M.; Batail, P. *J. Mater. Chem.* **1999**, *9*, 2373.
- Dolbecq, A.; Fourmigué, M.; Batail, P. *Bull. Soc. Chim. Fr.* **1996**, *133*, 83.
- Dolbecq, A.; Fourmigué, M.; Krebs, F. C.; Batail, P.; Canadell, E.; Clérac, R.; Coulon, C. *Chem. Eur. J.* **1996**, *2*, 1275.
- Perepichka, D. F.; Bryce, M. R.; Batsanov, A. S.; Howard, J. A. K.; Cuello, A. O.; Gray, M.; Rotello, V. M. *J. Org. Chem.* **2001**, *66*, 4517.
- Rindorf, G.; Thorup, N.; Lerstrup, K.; Bechgaard, K. *Synth. Met.* **1989**, *30*, 391.
- Mercier, N.; Giffard, M.; Pilet, G.; Allain, M.; Hudhomme, P.; Mabon, G.; Levillain, E.; Gorgues, A.; Riou, A. *Chem. Commun.* **2001**, 2722.
- (a) Golic, L.; Leban, I. *Croat. Chim. Acta* **1982**, *55*, 41. (b) James, M. N. G.; Matsushima, M. *Acta Crystallogr.* **1976**, *B32*, 1708. (c) Madsen, D.; Larsen, S. *Acta Crystallogr.* **1998**, *C54*, 1507.
- Kepert, C. J.; Heseck, D.; Beer, P. D.; Rosseinsky, M. *J. Angew. Chem., Int. Ed. Engl.* **1998**, *37*, 3158.
- Reported zwitterionic [TTF-CO<sub>2</sub>]<sup>+</sup> internal salts are extremely insoluble and decarboxylate upon warming: Kreitsberga, Y. N.; Neiland, O. Y. *J. Org. Chem. USSR (Engl. Trans.)* **1986**, 2131.
- Jeffrey, G. A. *An Introduction to Hydrogen Bonding*; Oxford University Press: Oxford, 1997.
- Dolbecq, A.; Fourmigué, M.; Batail, P. *Acta Crystallogr.* **1996**, *C52*, 1543.
- Bryce, M. R.; Skabara, P. J.; Moore, A. J.; Batsanov, A. S.; Howard, J. A. K.; Hoy, V. J. *Tetrahedron* **1997**, *53*, 17781.
- Liu, S.-X.; Neels, A.; Stoeckli-Evans, H.; Pilkington, M.; Wallis, J. D.; Decurtins, S. *Polyhedron* **2004**, *23*, 1185.
- Wang, C.; Bryce, M. R.; Batsanov, A. S.; Stanley, C. F.; Beeby, A.; Howard, J. A. K. *J. Chem. Soc., Perkin Trans. 2* **1997**, 1671.
- Moore, A. J.; Goldenberg, L. M.; Bryce, M. R.; Petty, M. C.; Moloney, J.; Howard, J. A. K.; Joyce, M. J.; Port, S. N. *J. Org. Chem.* **2000**, *65*, 8269.
- Legros, J.-P.; Dahan, F.; Binet, L.; Carcel, C.; Fabre, J.-M. *J. Mater. Chem.* **2000**, *10*, 2685.
- Batsanov, A. S.; Svenstrup, N.; Lau, J.; Bechern J.; Bryce, M. R.; Howard, J. A. K. *J. Chem. Soc., Chem. Commun.* **1995**, 1201.
- Blanchard, P.; Boubekeur, K.; Sallé, M.; Duguay, G.; Jubault, M.; Gorgues, A.; Martin, J. D.; Canadell, E.; Auban-Senzier, P.; Jérôme, D.; Batail, P. *Adv. Mater.* **1992**, *4*, 579.
- Dolbecq, A.; Fourmigué, M.; Batail, P.; Coulon, C. *Chem. Mater.* **1994**, *6*, 1413.
- Dolbecq, A.; Guirauden, A.; Fourmigué, M.; Boubekeur, K.; Batail, P.; Rohmer, M.-M.; Bénard, M.; Coulon, C.; Sallé, M.; Blanchard, P. *J. Chem. Soc., Dalton Trans.* **1999**, 1241.
- Li, H.; Zhang, D.; Zhang, B.; Yoa, Y.; Xu, W.; Zhu, D.; Wang, Z. *J. Mater. Chem.* **2000**, *10*, 2063.
- (a) Brammer, L.; Bruton, E. A.; Sherwood, P. *Cryst. Growth Des.* **2001**, *4*, 277. (b) Thallypally, P. K.; Nangia, A. *Cryst. Eng. Commun.* **2001**, 27.
- Legros, J.-P.; Dahan, F.; Binet, L.; Fabre, J.-M. *Synth. Met.* **1999**, *102*, 1632.
- Yao, Y.; Zeng, W.; Zhang, B.; Liu, Y.; Zhu, D. *Acta Crystallogr.* **2000**, *C56*, e90.
- Bernstein, J.; Etter, M. C.; Leiserowitz, L. In *Structure Correlation*; Bürgi, H.-B., Dunitz, J. D., Eds.; VCH: Weinheim, 1994; Vol. 2, Chapter 11.
- Leiserowitz, L.; Schmidt, G. M. *J. Chem. Soc. A* **1969**, 2372.
- Leiserowitz, L.; Tuval, M. *Acta Crystallogr.* **1978**, *B34*, 1230.
- Greenberg, A.; Breneman, C. M.; Liebman, J. F., Eds. *The Amide Linkage*; John Wiley & Sons: New York, 2000.
- Russel, V. A.; Ward, M. D. *Chem. Mater.* **1996**, *8*, 1654.
- Palacin, S.; Chin, D. N.; Simanek, E. E.; MacDonald, J. C.; Whitesides, G. M.; McBride, M. T.; Palmore, G. T. *R. J. Am. Chem. Soc.* **1997**, *119*, 11807.
- Lawrence, D. S.; Liang, T.; Levett, M. *Chem. Rev.* **1995**, *95*, 2229.
- Ono, G.; Izuoka, A.; Sugawara, T.; Sugawara, Y. *J. Mater. Chem.* **1998**, *8*, 1703.
- Heuzé, K.; Fourmigué, M.; Batail, P. *J. Mater. Chem.* **1999**, *9*, 2373.
- Allen, F. H.; Motherwell, W. D. S.; Raithby, P. R.; Shields, G. P.; Taylor, R. *New J. Chem.* **1999**, 25.
- Baudron, S. A.; Avarvari, N.; Batail, P.; Coulon, C.; Clérac, R.; Canadell, E.; Auban-Senzier, P. *J. Am. Chem. Soc.* **2003**, *125*, 11583.
- Mori, T. *Bull. Chem. Soc. Jpn.* **1998**, *71*, 2509.
- Batsanov, A. S.; Bryce, M. R.; Cooke, G.; Dhindsa, A. S.; Heaton, J. N.; Howard, J. A. K.; Moore, A. J.; Petty, M. C. *Chem. Mater.* **1994**, *6*, 1419.

- (64) Srikrishnan, T.; Parthasarathy, R. *Acta Crystallogr.* **1990**, *C46*, 1723.
- (65) Devic, T.; Avarvari, N.; Batail, P. *Chem. Eur. J.* **2004**, *10*, 3697.
- (66) Devic, T.; Batail, P.; Avarvari, N. *Chem. Commun.* **2004**, 1538.
- (67) Baudron, S. A.; Avarvari, N.; Canadell, E.; Auban-Senzier, P.; Batail, P. *Chem. Eur. J.* **2004**, *10*, 4498.
- (68) Bilton, C.; Allen, F. H.; Shields, G. P.; Howard, J. A. K. *Acta Crystallogr.* **2000**, *C56*, 849.
- (69) Neilands, O.; Belyakov, S.; Tilika, V.; Edzina, A. *J. Chem. Soc., Chem. Commun.* **1995**, 325.
- (70) Morita, Y.; Maki, S.; Ohmoto, M.; Kitagawa, H.; Okubo, T.; Mitani, T.; Nakasuji, K. *Org. Lett.* **2002**, *4*, 2185.
- (71) Goldenberg, L. M.; Neilands, O. *J. Electroanal. Chem.* **1999**, *463*, 212.
- (72) Moore, A. J.; Bryce, M. R.; Batsanov, A. S.; Heaton, J. N.; Lehmann, C. W.; Howard, J. A. K.; Robertson, N.; Underhill, A. E.; Perepichka, I. F. *J. Mater. Chem.* **1998**, *8*, 1541.
- (73) Allen, F. H.; Bird, C. M.; Rowland, R. S.; Raithby, P. R. *Acta Crystallogr.* **1997**, *B53*, 680.
- (74) Batsanov, A. S.; Bryce, M. R.; Cooke, G.; Heaton, J. N.; Howard, J. A. K. *J. Chem. Soc., Chem. Commun.* **1993**, 1701.
- (75) Batsanov, A. S.; Bryce, M. R.; Heaton, J. N.; Moore, A. J.; Skabara, P. J.; Howard, J. A. K.; Ort, E.; Viruela, P. M.; Viruela, R. *J. Mater. Chem.* **1995**, *5*, 1689.
- (76) Dautel, O. J.; Fourmigué, M. *J. Org. Chem.* **2000**, *65*, 6479.
- (77) Batsanov, A. S.; Bryce, M. R.; Cooke, G.; Dhindsa, A. S.; Heaton, J. N.; Howard, J. A. K.; Moore, A. J.; Petty, M. C. *Chem. Mater.* **1994**, *6*, 1419.
- (78) Hagler, A. T.; Leiserowitz, L. *J. Am. Chem. Soc.* **1978**, *100*, 5879.
- (79) Israelachvili, J. N. *Intermolecular Forces*; Academic Press: New York, 1985.
- (80) Blum, Z.; Hyde, S. T.; Ninham, B. W. *J. Phys. Chem.* **1993**, *97*, 661–665.
- (81) Forrest, S. R. *Chem. Rev.* **1997**, *97*, 1793–1896.
- (82) (a) Mas-Torrent, M.; Durkut, M.; Hadley, P.; Ribas, X.; Rovira, C. *J. Am. Chem. Soc.* **2004**, *126*, 984. (b) Bromley, S. T.; Mas-Torrent, M.; Hadley, P.; Rovira, C. *J. Am. Chem. Soc.* **2004**, *126*, 6544.
- (83) Heuzé, K.; Fourmigué, M.; Batail, P.; Canadell, E.; Auban-Senzier, P. *Chem. Eur. J.* **1999**, *5*, 2971.
- (84) Baudron, S. A.; Batail, P.; Rovira, C.; Canadell, E.; Clérac, R. *Chem. Commun.* **2003**, 1820.
- (85) Braga, D.; Grepioni, F. *Acc. Chem. Res.* **2000**, *33*, 601.
- (86) Jérôme, D. *Chem. Rev.* **2004**, *104*, 5565.
- (87) Heuzé, K.; Mézière, C.; Fourmigué, M.; Batail, P.; Coulon, C.; Canadell, E.; Auban-Senzier, P.; Jérôme, D. *Chem. Mater.* **2000**, *12*, 1898.
- (88) Baudron, S. A.; Mézière, C.; Heuzé, K.; Fourmigué, M.; Batail, P.; Molinié, P.; Auban-Senzier, P. *J. Solid State Chem.* **2002**, *168*, 668.
- (89) Ono, G.; Terao, H.; Higuchi, S.; Sugawara, T.; Izuoka, A.; Mochida, T. *J. Mater. Chem.* **2000**, *10*, 2277.
- (90) Giffard, M.; Riou, A.; Mabon, G.; Mercier, N.; Molinié, P.; Nguyen, T. P. *J. Mater. Chem.* **1999**, *9*, 851.
- (91) Braga, D.; Novoa, J. J.; Grepioni, F. *New J. Chem.* **2001**, *25*, 226.
- (92) Zaman, M. B.; Toyoda, J.; Morita, Y.; Nakamura, S.; Yamochi, H.; Saito, G.; Nishimura, K.; Yoneyama, N.; Enoki, T.; Nakasuji, K. *J. Mater. Chem.* **2001**, *11*, 2211.
- (93) Zaman, M. B.; Morita, Y.; Toyoda, J.; Yamochi, H.; Saito, G.; Yoneyama, N.; Enoki, T.; Nakasuji, K. *Chem. Lett.* **1997**, 729.
- (94) Zaman, M. B.; Toyoda, J.; Morita, Y.; Nakamura, S.; Yamochi, H.; Saito, G.; Nakasuji, K. *Synth. Met.* **1999**, *102*, 1691.
- (95) Horiuchi, S.; Yamochi, H.; Saito, G.; Sakaguchi, K.; Kusunoki, M. *J. Am. Chem. Soc.* **1996**, *118*, 8604.
- (96) Porter, L. C.; Wang, H. H.; Miller, M. M.; Williams, J. M. *Acta Crystallogr.* **1987**, *C43*, 2201.
- (97) Batsanov, A. S.; Moore, A. J.; Robertson, N.; Green, A.; Bryce, M. R.; Howard, J. A. K.; Underhill, A. E. *J. Mater. Chem.* **1997**, *7*, 387.
- (98) Taylor, R.; Kennard, O. *J. Am. Chem. Soc.* **1982**, *104*, 5063.
- (99) Desiraju, G. R. *Acc. Chem. Res.* **1991**, *24*, 270.
- (100) Aakeröy, C. B.; Evans, T. A.; Seddon, K. R.; Palinko, I. *New J. Chem.* **1999**, 145.
- (101) Steiner, T. *New J. Chem.* **1998**, 1099.
- (102) Desiraju, G. R. *J. Chem. Soc., Chem. Commun.* **1990**, 454.
- (103) Mayerle, J. J.; Torrance, J. B.; Crowley, J. I. *Acta Crystallogr.* **1979**, *B35*, 2988.
- (104) Frankenbach, G. M.; Beno, M. A.; Williams, J. M. *Acta Crystallogr.* **1991**, *C47*, 762.
- (105) Fourmigué, M.; Boubekeur, K.; Batail, P.; Renouard, J.; Jacob, G. *New J. Chem.* **1998**, *22*, 845.
- (106) Baumer, V. N.; Starodub, V. A. *Synth. Met.* **1984**, *9*, 467.
- (107) Hunter, C. A.; Sanders, J. K. M. *J. Am. Chem. Soc.* **1990**, *112*, 5525.
- (108) Horiuchi, S.; Okimoto, Y.; Kumai, R.; Tokura, Y. *J. Am. Chem. Soc.* **2001**, *123*, 665.
- (109) (a) Blessing, R. H.; Coppens, P. *Solid State Commun.* **1974**, *15*, 215. (b) Kistenmacher, T. J.; Phillips, T. E.; Cowan, D. O. *Acta Crystallogr.* **1974**, *B30*, 763.
- (110) Aharon-Shalom, E.; Becker, J. Y.; Bernstein, J.; Bittner, S.; Shaik, S. S. *Isr. J. Chem.* **1986**, *27*, 375.
- (111) Aumuller, A.; Erk, P.; Hunig, S.; von Schutz, J. U.; Werner, H.-P.; Wolf, H. C.; Klebe, G. *Chem. Ber.* **1991**, *124*, 1445.
- (112) Aumuller, A.; Erk, P.; Hunig, S.; Hadicke, E.; Peters, K.; von Schnering, H. G. *Chem. Ber.* **1991**, *124*, 2001.
- (113) Erk, P.; Hunig, S.; Klebe, G.; Metzenthin, T.; Werner, H.-P.; von Schutz, J.-U. *Liebigs Ann.* **1997**, 1235.
- (114) Aumuller, A.; Hadicke, E.; Hunig, S.; Schatzle, A.; von Schutz, J. U. *Angew. Chem., Int. Ed. Engl.* **1984**, *23*, 449.
- (115) Erk, P.; Hunig, S.; Klebe, G.; Krebs, M.; von Schutz, J. U. *Chem. Ber.* **1991**, *124*, 2005.
- (116) Devic, T.; Bertran, J. N.; Domercq, B.; Canadell, E.; Avarvari, N.; Auban-Senzier, P.; Fourmigué, M. *New J. Chem.* **2001**, *25*, 1418.
- (117) Guth, H.; Heger, G.; Drück, U. *Z. Kristallogr.* **1982**, *159*, 185.
- (118) Boitsov, S.; Songstad, J.; Toernroos, K. W. *Acta Crystallogr.* **2002**, *C58*, 066.
- (119) Morosin, B.; Nigrey, P. J. *Acta Crystallogr.* **1992**, *C48*, 1216.
- (120) Nigrey, P. J.; Duesler, E.; Wang, H. H.; Williams, J. M. *Acta Crystallogr.* **1987**, *C43*, 1073.
- (121) Korotkov, V. E.; Shibaeva, R. P. *Kristallografiya* **1991**, *36*, 1139.
- (122) Dautel, O. J.; Fourmigué, M.; Canadell, E. *Chem. Eur. J.* **2001**, *7*, 2635.
- (123) Ward, B. H.; Schlueter, J. A.; Geiser, U.; Wang, H. H.; Morales, E.; Parakka, J. P.; Thomas, S. Y.; Williams, J. M. *Chem. Mater.* **2000**, *12*, 343.
- (124) Geiser, U.; Schlueter, J. A.; Wang, H. H.; Kini, A. M.; Williams, J. M.; Sche, P. P.; Zakowicz, H. I.; VanZile, M. L.; Dudek, J. D. *J. Am. Chem. Soc.* **1996**, *118*, 9996.
- (125) Schlueter, J. A.; Ward, B. H.; Geiser, U.; Wang, H. H.; Kini, A. M.; Parakka, J.; Morales, E.; Koo, H.-J.; Whangbo, M.-H.; Winter, R. W.; Mohtasham, J.; Gard, G. L. *J. Mater. Chem.* **2001**, *11*, 2008.
- (126) Geiser, U.; Schlueter, J. A. *Chem. Rev.* **2004**, *104*, 5203.
- (127) (a) Guthrie, F. J. *Chem. Soc. Rev.* **1983**, *16*, 239. (b) Remsen, I.; Norris, J. F. *Am. Chem. J.* **1896**, *18*, 90.
- (128) Dumas, J. M.; Gomel, L.; Guérin, M. Molecular interactions involving organic halides. *The Chemistry of Functional Groups*, supplement D; Wiley: New York, 1983; pp 985–1020.
- (129) Legon, A. C. *Angew. Chem., Int. Ed. Engl.* **1999**, *38*, 2686–2714.
- (130) Ouvrard, C.; Le Questel, J.-Y.; Berthelot, M.; Laurence, C. *Acta Crystallogr. B* **2003**, *B59*, 512.
- (131) Metrangolo, P.; Resnati, G. *Chem. Eur. J.* **2001**, *7*, 2511.
- (132) Walsh, R. S.; Padgett, C. W.; Metrangolo, P.; Resnati, G.; Hanks, T. W.; Pennington, W. T. *Cryst. Growth Des.* **2001**, *1*, 165.
- (133) Corradi, E.; Meille, S. V.; Messina, M. T.; Metrangolo, P.; Resnati, G. *Angew. Chem., Int. Ed.* **2000**, *39*, 1782.
- (134) Desiraju, G. R.; Parthasarathy, R. *J. Am. Chem. Soc.* **1989**, *111*, 8725.
- (135) Price, S. L.; Stone, A. J.; Lucas, J.; Rowland, R. S.; Thornley, A. E. *J. Am. Chem. Soc.* **1994**, *116*, 4910.
- (136) Pauling, L. *The Nature of the Chemical Bond*; Cornell University Press: Ithaca, New York, 1942.
- (137) Bondi, A. J. *Phys. Chem.* **1964**, *68*, 441.
- (138) Nyburg, S. C.; Faerman, C. H. *Acta Crystallogr.* **1985**, *B41*, 274.
- (139) Imakubo, T.; Sawa, H.; Kato, R. *Synth. Met.* **1995**, *73*, 117.
- (140) Batsanov, A. S.; Bryce, M. R.; Chesney, A.; Howard, J. A. K.; John, D. E.; Moore, A. J.; Wood, C. L.; Gershtenman, H.; Becker, J. Y.; Khodorkovsky, V. Y.; Ellern, A.; Bernstein, J.; Perepichka, I. F.; Rotello, V.; Gray, M.; Cuello, A. O. *J. Mater. Chem.* **2001**, *11*, 2181.
- (141) Wang, C.; Ellern, A.; Khodorkovsky, V.; Bernstein, J.; Becker, J. Y. *J. Chem. Soc., Chem. Commun.* **1994**, 983.
- (142) Devic, T.; Domercq, B.; Auban-Senzier, P.; Molinié, P.; Fourmigué, M. *Eur. J. Inorg. Chem.* **2002**, 2844.
- (143) Shimizu, T.; Koizumi, T.; Yamaguchi, I.; Osakada, K.; Yamamoto, T. *Synthesis* **1998**, 259.
- (144) Wang, C.; Becker, J. Y.; Bernstein, J.; Ellern, A.; Khodorkovsky, V. J. *J. Mater. Chem.* **1995**, *5*, 1559.
- (145) Iyoda, M.; Kuwatani, Y.; Ogura, E.; Hara, K.; Suzuki, H.; Takano, T.; Takeda, K.; Takano, J.; Ugawa, K.; Yoshida, M.; Matsuyama, H.; Nishikawa, H.; Ikemoto, I.; Kato, T.; Yoneyama, N.; Nishijo, J.; Miyazaki, A.; Enoki, T. *Heterocycles* **2001**, *54*, 833.
- (146) Kux, U.; Suzuki, H.; Sasaki, S.; Iyoda, M. *Chem. Lett.* **1995**, 183.
- (147) Becker, J. Y.; Bernstein, J.; Bittner, S.; Shalal, L.; Shaik, S. S. *J. Chem. Soc., Chem. Commun.* **1991**, *9*, 22.
- (148) Iyoda, M.; Kuwatani, Y.; Hara, K.; Ogura, E.; Suzuki, H.; Ito, H.; Mori, T. *Chem. Lett.* **1997**, 599.
- (149) Mézière, C.; Fourmigué, M.; Fabre, J.-M. *C. R. Acad. Sci., Sér. II* **2000**, *3*, 387.
- (150) Fourmigué, M. Unpublished results.
- (151) Jørgensen, M.; Bechgaard, K. *Synthesis* **1989**, 207.

- (152) Iyoda, M.; Suzuki, H.; Sasaki, S.; Yoshino, H.; Kikuchi, K.; Saito, K.; Ikemoto, I.; Matsuyama, H.; Mori, T. *J. Mater. Chem.* **1996**, *6*, 501.
- (153) Iyoda, M.; Ogura, E.; Takano, T.; Hara, K.; Kuwatani, Y.; Kato, T.; Yoneyama, N.; Nishijo, J.; Miyazaki, A.; Enoki, T. *Chem. Lett.* **2000**, 680.
- (154) Domercq, B.; Devic, T.; Fourmigué, M.; Auban-Senzier, P.; Canadell, E. *J. Mater. Chem.* **2001**, *11*, 1570.
- (155) Kuwatani, Y.; Ogura, E.; Nishikawa, H.; Ikemoto, I.; Iyoda, M. *Chem. Lett.* **1997**, 817.
- (156) Gompper, R.; Hock, J.; Polborn, K.; Dormann, E.; Winter, H. *Adv. Mater.* **1995**, *7*, 41.
- (157) Devic, T.; Canadell, E.; Auban-Senzier, P.; Batail, P. *J. Mater. Chem.* **2004**, *14*, 135.
- (158) Devic, T.; Evain, M.; Moëlo, Y.; Canadell, E.; Auban-Senzier, P.; Fourmigué, M.; Batail, P. *J. Am. Chem. Soc.* **2003**, *125*, 3295.
- (159) Trigunayat, G. C. *Solid State Ionics* **1991**, *48*, 3.
- (160) Batsanov, A.S.; Lyubchik, S. B. *Acta Crystallogr., Sect. E: Struct. Rep. Online* **2003**, *59*, o326.
- (161) Imakubo, T.; Sawa, H.; Kato, R. *J. Chem. Soc., Chem. Commun.* **1995**, 1097.
- (162) Thoyon, D.; Okabe, K.; Imakubo, T.; Golhen, S.; Miyazaki, A.; Enoki, T.; Ouahab, L. *Mol. Cryst. Liq. Cryst.* **2002**, *376*, 25.
- (163) Ueda, K.; Sugimoto, T.; Faulmann, C.; Cassoux, P. *Eur. J. Inorg. Chem.* **2003**, 2333.
- (164) Imakubo, T.; Sawa, H.; Kato, R. *Synth. Met.* **1997**, *86*, 1847.
- (165) Imakubo, T.; Sawa, H.; Kato, R. *J. Chem. Soc., Chem. Commun.* **1995**, 1667.
- (166) Imakubo, T.; Miyake, A.; Sawa, H.; Kato, R. *Synth. Met.* **2001**, *120*, 927.
- (167) Imakubo, T.; Tajima, N.; Tamura, M.; Kato, R.; Nishio, Y.; Kajita, K. *J. Mater. Chem.* **2002**, *12*, 159.
- (168) Clemenson, P. I. *Coord. Chem. Rev.* **1990**, *106*, 171.
- (169) Nishijo, J.; Ogura, E.; Yamaura, J.; Miyazaki, A.; Enoki, T.; Takano, T.; Kuwatani, Y.; Iyoda, M. *Solid State Commun.* **2000**, *116*, 661.
- (170) Imakubo, T.; Maruyama, T.; Sawa, H.; Kobayashi, K. *Chem. Commun.* **1998**, 2021.
- (171) Suizi, R.; Imakubo, T. *Org. Bioorg. Chem.* **2003**, 3629.
- (172) Wangbo, M.-H.; Williams, J. M.; Schultz, A. J.; Emge, T. J.; Beno, M. A. *J. Am. Chem. Soc.* **1987**, *109*, 90.
- (173) Desiraju, G. R.; Harlow, R. L. *J. Am. Chem. Soc.* **1989**, *111*, 6757.
- (174) De Santis, A.; Forni, A.; Liantonio, R.; Metrangolo, P.; Pilati, T.; Resnati, G. *Chem. Eur. J.* **2003**, *9*, 3974.
- (175) Deluzet, A.; Rousseau, R.; Guilbaud, C.; Granger, I.; Boubekeur, K.; Batail, P.; Canadell, E.; Auban-Senzier, P.; Jerome, D. *Chem. Eur. J.* **2002**, *8*, 3884.
- (176) Schlueter, J. A.; Williams, J. M.; Geiser, U.; Wang, H. H.; Kini, A. M.; Kelly, M. E.; Dudek, J. D.; Naumann, D.; Roy, T. *Mol. Cryst. Liq. Cryst.* **1996**, *285*, 43.
- (177) Ghassemzadeh, M.; Harms, K.; Dehnicke, K. *Chem. Ber.* **1996**, *129*, 259.
- (178) Yamamoto, H. M.; Yamaura, J.-I.; Kato, R. *J. Mater. Chem.* **1998**, *8*, 15.
- (179) Yamamoto, H. M.; Yamaura, J.-I.; Kato, R. *J. Am. Chem. Soc.* **1998**, *120*, 5905.
- (180) Yamamoto, H. M.; Maeda, R.; Yamaura, J.-I.; Kato, R. *J. Mater. Chem.* **2001**, *11*, 1034.
- (181) Yamamoto, H. M.; Kato, R. *Chem. Lett.* **2000**, 970.

CR030645S